Distribution Agreement

In presenting this thesis or dissertation as a partial fulfillment of the requirements for an advanced degree from Emory University, I hereby grant to Emory University and its agents the non-exclusive license to archive, make accessible, and display my thesis or dissertation in whole or in part in all forms of media, now or hereafter known, including display on the world wide web. I understand that I may select some access restrictions as part of the online submission of this thesis or dissertation. I retain all ownership rights to the copyright of the thesis or dissertation. I also retain the right to use in future works (such as articles or books) all or part of this thesis or dissertation.

Signature:

_____ _____

Thayer King Darling Date

Unraveling the mechanisms by which CD8+ T cells and platelets contribute to cerebral malaria immunopathology

By

Thayer King Darling
Doctor of Philosophy

Graduate Division of Biological and Biomedical Science
Immunology and Molecular Pathogenesis

_____

Tracey Lamb, Ph.D.
Co-Advisor

_____

Jacob Kohlmeier, Ph.D.
Co-Advisor

_____

Brian Evavold, Ph.D.
Committee Member

_____

Malú Tansey, Ph.D.
Committee Member

_____

Sean Stowell, M.D., Ph.D.
Committee Member

Accepted:

_____

Lisa A. Tedesco, Ph.D.
Dean of the James T. Laney School of Graduate Studies

_____

Date

Unraveling the mechanisms by which CD8+ T cells and platelets contribute to cerebral malaria immunopathology

By

Thayer King Darling
B.S., University of Georgia, 2011

Co-Advisor: Tracey Lamb, Ph.D.

Co-Advisor: Jacob Kohlmeier, Ph.D.

An abstract of
A dissertation submitted to the Faculty of the
James T. Laney School of Graduate Studies of Emory University
in partial fulfillment of the requirements for the degree of
Doctor of Philosophy
in Graduate Division of Biological and Biomedical Science
Immunology and Molecular Pathogenesis
2019

Abstract

Unraveling the mechanisms by which CD8+ T cells and platelets contribute to cerebral malaria immunopathology

By Thayer King Darling

Malaria is a severe disease caused by infection with *Plasmodium* parasites. Despite continuing control efforts, reported malaria cases have increased in recent years. Cerebral malaria (CM) and malaria-associated acute lung injury/acute respiratory distress syndrome (MA-ALI/ARDS) are among the most severe complications of *Plasmodium falciparum* infection, yet the mechanisms underlying these diseases remain poorly understood. While these disease manifestations are complex and multifactorial, both CD8+ T cells and platelets have been described to play a role in the development of CM and MA-ALI/ARDS in mice as well as humans. However, the mechanisms by which CD8+ T cells and platelets contribute to exacerbation of organ pathology in the immune response to severe malaria have yet to be fully elucidated. Therefore, we were particularly interested in identifying molecular factors that may contribute to blood-brain barrier breakdown and increased lung vascular permeability in the development of these severe malaria syndromes.

Using a mouse model of experimental cerebral malaria (ECM), a disease which recapitulates key features of human CM including blood-brain barrier (BBB) dysfunction, we have identified a receptor tyrosine kinase, EphA2, essential for ECM development. *EphA2* is upregulated in brains of *Plasmodium berghei* ANKA (*Pb*A)-infected mice immediately prior to the onset of ECM symptoms, and *EphA2*-/- mice are protected from ECM. Interestingly, *EphA2* upregulation uniquely occurs in brains of mice infected with *Pb*A but not *Pb*NK65, a highly similar strain of *Plasmodium* that does not cause ECM. Furthermore, CD8+ T cells, which are required for ECM development, are not found in brains of *Pb*A-infected *EphA2*-/- mice. This reduction in brain CD8+ T cells is associated with enhanced endothelial cell junction integrity and reduced blood-brain barrier breakdown. These results indicate EphA2 may play a key role in ECM and could represent a distinguishing factor in the disparate disease phenotypes observed between these two malaria models.

In addition to CD8+ T cells, we address the role of platelets in the development of severe malaria using three different murine models of platelet dysfunction/depletion. We show that platelets are not required for control of blood-stage *Plasmodium* growth. On the contrary, platelet alpha-granules (α-granules) enhance parasite organ sequestration. In the absence of functional platelets, mice are protected from *Plasmodium*-associated lung and brain damage and death during ECM suggesting a key role for platelets and platelet α-granules, in particular, in mediating organ pathology during severe malaria.

Our findings reveal a key role for the receptor EphA2 and platelet α-granules in mediating CD8+T cell and platelet pathology in severe malaria. Given the increased incidence of malaria worldwide and paucity of CM and MA-ALI/ARDS treatment options, these observations could provide avenues into exploring novel therapeutics for this formidable disease.

Unraveling the mechanisms by which CD8+ T cells and platelets contribute to cerebral malaria immunopathology

By

Thayer King Darling
B.S., University of Georgia, 2011

Co-Advisor: Tracey Lamb, Ph.D.

Co-Advisor: Jacob Kohlmeier, Ph.D.

A dissertation submitted to the Faculty of the
James T. Laney School of Graduate Studies of Emory University
in partial fulfillment of the requirements for the degree of
Doctor of Philosophy
in Graduate Division of Biological and Biomedical Science
Immunology and Molecular Pathogenesis
2019

Acknowledgments

This journey towards completing my PhD would not have been possible without the support of a number of individuals.

First, I would like to thank my advisor, Dr. Tracey Lamb. From performing my first rotation with you back in 2013 until now, your scientific mentorship has been unwavering along the way. Thank you for always treating me as an equal and allowing me to explore scientific questions creatively while keeping me on track. Thank you for pushing me to apply for various opportunities from the very beginning of my graduate career. Even though for every success we have had over the years there have been several failures, each experience has molded me into the scientist that I am today. I have learned a tremendous amount from you over the past six years, and I will always be grateful for my time in your lab.

Second, I would like to thank past and present members of the Lamb lab. From early morning experiments to lab meetings and get-togethers outside of the lab, your support and kindness were always appreciated. Thank you for the conversations and ideas we have shared over the years. I am very grateful for all of the intellectual and experimental help you all provided along the way.

Third, I would like to thank my dissertation committee members. To Drs. Evavold, Kohlmeier, Stowell, and Tansey, thank you for your guidance. Each of you has been nothing but supportive from the very beginning, and I cannot imagine a better group of individuals to help shape my graduate career. You made each committee meeting a positive experience, and your optimism and wisdom when facing difficult scientific obstacles was immensely appreciated. I truly have unending gratitude for all of your counsel and kindness throughout the years.

Finally, I would like to thank my family. To my parents, Doug and Gerry, thank you for sparking my passion for science. From preschool through PhD, thank you for always putting education first and serving as role models for what can be achieved with hard work and dedication. Thank you for your patience, love, and unending support. You have taught me that nothing worth having comes easy, and you have instilled kindness, empathy, determination, sacrifice, and other lessons that are more important than anything I could learn in the lab. To my sisters, Ashley and Meagan, thank you for setting the precedent for what success looks like both within and outside of your careers – I can finally complete our trifecta of doctorates. And thank you for putting up with messages about mice on the family thread. Your senses of humor were always a much-needed respite during difficult times. Thank you all for always being proud of me, I wouldn't be here without you.

And to my husband, Josh, words will never be able to adequately thank you for all of your love and support over the years. This milestone is as much yours as it is mine. From working remotely to moving across the country, you have sacrificed an immeasurable amount for me on this winding road towards a PhD. I know that I can never repay you for all that you have done for me, but I will never stop trying. Through the many trials and tribulations along the way, thank you for always staying positive and believing in me. I am so lucky to have had such a loving and supportive partner throughout this journey, and I am unbelievably excited to begin the next chapter of our lives together. The best is yet to come.

Table of Contents

List of Figures

CHAPTER I

CHAPTER II

CHAPTER III

APPENDIX

CHAPTER I

Introduction

Chapter adapted from:

Darling TK and Lamb TJ (2019) Emerging Roles for Eph Receptors and Ephrin Ligands in Immunity. *Frontiers in Immunology*. 10:1473. doi: 10.3389/fimmu.2019.01473

Abstract

Eph receptors are the largest family of receptor tyrosine kinases and mediate a myriad of essential processes in humans from embryonic development to adult tissue homeostasis through interactions with membrane-bound ephrin ligands. The ubiquitous expression of Eph receptors and ephrin ligands among the cellular players of the immune system underscores the importance of these molecules in orchestrating an optimal immune response. This review provides an overview of the various roles of Eph receptors and ephrin ligands in immune cell development, activation, and migration. We also discuss the role of Eph receptors in disease pathogenesis as well as the implications of Eph receptors as future immunotherapy targets. Given the diverse and critical roles of Eph receptors and ephrin ligands throughout the immune system during both resting and activated states, this review aims to highlight the critical yet underappreciated roles of this family of signaling molecules in the immune system.

Significance

Malaria is the leading cause of death for children in sub-Saharan Africa (*1*). An estimated 200 million cases of malaria occur each year affecting people of all age ranges and resulting in one million annual deaths (*2*). Malaria is caused by infection with various species of the *Plasmodium* parasite (*3*), and transmission occurs when an infected *Anopheles* mosquito takes a blood meal. Plasmodium sporozoites enter the host and rapidly infect the liver before dividing and entering the bloodstream by infecting red blood cells (RBCs) (*4*). Research shows that limited immune responses occur against the pre-erythrocytic form of the parasite (*5*) and the response to the erythrocytic stage of the *Plasmodium* life cycle is responsible for the pathogenesis of infection. Therefore, it is essential that research on the development of antimalarial vaccines has a focus on controlling blood-stage parasitemia. The recently licensed RTS,S vaccine, a pre-erythrocytic

vaccine, is less than 50% effective (*6, 7*) and improvements are likely required. Children under five years of age living in sub-Saharan Africa are disproportionately affected by severe malaria complications which encompass a variety of conditions such as severe anemia, respiratory distress and cerebral malaria (*8*). Of the parasite strains that can infect humans, cerebral malaria is almost exclusively caused by infection with *Plasmodium falciparum* (*9*) and 15-20% of cerebral malaria cases are fatal. Currently, there are no specific therapeutics to treat cerebral malaria aside from quinine or artemisinin derivatives to aid in parasite control and clearance (*10*). Given the emerging parasite resistance associated with quinine and artemisinin derivatives, it is critical to identify and explore novel targets and therapeutics for this fatal disease. While the roles of Eph receptors in malaria are currently unknown to a large extent, their association with steady-state immune function as well as neurological disorders suggests a potential contribution of Eph receptor function to the development of cerebral malaria, in particular. Below we review the current understanding of Eph receptors in disease pathology and how members of this classical family of receptor tyrosine kinases may be involved in $CD8^+$ T cell dynamics during cerebral malaria representing a novel therapeutic target for antimalarial adjunctive treatments.

Eph receptors: a paradoxical family of kinases

The Eph (erythropoietin-producing hepatocellular carcinoma) receptors represent the largest known family of receptor tyrosine kinases in mammals (*11*). These receptors are critical for a variety of normal cellular processes during development and are key mediators of adult tissue homeostasis (*12-15*). First discovered in a human carcinoma cell line (*16*), the Eph family of receptors is now known to include two classes of receptors that consist of 9 EphA members and 5 EphB members classified according to sequence homology (*17*) **(Table 1)**. This group

Receptor	Expressed in mice and humans?	Ligand interactions
EphA1 (*16*)	Yes	**Ephrin-A4** > Ephrin-A1 > Ephrin-A3 > Ephrin-A2, Ephrin-A5
EphA2 (*18*)	Yes	**Ephrin-A1** > Ephrin-A5 > Ephrin-A4 > Ephrin-A3 > Ephrin-A2
EphA3 (*19*)	Yes	**Ephrin-A5** > Ephrin-A4 > Ephrin-A2 > Ephrin-A3 > Ephrin-A1
EphA4 (*20*)	Yes	**Ephrin-A4** > Ephrin-A5 > Ephrin-A1 > Ephrin-A2 > Ephrin-A3 *Can also bind all Ephrin-B ligands (1-3)
EphA5 (*21*)	Yes	**Ephrin-A5** > Ephrin-A3 > Ephrin-A4 > Ephrin-A2 > Ephrin-A1
EphA6 (*22*)	Yes	**Ephrin-A5** > Ephrin-A4 > Ephrin-A2 > Ephrin-A1 > Ephrin-A3
EphA7 (*23*)	Yes	**Ephrin-A5** > Ephrin-A3 > Ephrin-A4 > Ephrin-A1 > Ephrin-A2
EphA8 (*24*)	Yes	**Ephrin-A4, Ephrin-A5** > Ephrin-A1 > Ephrin-A3 > Ephrin-A2
EphA10 (inactive kinase) (*25*)	Yes	Ephrin-A1, Ephrin-A2, Ephrin-A3, Ephrin-A4, Ephrin-A5, (Binding affinities undetermined)
EphB1 (*26*)	Yes	**Ephrin-B2** > Ephrin-B1 > Ephrin-B3 *Can also bind Ephrin-A4
EphB2 (*24*)	Yes	**Ephrin-B2** > Ephrin-B1 > Ephrin-B3 *Can also bind all Ephrin-A ligands (1-5)
EphB3 (*27*)	Yes	**Ephrin-B2** > Ephrin-B1 > Ephrin-B3 *Can also bind Ephrin-A4
EphB4 (*28*)	Yes	**Ephrin-B2** > Ephrin-B1 > Ephrin-B3 *Can also bind Ephrin-A4
EphB6 (inactive kinase) (*29*)	Yes	**Ephrin-B2** > Ephrin-B1 > Ephrin-B3 *Can also bind Ephrin-A4
Additional references	(*17, 25, 29-37*)	

Table 1. List of Eph receptors expressed in both mice and humans along with potential binding partners and preferences for ephrin ligands.

of receptors function through interactions with membrane-bound ephrin (Eph receptor-interacting protein) ligands to mediate changes in cellular shape, motility, migration and proliferation (*12, 14, 38, 39*). The basic structures of Eph receptors and their ligands are shown in **Figure 1A**. All Eph receptors have a highly conserved overall structure with EphA and EphB receptors sharing the same structural features and domains. The primary sequence differences between EphA and EphB receptors reside in a region of the ligand binding domain determined to be a low-affinity ephrin binding site which is likely involved in determining ephrin subclass binding specificity (*40*). Given their high structural similarity, the differences in functional outcomes that result from activation of either EphA or EphB receptors can be primarily attributed to the spatial and temporal expression patterns of Eph receptors and ephrin ligands *in cis* on a cell and *in trans* on neighboring cells. In essence, activation of any given Eph receptor can have highly varied impacts on cellular processes depending on the cellular and microenvironmental context. EphA receptors bind promiscuously to ephrin-A ligands (5 members) while EphB receptors bind promiscuously to ephrin-B ligands (3 members) with some potential cross-talk between groups (*41*). In contrast to Eph receptors, the ephrin-A and ephrin-B ligand families have clear structural differences as ephrin-A ligands are tethered to the cell membrane through glycosylphosphatidylinositol (GPI) anchors while ephrin-B ligands have a short transmembrane domain and conserved cytoplasmic tail. Although it is widely accepted that clustering of membrane-bound Eph receptors and ephrin ligands is required to facilitate optimal signaling (*42*), research in cancer demonstrates that EphA2 expression on extracellular vesicles secreted from senescent cells can act on nearby ephrin-A1 expressing cancerous cells to contribute to proliferation (*43*). This indicates that cell-cell contact is not always necessary for the activation of downstream signaling upon Eph-

FIGURE 1

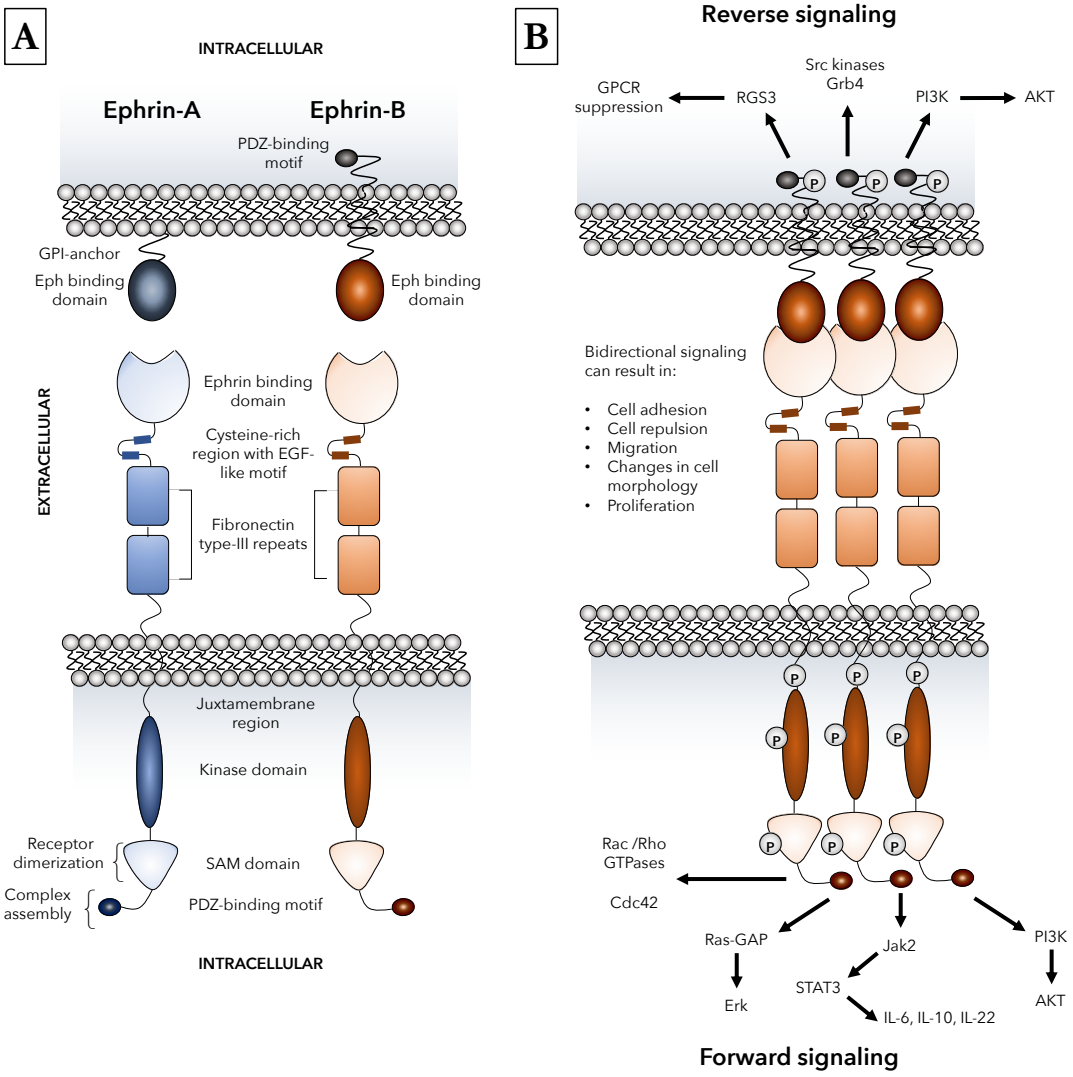
A
INTRACELLULAR
Ephrin-A
Ephrin-B
PDZ-binding motif
GPI-anchor
Eph binding domain
Eph binding domain
EXTRACELLULAR
Ephrin binding domain
Cysteine-rich region with EGF-like motif
Fibronectin type-III repeats
Juxtamembrane region
Kinase domain
Receptor dimerization
SAM domain
Complex assembly
PDZ-binding motif
INTRACELLULAR
B
Reverse signaling
GPCR suppression
RGS3
Src kinases Grb4
PI3K
AKT
Bidirectional signaling can result in:
• Cell adhesion
• Cell repulsion
• Migration
• Changes in cell morphology
• Proliferation
Rac /Rho GTPases
Cdc42
Ras-GAP
Erk
Jak2
STAT3
IL-6, IL-10, IL-22
PI3K
AKT
Forward signaling

Figure 1. Basic Eph receptor structure and signaling pathways. The structure of Eph receptors and their ligands is shown in **A**. Eph receptors are composed of an extracellular structure composed of an ephrin binding domain connected to two fibronectin type-III repeats by a cysteine-rich EGF-like motif. The juxtamembrane region connects the extracellular portion of the receptor to the intracellular kinase domain that is linked to a sterile alpha motif (SAM) domain and PDZ-binding motif. Two tyrosine residues on the juxtamembrane region mediate autophosphorylation. Eph receptors bind to ephrin ligands via an extracellular Eph binding domain. Ephrin-A ligands are GPI-anchored to the plasma membrane and signal through co-receptors that have not yet been fully defined. Ephrin-B ligands are transmembrane and are linked to an intracellular PDZ-binding motif via a linker containing 5 tyrosine resides for autophosphorylation. **(B)** Dimerization of Eph receptors is regulated by various processes including SAM domain interactions, ligand clustering, and interactions between cysteine-rich regions and ephrin binding domains on neighboring receptors. Receptor dimerization mediates the formation of heterocomplexes that are required for signaling and are assembled via the Eph receptor PDZ-binding motif. Formation of the heterocomplex mediates bi-directional signaling in which numerous signaling pathways known to play a role in immune cell function can be activated through both ephrin "reverse" and Eph "forward" signaling. These signaling events include activation of Rho GTPases, MAP kinases, PI3 kinase, Src family kinases, Jak-STAT molecules and RGS3 that has been shown to suppress G-protein coupled receptors including chemokine receptors. Abbreviations: P: representative of tyrosine phosphorylation sites; GPCRs: G-protein coupled receptors; RGS3: regulator of G-protein signaling 3; Grb4: cytoplasmic protein NCK2; PI3K: phosphatidylinositol 3-kinase; AKT: protein kinase B; Cdc42: cell division control protein 42 homolog; Ras-GAP: Ras-GTPase-activating protein; Erk: extracellular signal-regulated

(Figure 1 continued) kinases; Jak: Janus kinase; STAT: signal transducer and activator of transcription; IL: interleukin**.**

ephrin contact. The complexity of interactions conveyed by this promiscuous binding leads to considerable diversity in functional output upon Eph-ephrin binding.

A distinctive feature of Eph-ephrin interactions is the bidirectional signaling that occurs upon receptor-ligand binding and clustering which is termed forward signaling in Eph receptor-expressing cells and reverse signaling in ephrin ligand-expressing cells (*44-46*). Binding of Eph receptors to their ligands results in oligomerization and trans-phosphorylation leading to optimal kinase activity (*47, 48*). Importantly yet somewhat paradoxically, both cellular adhesion and repulsion can be consequences of Eph-ephrin binding between cells. High-affinity cell-cell binding events can lead to endocytosis of the receptor-ligand complex (*49-51*) or proteolytic cleavage of the ephrin extracellular domains (*52-54*) and cellular repulsion. On the other hand, Eph-ephrin adhesion is favored by reduced forward signaling (*55, 56*) and expression of Ephs and ephrins *in cis* (*57, 58*). There is also evidence that the fate decision between adhesion or repulsion can occur in a time-dependent manner where an initial adhesive event can later become a repulsive event (*49, 52*). The complexity provided by the signaling events downstream of Eph-ephrin binding allows for diverse functional consequences in a highly regulated and context-dependent manner, and examples of several potential signaling events that can occur upon Eph-ephrin clustering and ligation are shown in **Figure 1B**.

Expressed in most, if not all, adult tissues (*12, 59*), the Eph-ephrin signaling axis was initially most heavily studied for its complex role in embryonic and neural developmental processes such as cell segregation and migration, spatial organization of cell populations, tissue boundary formation, axonal guidance, and angiogenesis (*60, 61*). Also expressed on most cellular players of the immune system (**Table 2**), Eph-ephrin interactions have been implicated in various

	IMMUNE CELL SUBSETS				
	Platelets	**Monocytes & Macrophages**	**Dendritic cells**	**B cells**	**T cells**
Eph receptor protein expression	EphA4, EphB1, EphB2	EphA2, EphA4, EphB2, EphB4	EphA2, EphB1, EphB2, EphB3	EphA3, EphA4, EphA7, EphA10, EphB2, EphB6	EphA1, EphA3, EphA4, EphB3, EphB4, EphB6
Eph receptor functions	Platelet activation, thrombus formation	Cell spreading and adhesion, extravasation	Cell organization and trafficking	B cell activation, proliferation, and antibody production	IL-21 production in germinal centers, TCR signaling, T cell activation, migration, functionality
Cell-type specific disease relevance	*EphB2* mutation associated with platelet dysfunction and/or recurrent bleeding in humans	Liver fibrosis, Arteriosclerosis	EphA2 serves as a herpesvirus entry receptor on DCs	EphA4 associated with B-cell lymphoma and posttransplant lymphoproliferative disorder	EphA3, EphB3 and EphB6 involved in T cell malignancies
Ephrin ligand protein expression	Ephrin-B1	Ephrin-A1, Ephrin-A2, Ephrin-A4, Ephrin-B2	Unknown	Ephrin-A1, Ephrin-A4, Ephrin-B1	Ephrin-A1, Ephrin-B1, Ephrin-B2, Ephrin-B3
Ephrin ligand functions	Thrombus stability	Cell-cell contact/adhesion	Unknown	Cell-cell contact/adhesion, germinal center interactions and organization	Thymocyte development, T cell differentiation, activation, costimulation, migration
Cell-type specific disease relevance	Unknown	Atherosclerotic plaque formation	Unknown	Relation to chronic lymphocytic leukemia progression	Contribution to rheumatoid arthritis pathogenesis, possible involvement in multiple sclerosis

References	(*62-66*)	(*67-76*)	(*77-80*)	(*81-88*)	(*19, 85, 89-103*)

Table 2. Known protein expression profiles, functions, and disease contributions of Eph receptors and ephrin ligands on various immune cell subsets.

facets of immune surveillance including immune cell activation, migration, adhesion, and proliferation (*104-106*). In this review, we will discuss the emerging roles of Eph receptors and ephrin ligands in various aspects of immunity and disease pathogenesis as well as the implications of Eph receptors as future immunotherapy targets.

Impact of Eph receptor expression on stem cell fate

In order to understand how this unique family of receptors and ligands factors into immune system development and function, it is first necessary to review the effects of expression patterns of Eph receptors and their ligands on hematopoietic cells prior to divergence into different immune cell fates. There is evidence supporting a clear role for Eph receptors in cell fate decisions of hematopoietic progenitors prior to differentiation. EphB receptors in particular are important in the hematopoiesis of both red and white blood cells. Hematopoietic progenitor cells expressing EphB2 can be repulsed by bone marrow stromal cell-expressed Ephrin-B2, in turn mediating their subsequent differentiation into mature erythroid cells (*107*). Additionally, interactions between EphB4 and ephrin-B2 on bone marrow sinusoids and hematopoietic cells, respectively, aid in the mobilization of hematopoietic progenitor cells from the bone marrow (*108*). *In vitro*, ectopic EphB4 expression in hematopoietic cells promotes commitment to the megakaryocyte/erythroid lineage but not granulocytic or monocytic lineages (*109*). In the mouse small intestine, EphB2 is highly expressed on stem cells in crypts of villi while EphB3 is highly expressed on differentiated Paneth cells. The gradients of these receptors and their cognate ephrin-B1/B2 ligands tightly control cellular positioning and stem-cell differentiation and proliferation (*110, 111*). Various combinations and expression levels of Eph and ephrin family members have also been found on $CD34^+$ stem cells in both the bone marrow (*112*) and peripheral blood (*113*). Since expression differs

depending on hematopoietic stem cell location (bone marrow and blood) and other microenvironmental factors, expression patterns are likely important for both early development and later function of these cells prior to lineage commitment.

Roles of Ephs and ephrins in immune cell activation

One of the initial processes in mounting an immune response is the activation of immune cells. There is evidence that Eph receptors and ephrin ligands may mediate immune cell activation. However, given the sparse number of reports in the literature it remains an open question of how signaling emanating from Eph-ephrin ligation influences activation and how this process is influenced by expression of these molecules *in cis* and *in trans* on different immune cell subsets. Furthermore, in the case of innate immune cells, initial recognition leads to activation that can be amplified through feedback loops once the adaptive immune response has been initiated. Below we outline what is currently known about the involvement of Eph receptors in activating both innate and adaptive immune cells.

Innate immune cells

There are very few reports on the contribution of Eph receptors and ephrin ligands to the activation of innate immune cells. However, there is evidence suggesting a role for Eph receptors, specifically EphB2, in modulating dendritic cell (DC) responsiveness to toll-like receptor (TLR) ligation by pathogen-associated molecular patterns (*78*). Although not currently understood, it is possible that TLR signaling pathways intersect with EphB forward signaling events leading to a modulation of NFκB activation which is central to many immune cell activation pathways. Given the widespread expression of Eph receptors and TLRs on

many innate immune cells (**Table 2**), it would be surprising if this is not a more widespread phenomenon although this remains to be tested in other innate immune cell types.

B cells

Eph receptors and ephrins have been identified on both human (*81, 87, 114*) and mouse (*84*) B cells. Eph receptors and ephrin ligands are also expressed differentially on naïve and activated B cells (*81*). This suggests that they may contribute to processes facilitating B cell activation as exemplified by naïve human B cells which upregulate EphB2 leading to increased proliferation and antibody production. In B cells, EphB2 has been demonstrated to be regulated by the microRNA miR-185 and its effects on B cell activation appear to occur at least in part through interactions between EphB2 and the Src-p65 and Notch1 signaling pathways (*86*). Thus, B cells may modulate expression of different Eph and/or ephrin members in order to facilitate their development, activation, differentiation, and functionality. Given the importance of cell-cell contact and localization to specific anatomical niches to the development, activation and maturation of B cells, it seems likely that differential expression of Eph receptors and ephrin ligands could also contribute to B cell specialization into various canonical B cell fates.

T cells

Ephs and ephrins have been detected on human peripheral T cells with one study showing between 10-12% of $CD4^+$ and $CD8^+$ T cells expressing EphB6 (*115*). EphB receptors reported to be expressed on mouse naïve splenic $CD4^+$ and $CD8^+$ T cells include EphB1, EphB2, EphB3 and EphB6. Expression of all three ephrin-B ligands on T cells has also been demonstrated (*97, 100, 116*), but co-expression patterns of the ligands and receptors on T cells

have not yet been determined. Given the fact that Eph receptors and ephrins are also present on antigen presenting cells such as DCs(*77-80*), expression of these molecules on T cells suggests a potential role in T cell activation and differentiation.

Multiple studies have demonstrated that all three ephrin-B ligands can influence cooperation between T cells, T cell co-stimulation, and enhancing signaling through the T cell receptor (TCR). EphB receptors and TCRs colocalize in signaling rafts on the surface of activated T cells. Additionally, ephrin-B1 mediated stimulation of T cells through EphB receptors increases both phosphorylation of LAT and activation of the signaling molecules p38 and p44/42 MAPK (*97, 100*) providing a mechanistic explanation for how Eph receptors and components of the TCR complex may interact. Specifically, EphB6 has been shown to have a critical role in T cell activation with EphB6 deficient mice displaying reduced activation, phosphorylation, and/or recruitment of the T cell signaling molecules ZAP-70, LAT, SLP-76, PLCγ1, and P44/42 MAPK (*117*). Administration of anti-EphB6 antibodies, which can cause EphB6 clustering and subsequent signaling on T cells, increases the response of mature T cells to weak TCR ligation as measured by canonical activation marker expression (CD25, CD69) and cytokine production (interferon (IFN)-γ, interleukin (IL)-6) as well as T cell proliferation (*115*). In support of its role in enhancing TCR signal strength, EphB6 cross-linking in a T cell line sensitive to strong TCR signaling leads to enhanced apoptosis (*118*) which supports the finding that strong Eph receptor activation can induce apoptotic pathways (*44, 119*). This is in contrast to EphA receptors which prevent apoptosis in thymocytes (*120*) and we speculate that this could also apply to peripheral mature T cells participating in an immune response.

More recently, it has been suggested that EphB-ephrin-B signaling may also provide negative feedback during T cell activation. Ephrin-B1 and ephrin-B2, but not ephrin-B3, co-stimulated T cells at low concentrations but inhibited T cell activation at higher concentrations. This inhibition at high ephrin-B1/B2 concentrations likely occurs through inducing recruitment of the SHP1 phosphatase in stimulated T cells resulting in reduced phosphorylation of the signaling molecules Lck, Erk, and Akt (*93*). Additional data shows that mixed lymphocyte reaction activated cells pulsed with EphB2-Fc or ephrin-B2-Fc recombinant chimeric proteins downregulate key activation molecules including IL-2, IFN-γ, tumor necrosis factor-α (TNF-α) and IL-17 (*96*). These data suggest that the context-dependent expression of a combination of EphB receptors and ephrin-B ligands on T cells may serve an immunomodulatory role in different microenvironments.

In addition to activation, it is possible that regulation of Eph receptors and ephrin ligands can influence T cell differentiation into various T cell subsets. EphA-ephrin-A interactions can preferentially skew the differentiation of activated human $CD4^+$ T cells to a T helper (Th) type 1, rather than a Th2, phenotype upon cross-linking of ephrin-A ligands in the presence of α-CD3/α-CD28 activating antibodies via the suppression of IL-2 and IL-4 (*99*). This indicates that reverse signaling in ephrin-A ligand expressing T cells is able to intersect with other currently unidentified signaling pathways in order to suppress differentiation into a Th2 cell fate.

Eph-ephrin interactions mediate immune cell trafficking

An emerging role for Eph receptors and ephrin ligands in immune cell trafficking has been a focus of recent research. Cell migration is a fundamental process required for optimal immune

system functioning. Migration occurs both locally, where cells are required to move within lymphoid organs such as the spleen in order to interact with other immune cells, and systemically during routine immune surveillance and response to damage or infection. Several key events in local and systemic immune cell trafficking that involve Eph-ephrin interactions in both steady and activated states of the immune system are shown in **Figure 2** and discussed in detail below.

Localized immune cell migration within lymphoid organs

Thymic movement of T cells during development

It is not surprising that members of the Eph family would mediate a process such as T cell maturation given their well-established roles in tissue organization and cell migration in numerous organ systems. During T cell maturation, immature thymocytes undergo multiple steps of selection in the thymus requiring extended cell-cell contact with various cell types such as thymic stromal cells. It is quite possible that Eph-ephrin interactions may mediate adhesion and aid in the movement of maturing T cells through different thymic compartments during this process. Indeed, the expression of nearly all Eph receptors and ephrin ligands, with the exception of a few, has been detected in the thymus (*29, 121*). In the fetal thymus, EphB2 and EphB3 appear to be crucial for the successful development of thymic epithelial cells (*122*). Furthermore, EphB2 is implicated in mediating the colonization of T cell progenitor cells during fetal thymus colonization (*123*). As such, the presence of EphB2 and ephrin-B1/B2 ligands on thymocytes and thymic epithelial cells is essential for the correct organization of the thymic medulla (*124*). EphB6 is highly expressed in thymocytes and in mice between 50-70% of T cells in the thymus express EphB6 including $CD4^+CD8^+$ double positive as well as $CD4^+$ and $CD8^+$ single positive T cells (*117*). However, only around 8-17% of peripheral

FIGURE 2

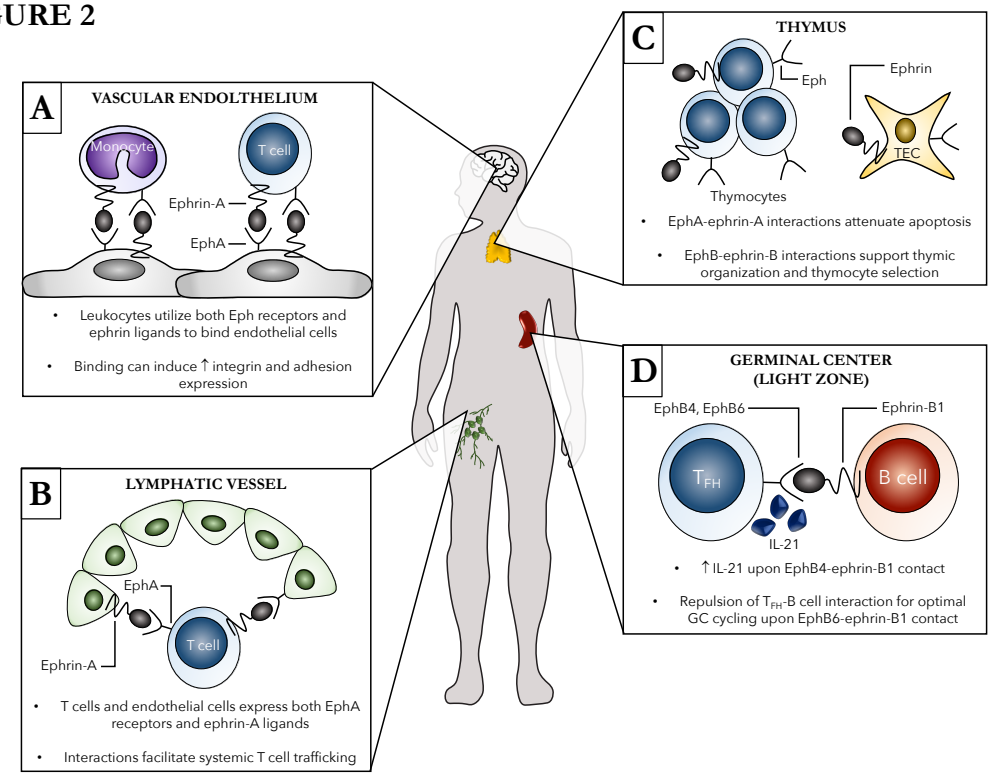
A
VASCULAR ENDOLTHELIUM
Monocyte
T cell
Ephrin-A
EphA
• Leukocytes utilize both Eph receptors and ephrin ligands to bind endothelial cells
• Binding can induce ↑ integrin and adhesion expression
B
LYMPHATIC VESSEL
EphA
T cell
Ephrin-A
• T cells and endothelial cells express both EphA receptors and ephrin-A ligands
• Interactions facilitate systemic T cell trafficking
C
THYMUS
Eph
Ephrin
TEC
Thymocytes
• EphA-ephrin-A interactions attenuate apoptosis
• EphB-ephrin-B interactions support thymic organization and thymocyte selection
D
GERMINAL CENTER (LIGHT ZONE)
EphB4, EphB6
Ephrin-B1
TFH
B cell
IL-21
• ↑IL-21 upon EphB4-ephrin-B1 contact
• Repulsion of TFH-B cell interaction for optimal GC cycling upon EphB6-ephrin-B1 contact

Figure 2. Examples of the contribution of Eph receptors and ephrin ligands to both localized and systemic immune cell trafficking. Several systemic (A and B) and localized (C and D) roles of Eph-ephrin interactions in immunity are shown. **(A)** Both leukocytes, such as monocytes and T cells, and vascular endothelial cells, shown here in the brain as an example, express various Eph receptors and ephrin ligands. Eph-ephrin interactions can aid in processes such as leukocyte chemotaxis, adhesion, and transmigration of the vascular endothelium. These binding events can subsequently induce increased expression of adhesion molecules and integrins leading to enhanced cell-cell contact. **(B)** EphA receptors, primarily EphA2, on high endothelial venules (HEVs) of lymph nodes can interact with ephrin-A ligand-expressing T cells to facilitate trafficking between the blood and lymph. Additionally, ephrin-A1 on HEVs can bind EphA receptors on circulating peripheral T cells leading to changes in actin polymerization in the T cell and initiating subsequent chemotaxis. **(C)** Thymic organization as well as thymocyte development are heavily dependent on Eph-ephrin interactions. The Eph B family members are particularly important in these processes, with both single- and double-positive thymocytes as well as thymic epithelial cells (TECs) expressing several EphB receptors and ephrin-B ligands to facilitate cellular organization of the thymus and thymocyte selection. **(D)** EphB-ephrin-B interactions are critical for optimal germinal center interactions between B cells and T follicular helper (T_{FH}). Ephrin-B1 marks a subpopulation of germinal center memory B cells and binding to EphB4 and EphB6 on T_{FH} cells induces IL-21 production from the T_{FH} cells and repulsion, respectively, both required for optimal germinal center B cell cycling.

mature $CD4^+$ and $CD8^+$ T cells in mice are $EphB6^+$ (*117*) indicating a potential role for EphB6 and its cognate ligand in mediating T cell retention in the thymus during development.

Although there have not been a large number of studies that address the role of Eph-ephrin interactions in T cell migration and adhesion within the thymus, such interactions appear to be critical for modulating apoptosis of thymocytes and are therefore likely critical in T cell selection processes. Distinct, yet overlapping, expression patterns of EphA receptors and ephrin-A ligands are observed in the rat thymus, and disruption of these interactions in a thymic culture model with EphA-Fc or ephrin-A-Fc recombinant chimeric proteins leads to an increase in apoptosis of double positive $CD4^+CD8^+$ T cells (*125*). This is in contrast to one study that showed ligation of EphA receptors with ephrin-A1 ligand can prevent apoptosis in thymocytes (*120*) but in agreement with a mouse study that used recombinant EphB2-Fc or ephrin-B1-Fc in thymic organ cultures *in vitro* to show reduced numbers of thymocytes via increased apoptosis (*126*). An overwhelming number of *in vivo* mouse models involving both Eph receptor subfamilies support the conclusion that Eph-ephrin interactions prevent apoptosis of thymocytes. Mice with selective T cell deficiency of ephrin-B1 and ephrin-B2 have significantly reduced numbers of double positive and single positive T cells in the thymus compared with intact littermate control mice (*127*). However, the lack of an effect in mice with a selective T cell deficiency in ephrin-B2 only (*92*) demonstrates the redundancy of this family of molecules as well as the ability of these receptors and ligands to potentially compensate for one another. Reduced thymic cellularity is also observed in the absence of EphB2, EphB3 (*128*) and EphA4 (*129*) in mice again suggesting a critical role for Eph receptors in preventing apoptosis of thymocytes during T cell thymic maturation.

Movement of immune cells in the context of germinal centers

Germinal centers (GCs) are key immunological structures in secondary lymphoid organs that form to facilitate the interaction between T follicular helper (Tfh) cells and activated B cells and to aid in the development of a robust humoral immune response. During an early GC reaction, activated Tfh cells interact with their cognate antigen-specific B cells to promote B cell proliferation and differentiation into plasma cells and memory B cells (*130*). With T and B cells activated in different zones within the GC, this cellular interaction requires movement of T cells into the B cell zone as induced by the chemokine CXCL13 (previously known as B-cell attracting chemokine-1) along with subsequent exit of antibody-secreting plasma cells and memory B cells from the GC. In order for these extensive cell cycling and cell-cell contact events to successfully occur in the GC, both attractive and repulsive events between cells are required.

One of the more recently discovered immunological roles of the Eph-ephrin signaling system involves the generation of GC B cell responses. Ephrin-B1, a ligand that can bind to several EphB receptors, was recently shown to be a marker of mature GC B cells and may specifically differentiate early GC memory precursor B cells from other subsets of GC B cells (*84*). The development of an optimal humoral immune response requires specific temporal interactions to occur between Tfh cells and GC B cells. Ephrin-B1 has been shown to be involved in the localized interaction between B cells and Tfh cells in the GC microenvironment (*85*). Specifically, GC B cell-expressed ephrin-B1 can inhibit recruitment and retention of Tfh cells in the GC and is required for GC B cells to induce optimal levels of IL-21 from Tfh cells via EphB4 forward signaling (*85*). Given the key role of IL-21 in plasma cell formation and affinity

maturation, GC B cell-expressed ephrin-B1 is therefore a key molecule required for the optimal functioning of GC interactions as a whole.

Migration of immune cells systemically

Directional trafficking of immune cells throughout the body is driven in part by chemokine receptors expressed on immune cells that respond to chemokines secreted by distal cells. The process of systemic cell migration is facilitated by adhesion molecules such as integrins expressed on vascular endothelial cells and their ligands expressed on trafficking immune cells. Like integrins, Ephs and ephrins are also expressed in the vasculature throughout the body (*59, 131, 132*). Given the widespread expression of Eph receptors and ephrin ligands on immune cells, the Eph-ephrin family of molecules may also be an important family of molecules facilitating trafficking of immune cells to the site of damage and inflammation.

The Eph-ephrin system has been shown to participate in multiple steps of monocyte trafficking including chemotaxis, adhesion (*70*), and vascular endothelial transmigration (*74*). In particular, expression of the receptors and ligands EphA2, EphA4, ephrin-A1, ephrin-A2, and ephrin-A4 is upregulated on mouse and human classical monocyte subsets at both the RNA and protein level, and these molecules can contribute to adhesion of monocytes to integrin-coated surfaces (*73, 76, 133*). One example of how Eph receptor signaling may mediate monocyte retention at the site of inflammation involves the interaction between ephrin-A1 on monocytes and EphA4 on endothelial cells. Upon endothelial EphA4 activation, the RhoA signaling pathway is activated leading to increased actin filament polymerization and subsequently enhanced monocyte-endothelial cell adhesion (*70*). Overall, the signaling events downstream of Eph-ephrin activation are likely to participate in crosstalk with integrin

molecular pathways and have been hypothesized to facilitate adhesion of monocytes to other Eph or ephrin-expressing cells.

Human DCs are also known to express members of the EphA (EphA2, EphA4, EphA7) and EphB (EphB1, EphB2, EphB3, EphB6) subfamilies (*70, 77, 78*). Similar to monocytes, Eph receptors could potentially contribute to DC trafficking and adhesion by allowing for localization to sites of damage or infection in the body with some evidence suggesting that crosstalk between Eph receptors and integrins, particularly β1 integrin, may facilitate DC adhesion (*134*). Interestingly, different subsets of DCs such as Langerhans cells (*135*), interstitial DCs, and plasmacytoid DCs (*80*) have unique patterns of Eph receptor expression. Although the reasons for these unique expression patterns remain unknown, it is possible that Eph receptors may contribute to the locational and functional specificity observed in these different DC subsets.

In the adaptive arm of the immune system, members of the EphA-ephrin-A family have been associated with B and T cell trafficking in several studies. The expression of EphA2 on high endothelial venules (HEVs) in human lymph nodes (*136*) suggests a role in immune cell trafficking. In support of this data, initiation of ephrin-A reverse signaling on T cells alters T cell trafficking by directing the T cells to enter lymph nodes upon injection into recipient mice (*137*). Although the specific member(s) of the ephrin-A ligand family important for this phenomenon is currently unknown, EphA2 has been shown to be important in mediating T cell trafficking between the blood and lymph nodes through interactions with ephrin-A4 on peripheral T cells (*136*). Along the same lines, ephrin-A1 is also expressed on HEV endothelial cells, and engagement of EphA receptors on the surface of both $CD8^+$ and $CD4^+$ T cells

directly stimulates chemotaxis through effects of this ligation on actin polymerization (*138*). Specifically, the migration that is induced upon stimulation of EphA receptors on T cells with ephrin-A ligands involves activation of a variety of signaling molecules including Lck, Pyk2, PI3K, Vav1, and Rho GTPase (*139*). More recently, it has also been shown that activation of EphA2 on endothelial cells with ephrin-A1 leads to NFAT activation and subsequent upregulation of vascular cellular adhesion molecule 1 (VCAM-1) which aids in leukocyte recruitment by facilitating cellular adhesion (*140*). Collectively, these studies indicate a key role for Eph molecules, particularly EphA2, in optimal adaptive immune cell trafficking to sites of inflammation.

Interestingly, the expression of ephrin-A ligands on the various subsets of $CD4^+$ and $CD8^+$ T cells differs (*103*) and thus EphA-ephrin-A expression patterns may contribute to the differing migratory potential observed in naïve, effector, and memory T cells. Expression of ephrin-B ligands has also been implicated in T cell trafficking to inflamed paws during a collagen-induced arthritis mouse model (*91*) as well as to the central nervous system in the experimental autoimmune encephalomyelitis (EAE) mouse model (*95*) underlining a role for both subfamilies in T cell trafficking to distal sites of inflammation in the body. Interplay between Eph-ephrin interactions and chemokines has yet to be well-studied but T cell chemotaxis in response to the chemokines stromal cell derived factor-1α (SDF-1α, also known as CXCL12) and macrophage inflammatory protein-3β (MIP-3β, also known as CCL19) can also be modulated by both ephrin-A and ephrin-B ligands (*141*) implicating both subfamilies in T cell trafficking in response to chemokine gradients.

Involvement of Eph receptors and ephrin ligands in disease pathogenesis

The ubiquitous expression profile of Ephs and ephrins throughout the human body makes them plausible candidates for mediating a variety of immunological processes. However, the widespread expression pattern along with the characteristic tyrosine kinase activity associated with Eph receptors also renders them highly likely to contribute to certain pathological conditions. Evolving research implicates various members of this family in a growing number of immune-mediated pathological conditions (*142-144*) as well as the pathogenesis of various diseases (*13, 145-147*). Thus, Eph receptors and ephrin ligands have become attractive therapeutic targets for several diseases including cancer, neurological disorders, and infectious diseases (*83, 145, 148-154*). In the remaining sections, we discuss what is currently known about the involvement of the Eph-ephrin family in both non-infectious and infectious diseases to convey the complexity of how these molecules contribute to various diseases.

Cancer

The first Eph receptor was identified in 1987 (*16*) from a human carcinoma cell line in a screen for oncogenic tyrosine kinases. It is therefore not surprising that a strong link between Eph receptors and cancer has emerged in the years since their discovery. Various Eph receptors and ephrin ligands are expressed in cancer cells as well as cells in the tumor microenvironment allowing for cell-cell communication within these compartments (*155, 156*). In the tumor microenvironment, upregulation of ephrin-A2, ephrin-A3, EphB2, and EphB4, to name a few, on vascular cells in response to tumor factors has been the most well studied (*157, 158*). EphA2 and EphB4 are upregulated in many types of cancers and are associated with increases in cancer malignancy and poor prognosis (*159-162*). Expression of several EphB receptors has also been inversely correlated with colorectal cancer where decreased expression is associated with increased malignancy (*163*).

As many Eph receptors and ephrin ligands are expressed on T and B cells **(Table 2)** and can play critical roles in cell development, differentiation, activation, and proliferation, it is predictable that aberrant expression or activation of these molecules on adaptive immune cells could contribute to hematologic malignancies. EphA3 has been of particular interest to the cancer research field as it was originally identified in an acute lymphoblastic leukemia cell line and expression can be detected in many T cell lymphomas but not generally in T cells from healthy individuals (*19, 88, 102, 164*). Given its unique expression on malignant T cells, EphA3 has strong potential to serve as a therapeutic target for $EphA3^+$ T cell lymphomas with minimal detrimental effects on healthy T cells. Indeed, an anti-EphA3 monoclonal antibody has already been the subject of a Phase I clinical trial in patients with refractory hematologic malignancies (*165*). In addition to its role in T cell lymphomas, EphA3 also plays a role in multiple myeloma angiogenesis (*166*) suggesting that an effective anti-EphA3 therapy could be potentially utilized for treatment of both T and B cell malignancies. Along with EphA3, expression of the receptors EphA2, EphB3, and EphB6 has also been identified in many malignant T lymphocytes (*101, 167*). The potential involvement of these receptors in promoting survival of malignant immune cells suggests that they may also hold promise as future therapeutic targets. However, Eph receptors may also be involved in lymphoma suppression as has been shown in the case of a soluble form of EphA7 (*168*) and for EphB4 (*169*). This indicates that great care must be taken in designing future anti-Eph therapies to ensure specificity towards targeting particular Eph receptors of interest that may contribute to malignancies while avoiding targeting those that may benefit the host anti-tumor immune response.

Paradoxically, both an increase and a decrease in Eph receptor expression has been associated with cancer progression consistent with the functional complexity of interactions between different Eph-ephrin family members. For the most part, the roles for Eph receptors in malignancies have been investigated from a cellular biology perspective. For example, Eph receptor forward signaling can inhibit cancer cell migration, proliferation, and survival as well as tumor growth in mice (*170*). Angiogenesis is essential for both tumor growth and metastasis and some evidence suggests that interactions between EphA2 and ephrin-A1 (*61, 160*) as well as EphB4 and ephrin-B2 (*61, 160*) on tumor cells and vascular cells can lead to increased angiogenesis and tumor vascularization. Several recent studies have aimed to alter or redirect T cells to target Eph receptors on cancerous cells using unique approaches including the generation of chimeric antigen receptor (CAR) T cells in which the T cell receptor recognizes EphA2 (*171-173*). A second approach which involves administering a bi-specific antibody that recognizes EphA10 expressed on breast cancer cells as well as CD3 expressed on T cells aims to redirect cytotoxic $CD8^+$ T cells to attack malignant $EphA2^+$ cells (*174*). However, these studies have not comprehensively addressed the potentially negative effects that Eph-ephrin expression on T cells may have on the target cells, which often will also express the same receptors and their ligands. While the contribution of Eph-ephrin expression on cancerous cells to disease progression has been thoroughly investigated, the crucial role of the immune response in the recognition and containment of malignant cells is often overlooked. Given the nearly ubiquitous expression of Eph receptors on immune cells, the function that these receptors play in cancer immunology must also be understood in order to rationally design Eph-based anti-cancer therapeutics that incorporate the contributions of Eph receptors to the immune control of cancers.

Atherosclerosis

Atherosclerosis is a condition characterized by the hardening and narrowing of the arteries which can impede blood flow and lead to heart attack and stroke. Damage to the vascular endothelium triggers the process of atherosclerosis, and activation of platelets by subendothelial matrix-derived molecules such as collagen and fibronectin triggers the adhesion of platelets onto the endothelium. This, in turn, initiates the formation of plaques that harbor immune cells such as monocytes and macrophages which have migrated to the plaque in response to chemotactic signals (*175*).

Platelets, anuclear cell fragments derived from megakaryocytes, are components of the immune system capable of exerting effects on both the innate and adaptive branches. Human platelets express several members of the Eph-ephrin family including EphA4, EphB1, EphB2 and ephrin-B1. Forward signaling through the EphB2 receptor on platelets is associated with both thrombus formation and platelet activation in the absence of ligand contact (*66*). This suggests an inherent role of the Eph cytoplasmic signaling domain in contributing to platelet function. The key contribution of EphB2 to platelet activation and optimal functioning is also supported by the association between mutations in the human *EphB2* gene and platelet dysfunction (*62*). Ligation of this family of molecules on platelets may contribute to granule secretion along with adhesive interactions between platelets. Subsequent platelet aggregation and thrombus formation can then follow mediated by $\alpha_{IIb}\beta_3$ integrin (*176-178*). Platelet granule release upon platelet activation is a highly inflammatory event. As such, Eph-mediated platelet activation is likely a key event mediating the immunopathogenic aspects of atherosclerosis.

In addition to platelets, other cells of the immune system can influence and enhance the inflammatory milieu of atherosclerotic plaques via Eph-ephrin interactions. Several studies have demonstrated a positive correlation between expression of EphB2, EphB4, ephrin-B1, and ephrin-B2 with the macrophage content of atherosclerotic plaques. These particular members of the Eph-ephrin family can contribute to the recruitment (*179*) and proinflammatory activation (*67*) of monocytes. Inflammation is likely further compounded by a suppression of localized chemotactic gradients by monocytes and/or macrophages leading to retention of these cells within lesions and augmentation of inflammatory responses (*180*). More work is needed to define precisely how Eph-ephrin interactions contribute to the pathogenesis of atherosclerosis. However, the abilities of these molecules to modulate the activation and chemotaxis of monocytes and macrophages, key events mediating plaque formation and growth, suggest a potential therapeutic avenue for this disease.

Fibrosis

Fibrosis describes the scarring of tissue that occurs through excess production of extracellular matrix proteins in an attempt to repair damaged tissue. While the causes of fibrosis can be highly varied, the general process is thought to result from chronic inflammation leading to the activation of myofibroblasts that produce molecules such as collagen and glycosaminoglycans in response to immune mediators such as transforming growth factor (TGF)-β (*181*). Recently, Eph receptors and their ligands have been implicated in the development of organ fibrosis. EphB2 has been identified as a pro-fibrogenic molecule that is essential for the development of liver fibrosis from both infectious and non-infectious etiologies (*72*). By mediating trafficking of ephrin-B-expressing macrophages to the liver, EphB2 can promote inflammatory signaling pathways that stimulate the differentiation of

hepatic stellate cells into fibrogenic myofibroblasts. In a separate model of lung fibrosis, cleavage of the ligand ephrin-B2 on fibroblasts by the disintegrin and metalloproteinase domain-containing protein ADAM10 leads to increased fibroblast activation and subsequently increased skin and lung fibrosis (*182*). It is anticipated that similar processes involving Eph-ephrin interactions may underlie other fibrotic conditions such as systemic scleroderma.

Diseases of the Central Nervous System

Eph-ephrin interactions play a key role in neurological development, and neurological disorders can stem from dysfunctional Eph-ephrin interactions. Upregulation of EphA4 expression has been consistently observed after traumatic brain injury in both primates (*183*) and humans (*184*). Similarly, EphA4, along with several other Eph receptors, appears to inhibit neuronal regrowth and recovery after spinal cord injury in mice (*185*).

Multiple sclerosis (MS) is a demyelinating disease in which the nerve cells of the brain become demyelinated and exposed rendering them unable to communicate efficiently. This leads to a variety of physical symptoms such as muscle weakness and poor coordination. It is the most common immune-mediated disease of the central nervous system (*186*) in which auto-reactive $CD4^+$ T cells play a central role in contributing to the induction of inflammation and lesion formation in the brain and spinal cord. Increased expression of ephrin-A1, EphA3, EphA4, and EphA7 has been observed in axons of multiple sclerosis lesions (*187*). Ephrin-B1 and ephrin-B2 were also shown recently to be involved in T cell migration to the central nervous system in both the mouse model of EAE and in human MS (*95*) which indicates the potential importance of these molecules in mediating this disease. However, there remains a significant

amount of knowledge to be gained before the full contribution of the Eph-ephrin molecules to MS can be fully understood.

Other diseases of the central nervous system that may involve Eph-ephrin interactions include Parkinson's disease (*188*) and Alzheimer's disease (*189*). Although studies thus far have only identified correlations between Eph expression and disease severity, the known roles for Ephs and ephrins in the immune system outlined in this review make these correlations worthy of further investigation.

Infectious diseases

Given the central role of the immune system in defense against infectious pathogens, there is a surprising lack of reports regarding the involvement of Eph receptors in this regard although this has become a greater focus of research in recent years. A clear role for Ephs as viral entry receptors has been shown for Nipah and Hendra viruses (ephrin-B2 and ephrin-B3) (*190, 191*), Kaposi's sarcoma-associated herpesvirus (EphA2) (*79, 192*), and Epstein-Barr virus (EphA4 and EphA2) (*83, 152, 153*). Similarly, it was also recently described that the sporozoite stage of the *Plasmodium* parasite, the causative agent of malaria, engages EphA2 on liver hepatocytes in order to establish a productive infection (*154, 193*) although additional entry receptors may be involved in this process as well (*194*). EphA2 is also used by the fungal pathogen *Cryptococcus neoformans* to traverse the blood-brain barrier in order to gain entry into the brain (*150*).

In addition to facilitating entry, it is likely that the ubiquitous expression of Eph receptors and ephrin ligands on the majority of cells in the immune system facilitates immune defense,

although reports in support of this idea are currently sparse. One of the challenges in the study of Eph-ephrin molecules is the redundancy that can occur with respect to binding of Eph receptors to multiple ephrin ligands. Although one study demonstrates no effect of B cell-specific ephrin-B1 ligand deficiency on GC formation, plasmablast production, or B cell class-switching in mice after infection with either influenza virus or acute lymphocytic choriomeningitis virus (LCMV Armstrong) (*84*), compensatory activities of other ephrin-B ligands may mask a potential role of the ephrin-B ligands in general. For example, a T cell-specific dual deletion of both ephrin-B1 and ephrin-B2 does in fact lead to a defective immune response against the LCMV virus (*127*). One additional study demonstrates that *Mycobacterium tuberculosis* can manipulate EphA2 and ephrin-A1 expression in order to support granuloma formation (*195*) which, in turn, aids in bacterial immune evasion. These reports suggest that these molecules do play a role in the activation and regulation of immune responses against pathogens further highlighting the importance of this consideration in future therapeutic designs.

$CD4^+$ and $CD8^+$ T cells contribute to protective immune responses in malaria

While the roles of various adaptive immune cells in malaria have been studied, many facets of malaria T cell immunology are still unknown. The role of the T-cell mediated immune response during malaria, in particular, is poorly understood. Mice deficient in $CD8^+$ T cells are defective in controlling blood-stage parasitemia suggesting an important contribution of $CD8^+$ T cells in the adaptive immune response involved in controlling parasitemia. In the absence of $CD8^+$ T cells, peripheral IFN-γ levels drop significantly (*196*). While studies have shown that $CD4^+$ and $CD8^+$ T cells are activated by blood-stage parasites and expand during acute infection, none have determined how low-affinity T cells contribute to the anti-*Plasmodium*

immune response. Blood-stage *Plasmodium* infection leads to robust $CD4^+$ and $CD8^+$ T cell activation with expansion of subsets resembling conventional effector and memory T cells (*197*). The requirement of $CD4^+$ T cells for the generation of protective anti-blood-stage immune effector mechanisms has been well-documented (*198-200*). $CD8^+$ T cells become activated during the liver-stage of the parasite life cycle (*201*), but the function of $CD8^+$ T cells against blood-stages of the *Plasmodium* parasite is unknown. In the absence of $CD8^+$ T cell activation, mice infected with *P. chabaudi* experience uncontrolled parasitemia and die 10-15 days post-infection (*202*). Transfer of $CD8^+$ T cells from mice infected with a different *Plasmodium* strain into mice lacking $CD8^+$ T cells partially protected from a lethal challenge infection (*203*). Further, β_2-microglobulin knockout mice lacking mature $CD8^+$ T cells experience significantly higher *P. chabaudi* AS parasitemia compared to C57BL/6J control mice indicating a role for $CD8^+$ T cells in controlling acute blood-stage infection *(unpublished)*. $CD8^+$ T cells that expand during malaria have been shown to be a major source of the pro-inflammatory cytokine IFN-γ that can control the blood stages of *Plasmodium* parasites (*196*) and may function to reduce blood-stage parasitemia. However, IFN-γ production from *Plasmodium*-reactive $CD8^+$ T cells has also been implicated in the development of acute pathology in the experimental cerebral malaria *P. berghei* ANKA model in part by their production of IFN-γ (*204, 205*). Defining the role of protective $CD8^+$ T cells during *Plasmodium* infection is essential for creating functional benchmarks of T cell responses that can be incorporated into future malaria vaccine candidates.

Brain leukocyte accumulation is essential for cerebral malaria development

It has been well established that $CD8^+$ T cells are required for the development of ECM (*138, 206*). However, the precise mechanisms for $CD8^+$ T cell retention in the brain at the onset of ECM allowing for subsequent BBB breakdown remain unclear. Intravital microscopy experiments clearly show $CD8^+$ T cells (*207*) and other leukocytes (*208*) accumulate and arrest in the brain microvasculature at the onset of ECM in *Pb*ANKA infection compared to non-lethal *Plasmodium* infections. Parasite sequestration has also been shown to be required for the development of ECM (*209*), and local antigen availability in the brain is also thought to be key in $CD8^+$ T cell retention in the brain (*210, 211*). Histology of human brain tissue from patients who succumbed to CM-associated fatality indicates the presence and accumulation of both platelets and leukocytes in the brain microvasculature throughout the cerebral cortex (*212, 213*) in regions where iRBCs have also sequestered. Additionally, while the role of CD8+ T cells in human CM has been widely debated (*214-216*), a recent study has demonstrated the presence of CD8+ T cells in brain sections from humans who died as a result of retinopathy-confirmed CM (*217*). In support of this phenomenon, similar observations have been made in a mouse model of cerebral malaria (*218*) (as described in detail below in the experimental techniques section) that mimics several key aspects of human CM and is known as experimental cerebral malaria (ECM). Development of ECM requires activation of $CD8^+$ splenic dendritic cells (*219, 220*), which leads to trafficking of *Plasmodium* antigen-reactive $CD8^+$ T cells to the brain (*221, 222*) at the onset of ECM symptoms. Brain endothelial cells can then cross-present parasite antigen, generally after phagocytosing free merozoites, to $CD8^+$ T cells in an interferon-gamma (IFN-γ) dependent manner (*223, 224*). Consequently, these activated, parasite-specific $CD8^+$ T cells can exert their effect through release of molecules such as perforin (*225*) and granzyme B (*209*) leading to endothelial apoptosis and presumably disruption of endothelial tight junction integrity (*207*) as well. Of note, mice

lacking $CD8^+$ T cells are protected from ECM (*206, 226*) indicating its essential role for the development of disease. However, the molecular interaction(s) mediating $CD8^+$ T cell adhesion to brain microvessels during ECM remains elusive. It was previously believed that ICAM-1 mediated this $CD8^+$ T cell-endothelial cell interaction, yet several groups have shown in recent years that endothelial cell expression of ICAM-1 is not required for the development of ECM (*227, 228*) although it is known to be involved in the sequestration of iRBCs to the brain endothelium in both humans (*229, 230*) and mice (*231*).

Blood-brain barrier breakdown is a hallmark of cerebral malaria

Cerebral malaria (CM) develops, in part, due to responses generated against sequestered *Plasmodium*-infected red blood cells (iRBCs) in the brain microvasculature resulting in a pro-inflammatory immune response, vascular occlusion, and subsequent decrease in microvascular blood flow (*232, 233*). *Plasmodium* parasites remodel the surface of iRBCs allowing for binding of parasite-derived surface proteins to receptors on the endothelium such as intercellular adhesion molecule-1 (ICAM-1) (*234*), CD36 (*235, 236*), and/or endothelial protein C receptor (EPCR) (*237*), providing a mechanism for sequestration of iRBCs from the peripheral circulation. Inflammation-mediated breakdown of the blood-brain barrier (BBB) due to the presence of sequestered parasites occurs and leads to hemorrhaging, vascular leakage, and death (*238-240*). The precise mechanisms that occur during CM leading to BBB breakdown have not been entirely elucidated, but data from mouse models suggests it partially involves apoptosis of endothelial cells induced by leukocytes, such as $CD8^+$ T cells (*223, 241*). However, it is likely that there are other $CD8^+$ T cell-induced mechanisms involving perforin and granzyme B that account for the disassembly of endothelial tight junctions and subsequent vascular leakage associated with ECM (*207*). Recent evidence in the field suggests that while

$CD8^+$ T cells can directly cause apoptosis in brain endothelial cells cross-presenting parasite peptides on MHC I (*223, 224*), a mechanism that has yet to be determined likely contributes more to disassembly of tight junctions between brain endothelial cells leading to vascular leakage and ECM development (*207*). The importance of EphA2 in the maintenance of endothelial cell junctions forming the BBB has been previously shown (*242, 243*). While the involvement of tyrosine kinases in the breakdown of the BBB has been shown previously (*240*), the kinase(s) responsible for this phenomenon is unknown. EphA2 kinase activity may be involved in this process. Nonetheless, further elucidation of the precise mechanisms and cellular interactions resulting in BBB breakdown during ECM is necessary.

EphA2 has been implicated in endothelial junction disruption

EphA2 has previously been shown to co-localize with tight junction proteins. Upon ephrin A1 ligand binding, the activation and phosphorylation of EphA2, but not other Eph receptors, has been shown to directly enhance breakdown of tight junctions in human brain microvascular endothelial cells (*243*). A similar role for EphA2 moderating tight junction permeability has been observed in the lungs (*244*) and various other cell types (*245*), supporting a potential role for EphA2 activation in the blood-brain barrier (BBB) breakdown and vascular permeability associated with ECM. Substantial mechanistic data exists supporting dichotomous functional consequences of Eph-ephrin interactions which suggests that EphA2 may be playing dual roles in cerebral malaria including mediating $CD8^+$ T cell adhesion to brain endothelial cells (adhesion) and contributing to blood-brain barrier breakdown (repulsion).

Platelets play an early role in cerebral malaria development

Unlike CD8+ T cells whose relevance to human CM has only recently been demonstrated, platelets have long been known to be modulated by and participate in the immune response to *Plasmodium* infection. Thrombocytopenia has been observed in both mice (*246, 247*) and humans (*248-250*) with severe malaria and may, in part, be due to suppressive effects that the *Plasmodium* parasite exerts on the process of hematopoiesis in the bone marrow. Along with being a correlate of severe malaria, there is also substantial evidence that platelets may be directly involved in enhancing severe malaria-associated organ pathology. For instance, platelets have been found in the lung and brain microvasculature in histological sections from patients who died of severe malaria (*251-254*) and could be serving to enhance *Plasmodium* sequestration given their abilities to interact directly with infected red blood cells (*255, 256*). While these findings only identify a correlation, additional studies suggest direct mechanisms by which platelets could contribute to increased inflammation and organ damage in severe malaria. In human CM, endothelial cell activation in the brain is a key feature of disease development. Platelets have been shown to have the capacity to release cytokines (*257*) and extracellular vesicles (*258, 259*) which contain bioactive components that can activate endothelial cells. Upon endothelial activation, platelet-released von Willebrand factor strings are transferred to the endothelium which enhances parasite sequestration (*260*). Additionally, they can mediate adhesion of immune cells to endothelial cells (*261, 262*) and the sequestration of immune cells in the vasculature of organs such as the lungs and brain has the potential to enhance organ pathology in CM.

In mice, while the requirement of CD8+ T cells has primarily been shown to be critical at the onset of ECM around days 5-6 post-infection with *Plasmodium*, the pathogenic role of platelets begins much earlier. Thrombocytopenia protects against ECM (*263*), and antibody-mediated

depletion of platelets one day post-infection with *Pb*A prevents death from ECM in mice while platelet depletion any later does not provide any protection from ECM-associated death (*264*). This suggests that an early function of platelets, either direct or indirect, sets the stage for the development of the immune-associated symptoms of ECM. Similar to what has been observed in humans, ultra large von Willebrand factor strings were also recently found to be deposited by platelets onto the brain endothelium during ECM, and mice deficient in von Willebrand factor are significantly protected against blood-brain barrier breakdown and experience a significantly delayed death from ECM (*265*). However, given that the reduced blood-brain barrier permeability and delayed onset of death were not absolute in *vWF-/-* mice and only provided partial protection compared to the effects of platelet depletion, it is likely that other platelet factors are critical to mediating disease.

Although there is clear evidence for a pathogenic role of platelets in ECM, there are several studies which suggest that platelets can mediate protection from *Plasmodium* infection, primarily through their ability to interact with and kill *Plasmodium*-infected red blood cells (*255, 266-268*). However, these studies present several issues. First of all, they primarily utilize non-severe mouse models of malaria which induce drastically different immune responses and pathology in comparison to severe mouse models of malaria. Second of all, much of the data relies on *in vitro* experiments in which physiological ratios of platelets to red blood cells are not utilized and other components of the immune system are not present. Therefore, the current evidence overwhelmingly supports a pathogenic, and not protective, role for platelets in the development of ECM although the mechanisms by which they influence the immune response remain to be discovered. Additionally, it is likely that the function of platelets in non-severe and severe malaria can be highly context dependent with different parasite strains eliciting

diverse responses from platelets (*269*). The identification of additional platelet components and mechanisms that are responsible for inducing organ damage and death during ECM would have great translational potential given the similar role of platelets in both mouse and human cerebral malaria.

Dissertation overview

There is overwhelming evidence to support the fact that both CD8+ T cells and platelets are involved in the immune response to *Plasmodium* infection. However, despite extensive research significant questions still remain regarding the mechanisms by which these cells may contribute to either infection control or immunopathology in the context of severe malaria. In the case of CD8+ T cells, while they are known to be required for the development of ECM in mice and have recently be correlated with human CM as well, the molecules involved in mediating CD8+ T cell retention in the brain microvasculature and subsequent blood-brain barrier breakdown remain unknown. In the case of platelets, there is a debate in the field as to whether platelets are protective by inhibiting parasite growth or pathogenic by exacerbating organ pathology through either direct or indirect mechanisms.

In this dissertation, we provide evidence that the receptor tyrosine kinase EphA2 is a key contributor to malaria-associated blood-brain barrier breakdown likely through its effects on inducing inflammation and disrupting brain endothelial junctions (Chapter II). In the absence of EphA2, pathogenic CD8+ T cells are unable to be recruited and retained in the brain which results in reduced brain immunopathology and enhanced survival. In addition to CD8+ T cells, we demonstrate that platelets also play a key pathogenic role in ECM development by identifying platelet α-granules as required for *Plasmodium*-induced lung and brain pathology

and death in mice (Chapter III). Finally, we summarize our collective findings, outline potential ways in which CD8+ T cells and platelets may be linked in the pathologic immune response to malaria, and discuss the relevance of this research beyond malaria and into other infectious and non-infectious diseases in which our work could help guide novel therapeutic intervention strategies in the future (Chapter IV).

CHAPTER II

EphA2 contributes to disruption of the blood-brain barrier in cerebral malaria

Chapter adapted from:

Darling TK, Mimche PN, Bray CF, Umaru B, Brady LM, Stone C, Eboumbou Moukoko CE, Lane TE, Ayong LS, and Lamb TJ (2019) EphA2 contributes to disruption of the blood-brain barrier in cerebral malaria. Revised and Resubmitted.

Figure attributions:

Figures 1 and 3-7 were contributed primarily by myself with data in each figure contributed by P. Mimche. Figures 2 and 8 as well as supplemental figures 1-2 were contributed by myself, supplemental figures 2 and 4 were contributed by P. Mimche, and supplemental figures 3 and 5 were contributed by both myself and P. Mimche. C. Bray and L. Brady contributed technical assistance. B. Umaru contributed to figure 4 and supplemental figure 4. C. Stone contributed to supplemental figure 2.

Abstract

Disruption of blood-brain barrier (BBB) function is a key feature of cerebral malaria. Increased barrier permeability occurs due to disassembly of tight and adherens junctions between endothelial cells, yet the mechanisms governing junction disassembly and vascular permeability during cerebral malaria remain poorly characterized. We found that EphA2 is a principal receptor tyrosine kinase mediating BBB breakdown during *Plasmodium* infection. Upregulated on brain microvascular endothelial cells in response to inflammatory cytokines, EphA2 is required for the loss of junction proteins on mouse and human brain microvascular endothelial cells. Furthermore, EphA2 is necessary for CD8+ T cell brain infiltration and subsequent BBB breakdown in a mouse model of cerebral malaria. Blocking EphA2 protects against BBB breakdown highlighting EphA2 as a potential therapeutic target for cerebral malaria.

Author Summary

Malaria is a disease caused by transmission of the mosquito-borne *Plasmodium* parasite that remains a severe global public health issue. Advancements in parasite control measures such as prevention, treatment, and surveillance have reduced the incidence of malaria worldwide. However, current reports indicate that progress towards reducing global malaria cases and deaths in recent years has stalled. Therefore, it is imperative that we continue to explore new therapeutic avenues that can synergize with existing treatment methods. In particular, there is currently no adjunctive treatment available for cerebral malaria which is a serious complication of *Plasmodium* infection characterized by blood-brain barrier breakdown. Here, we have identified that a receptor EphA2 is required for the breakdown of the blood-brain barrier during *Plasmodium* infection in mice. We found that expression of this receptor is critical for

inducing brain inflammation, recruiting immune cells to the brain, and disruption brain endothelial cell junctions. Inhibiting activation of this receptor using two different treatment approaches also prevented blood-brain barrier breakdown in mice. Thus, along with identifying a new molecule critical for cerebral malaria in mice we also provide a basis for exploring this receptor as a novel therapeutic target in human cerebral malaria in the future.

Introduction

Cerebral malaria (CM) is a severe manifestation of infection with the *Plasmodium falciparum* (*Pf*) parasite and has a 20% fatality rate (*270*). Presenting as a plethora of neurological symptoms that lead to coma, pediatric CM is a complex disease that has been shown to involve alterations to, and breakdown of, the blood-brain barrier (BBB) (*271-274*). This is thought to result from vascular activation in response to sequestration of *Plasmodium*-infected red blood cells (pRBCs) on the endothelium via adhesion molecules that include endothelial protein C receptor (EPCR) (*237*) and intercellular adhesion molecule 1 (ICAM-1) (*228, 275*). Infection of mice with *Plasmodium berghei* ANKA (*Pb*A) has been used to demonstrate the importance of inflammatory cytokines such as interferon-γ (IFN-γ) (*218*) and tumor necrosis factor-β, also known as lymphotoxin-α (LT-α) (*276*), in the development of experimental cerebral malaria (ECM), a disease that shares several key features with human CM (*277, 278*). Inflammation in ECM is T cell-mediated with CD8+ T cells playing a critical role in breakdown of the BBB (*205, 207, 279, 280*). However, apoptosis of brain endothelial cells does not appear to be sufficient to cause significant disruption of the barrier (*207, 240*). The molecular mechanisms underlying BBB breakdown during *Plasmodium* infection are poorly understood, but the

disruption of endothelial junctions is thought to be instrumental in this pathophysiological process.

Activation of receptor tyrosine kinases has been previously shown to play a role in endothelial junction disruption (*281*) and barrier integrity during ECM which can be maintained by global inhibition of the receptor tyrosine kinase family (*240*). However, therapeutic potential of this observation is limited by the simultaneous inhibition of receptor tyrosine kinases that are also involved in mounting an effective immune response (*282*) which could detrimentally affect control of *Plasmodium* infection. Identification of the major receptor tyrosine kinases necessary for junction disruption during CM is required to capitalize on strategies to specifically target receptor tyrosine kinases for therapeutic benefit.

Erythropoietin-producing hepatocellular (Eph) receptors constitute the largest family of receptor tyrosine kinases in humans and are ubiquitously expressed in nearly all tissues, including the brain (*283*) in both mice and humans. There are nine different functional EphA receptors in the mouse and human genome (EphA1-EphA9) that have the ability to interact with five membrane-bound Eph receptor interacting (ephrin) ligands (ephrin-A1-ephrin-A5) with varying affinities (*12*). The unique expression patterns of EphA receptors and ephrin-A ligands in different tissues and cell types allows for functional specificity, and EphA-ephrin-A binding between cells canonically leads to events such as cellular migration, adhesion, and changes in cellular morphology (*15*). As the interaction between EphA receptors and membrane-bound ephrin-A ligands is of high-affinity, this initial binding event will often lead to strong adhesion between the two cells involved. This can progress to either extended adhesion or repulsion and separation of the two cell surfaces once signaling pathways are

propagated depending on the context (*12*). As a prime example of these multifunctional receptors, one particular EphA family member, EphA2, can be utilized by CD8+ T cells for chemotaxis (*139*) and adhesion (*98*). Additionally, EphA2 has also been previously shown to be instrumental in the disassembly of both tight and adherens junction protein complexes on endothelial cells reducing cell-cell contact (*243, 284*). Given that EphA receptors play a role in regulating both brain endothelial junction formation and immune cell migration and adhesion, processes highly relevant to the development of CM, here we have investigated the role of EphA receptors in malaria-associated BBB breakdown. We found that EphA2 is upregulated on both human and mouse primary brain microvascular endothelial cells in response to tumor necrosis factor family cytokines. In mice, EphA2 is upregulated by LT-α, a cytokine required for BBB breakdown in *Pb*A infection (*276, 285*). EphA2 deficient mice exhibit significantly improved survival in comparison to EphA2 sufficient mice, likely as a result of reduced CD8+ T cell brain infiltration and inflammation along with maintenance of brain microvascular endothelial cell junctions. Collectively, this results in enhanced BBB integrity. Interestingly, brain EphA2 upregulation is a unique feature of infection with the ECM-causing *Pb*A strain and does not occur upon infection with strains that do not cause ECM. This suggests EphA2 upregulation on brain microvascular endothelial cells is critical for *Plasmodium*-associated cerebral pathology. Blocking the interaction between EphA2 and its cognate ephrin-A ligands increases the integrity of the BBB during ECM which demonstrates a rationale for exploring EphA2 antagonism as a novel therapeutic strategy for maintaining BBB integrity during CM.

Results

EphA2 is required for blood-brain barrier breakdown and the development of ECM

Given the known roles of EphA receptors in mediating cellular interactions in the brain, we first determined if members of the EphA family of receptors were modulated at the onset of ECM. A comparison of the transcriptional profile of the EphA receptor subfamily in whole brain tissue isolated from mice infected with *Pb*A revealed a significant upregulation of *EphA2* transcript at day 6 post-infection (**Fig 1A**) at the onset of ECM symptoms along with a slight upregulation of *EphA1* transcript. In the absence of EphA2, *Pb*A-infected mice maintained an intact BBB (**Fig 1B**) at the onset of ECM in comparison to EphA2 sufficient mice. However, there was no significant difference in the parasite burden in *EphA2-/-* and *EphA2+/+* mice when assessing the levels of parasites by *Pb*A luciferase expression in the brain (**Fig 1C, left, and Fig S1A**), parasite mRNA in the brain (**Fig 1C, right**), or peripheral parasitemia (**Fig 1D, top**). However, *EphA2-/-* mice did have significantly less *Pb*A accumulation in the spleen and liver compared to *EphA2+/+* control mice (**Fig S1B**). The maintained BBB integrity observed in *Pb*A-infected *EphA2-/-* mice translated into significantly improved survival compared to *EphA2+/+* control mice (**Fig 1D, bottom**). Maintenance of BBB integrity and improved survival were also associated with a failure of CD8+ T cells, including *Plasmodium*-reactive GAP50+CD8+ T cells (*223*), to accumulate in the cerebral microvasculature (**Fig 1E**). No compensatory transcriptional upregulation of other EphA receptors occurred in the brains of *EphA2-/-* mice infected with *Pb*A **(Fig 1F)** indicating that the upregulation of EphA2 in *Plasmodium* infection is independently regulated from other EphA receptors. Using the previously identified CD8+ T cell *Plasmodium*-reactive tetramers GAP50 and F4 (*223, 286, 287*) and analyzing IFN-γ and Granzyme B which are essential molecules for ECM development (*205, 279*), we found that the absence of CD8+ T cells observed in the brains of *EphA2-/-* mice was not due to a defect in the splenic expansion or egress of highly functional *Plasmodium*-reactive CD8+ T cells (**Fig 2A-C**) but rather on a failure of CD8+ T cells to

accumulate in the brain microvasculature in the absence of EphA2. *EphA2-/-* mice had significantly higher numbers of circulating *Plasmodium*-reactive CD8+ T cells in their bloodstream (**Fig 2A**) demonstrating that mice are able to mount a robust CD8+ T cell response against the parasite in the absence of EphA2.

EphA2 **is upregulated in human and mouse primary brain endothelial cells in response to inflammatory cytokines**

EphA2 expression on endothelial cells has previously been associated with impairment of junction formation (*243*). Since the majority of pRBCs (*207*) and CD8+ T cells (*288*) are known to adhere to the brain microvascular endothelium on the luminal surface of blood vessels during ECM, we sought to determine the impact of *Pb*A infection specifically on endothelial-expressed EphA2. We confirmed that EphA2 is upregulated at the protein level in brains of *Pb*A-infected wild-type mice and colocalizes primarily with the brain vasculature (**Fig S2**). To determine if the pRBCs or inflammatory cytokines were responsible for this observed upregulation of EphA2 on brain endothelial cells, we isolated both human primary brain microvascular endothelial cells (HBMECs) and mouse primary brain microvascular endothelial cells (MBMECs) as confirmed by staining for the endothelial-specific markers von Willebrand factor (VWF) **(Fig 3A, left)** and CD31 **(Fig 3A, right)** and the formation of cell-cell contacts by transmission electron microscopy **(Fig 3B)**. We cultured the cell monolayers with their respective parasites (*Pf* pRBCs with HBMECs and *Pb*A pRBCs with MBMECs) along with the inflammatory cytokines tumor necrosis factor-alpha (TNF-α) and LT-α which are known to be produced in the brain during *Plasmodium* infections. *EphA2* expression was significantly increased in HBMECs pulsed with TNF-α (**Fig 3C**). The addition of *Plasmodium falciparum*-infected red blood cells (*Pf* pRBC) had no synergistic effect which supports previous

studies showing upregulation of *EphA2* in human microvascular endothelial cells and monocytes by TNF-α (*73, 289*). On the other hand, MBMECs upregulated *EphA2* primarily in response to LT-α (**Fig 3D-E**). This result is biologically significant because production of TNF-β/LT-α by non-hematopoietic cells in *Pb*A infection is required for ECM development (*276*). The *Pb*A-associated upregulation of *EphA2* mRNA appeared specific to the brain tissue as transcript levels remained essentially unchanged in liver and lung tissues (**Fig S3A-B**). Furthermore, *Plasmodium*-reactive CD8+ T cell accumulation in pulmonary tissue was identical in the presence or absence of EphA2 (**Fig S3C-D**). This brain-specific *EphA2* upregulation likely results from the fact that *LT-a* is only upregulated in the brain during ECM with little to no increase in *LT-a* mRNA levels in the liver, lung, or spleen at day 6 post-infection with *Pb*A **(Fig 3F)**. In agreement with these observations, *EphA2* transcript was not upregulated in the brains of LT-α deficient and tumor necrosis factor receptor 2 (TNFR2) deficient mice infected with *Pb*A in contrast with wild-type mice (**Fig 3G**). Additionally, treatment of *Pb*A-infected C57BL/6J mice with an anti-TNFR2 blocking antibody resulted in significantly reduced mRNA levels of both *LT-α* and *EphA2* in the brain in comparison to isotype control treated mice **(Fig 3H)**. These data provide further support for the role of LT-α in inducing *EphA2* upregulation in the brains of mice at the onset of ECM.

Ephrin-A ligands are upregulated during *Plasmodium* infection

Ephrin-A ligands are the cognate ligands for Eph receptors and are expressed on a variety of tissues and cell types. Upon binding to Eph receptors, they can be cleaved by matrix metalloproteinases (MMPs) and a disintegrin and metalloproteinase domain-containing (ADAMs) proteins, a family of zinc proteases (*290-293*). This occurs particularly in

inflammatory environments (*294, 295*) resulting in the release of soluble ligand fragments into the bloodstream. As cell membrane-bound ephrin dimer complexes are thought to be a requirement to induce Eph receptor downstream signaling (*296, 297*), soluble ephrin ligands are not generally believed to activate Eph receptors although there is some evidence that this can occur (*298*). As each Eph receptor, including EphA2, can promiscuously bind to several ephrin ligands (ephrin-A1-5) with varying affinities, we focused on the main high affinity ligand for EphA2, ephrin-A1, along with a secondary ligand for EphA2, ephrin-A5 (*47, 299, 300*). Like EphA2, ephrin-A1 ligand expression is known to be induced by TNF family members (*301-303*). Therefore, we analyzed expression of *ephrin-A1* in HBMECs and MBMECs upon incubation with pRBCs, TNF-α, or LT-α alone or in varying combinations. We found that TNF-α was the primary driver of *ephrin-A1* transcription in both HBMECs and MBMECs with pRBCs having no apparent effect (**Fig 4A-B**). However, *P. falciparum* did significantly upregulate *ephrin-A1* ligand and *ephrin-A5* ligand expression on peripheral blood mononuclear cells (PBMCs) isolated from healthy individuals not previously exposed to malaria in a dose-dependent manner *in vitro* (**Fig S4A-B**). Cells upregulating these ephrin ligands included, but were not limited to, CD3+ T cells (**Fig S4C-D**). Transcription of *ephrin-A1* and *ephrin-A5* ligands was also modulated in splenic T cells isolated from *Pb*A-infected mice at day 5 post-infection prior to their egress from the spleen (**Fig S4E**).

Given this significant induction of *ephrin-A1* transcript in both mouse and human brain endothelial cells and leukocytes, we next tested whether soluble ephrin-A ligands are released into the bloodstream during *Plasmodium* infection. We detected soluble ephrin-A1 ligand in the plasma of *P. falciparum*-infected pediatric patients, where those patients experiencing neurological manifestations had a significantly higher concentration of soluble ephrin-A1

ligand compared to uninfected patients ($F_{2,149}$=3.61; P=0.029) when patient age and parasite burden were taken into consideration (Uninfected = 54.1±6.6 months with 0±0 parasites/μL blood; Uncomplicated = 72.3±6.5 months with 83,034±17,019 parasites/μL blood; Neurological = 46.1±6.0 months with 142,598±23,138 parasites/μL blood) (**Fig 4C**). Unlike ephrin-A1 ligand, there was no correlation between the presence of soluble EphA2 receptor in the plasma and neurological symptoms in the same cohort of pediatric patients ($F_{2,149}$=1.6; P=0.206) (**Fig S4F**). Soluble ephrin-A1 ligands were also detected in the plasma of C57BL/6J mice infected with *Plasmodium* (**Fig 4D**) at significantly higher levels than naïve mice. However, ephrin-A1 ligand was also highly prevalent in plasma of mice infected with a parasite strain related to *Pb*A, *Plasmodium berghei* NK65 (*Pb*NK65), which does not cause ECM but causes inflammation and pathology in other organs, particularly the lungs (*304*). This data indicates that general inflammation is likely leading to increased levels of soluble ephrin-A1 ligand and that this phenomenon is not limited to neurological disease.

As the shedding of ephrin-A ligands is believed to occur subsequent to binding EphA receptors, we investigated if *EphA2*-/- MBMECs had a defect in the release of soluble ephrin-A1 ligand. We found that ephrin-A1 ligand was shed by *EphA2*+/+ MBMECs primarily in response to TNF-α (**Fig 4E**). On the contrary, *EphA2*-/- MBMECs released little to no ephrin-A1 ligand suggesting that the presence of EphA2 on brain endothelial cells can mediate ephrin-A1 cleavage and release. This could potentially occur through interactions with ADAMs and MMPs which are modulated during *Plasmodium* infection **(Fig S5A-B)** and can cleave ephrin-A1 ligands (*143, 290-293, 305*). However, there was no significant difference in levels of plasma ephrin-A1 ligand between *Pb*A-infected *EphA2*-/- and *EphA2*+/+ mice (**Fig 4F**). This indicates that ephrin-A1 ligands can be shed in an EphA2-independent manner from

other organ sites and cell types during infection, likely through interactions with other EphA receptors that ephrin-A1 is able to bind. Collectively, this data suggests that although ephrin-A ligand upregulation and shedding are induced during the inflammatory immune response to malaria, the modulation and expression of the membrane-bound receptor, EphA2, is likely more of a critical factor influencing susceptibility to ECM.

EphA2 expression in the brain is a hallmark of pathogenesis in ECM

CD8+ T cell accumulation in the brain is necessary (*226*) but not sufficient (*223*) for the development of ECM. Previous studies have attributed CD8+ T cell participation in ECM in the brain microvasculature as dependent on MHC-I cross-presentation of malaria peptides, a phenomenon driven by IFN-γ. In addition to pMHC-I/TCR interactions, we hypothesized that a signal provided by EphA2 ligation is required to mediate BBB disruption.

In support of this hypothesis, upregulation of *EphA2* was not observed in brains of C57BL/6J mice infected with *Pb*NK65 or another *Plasmodium* strain, *Plasmodium chabaudi* AS (*Pc*AS), neither of which causes ECM (**Fig 5A, left**). Significant upregulation only occurs in the brains of mice infected with the ECM-causing strain *Pb*A **(Fig 1A)**. We found no upregulation of ephrin-A1 ligand in the brains of mice infected with either *Pb*A or *Pb*NK65 **(Fig 5A, right)** suggesting that this is not a factor required for the development of ECM. *Pb*NK65 infection of C57BL/6J mice led to equivalent levels of *Plasmodium* transcript **(Fig 5B)** and accumulation of *Plasmodium*-reactive CD8+ T cells in the brain at day 6 post-infection to those measured in *Pb*A infection (**Fig 5C**) consistent with previous reports (*207, 223, 286*). CD8+ T cells found in the brains of *Pb*NK65-infected mice expressed similar levels of surface EphA2 (**Fig 5D**) and ephrin-A1 ligand (**Fig 5E**) to those that accumulated in brains of *Pb*A-infected C57BL/6J

mice at the onset of ECM. However, unlike *Pb*A-induced CD8+ T cell accumulation in the brain which we found was dependent on EphA2 (**Fig 1E**), *Plasmodium*-reactive CD8+ T cells were found at equal numbers in the brains of *Pb*NK65-infected *EphA2*-/- mice compared to *EphA2*+/+ control mice (**Fig 5F**). This is likely due to the fact that levels of chemokines responsible for CD8+ T cell recruitment to the brain are present at equivalent levels in the brains of *Pb*NK65-infected *EphA2*+/+ and *EphA2*-/- mice **(Fig 5G)** suggesting that CD8+ T cells are recruited to the brain independently of EphA2 in this non-ECM malaria model.

There are considerable challenges in obtaining brain sections from children who have died from CM as well as control brain sections precluding confirmation that endothelial-expressed EphA2 is the main correlate of BBB breakdown in CM. However, these data from mouse models of *Plasmodium* infection suggest that EphA2 expression on endothelial cells, which is mediated by the interactions of sequestered pRBCs with MBMECs, is a critical mediator of ECM pathogenesis. While expression of *ephrin-A1* ligand in whole brains **(Fig 5A)** and CD8+ T cells **(Fig 5C)** along with soluble ephrin-A1 ligand in the plasma **(Fig 4D)** are similar in *Pb*A and *Pb*NK65 infections, the differential requirement of EphA2 for CD8+ T cell accumulation in the brain in these two mouse models of malaria suggests that the unique and significant difference in brain EphA2 expression may be a contributing factor to the different neurological damage that occurs in these two *Plasmodium* models.

EphA2 deficiency leads to a reduced neuroinflammatory response to *Pb*A

To determine why CD8+ T cells did not accumulate in the brains of *Pb*A-infected *EphA2*-/- mice despite their abundance in the bloodstream, we examined if there was a defect in the inflammatory response in *EphA2*-/- mice compared to *EphA2*+/+ littermate control mice.

Transcription of inflammatory cytokines associated with *Pb*A pathogenesis was significantly reduced in brains of *EphA2-/-* mice compared to littermate control mice (**Fig 6A**). In contrast to what was observed in the brains of *Pb*NK65-infected *EphA2-/-* mice **(Fig 5G)**, *Pb*A-infected *EphA2-/-* mice exhibited a significant reduction in the mRNA levels of key chemokines responsible for CD8+ T cell recruitment to the brain during ECM (**Fig 6B**). This suggests that *Plasmodium*-reactive CD8+ T cells do not accumulate in the brain microvasculature of *EphA2-/-* mice because the chemokine signals required for their recruitment to the brain are not present at sufficient levels.

Plasmodium-infected RBCs are able to induce a potent inflammatory response in endothelial cells *in vitro*(*306*). This includes inducing the production of C-X-C motif chemokine 10 (CXCL10/IP-10)(*307, 308*), C-C motif chemokine ligand 2 (CCL2/MCP1)(*309*), and C-C motif chemokine ligand 5 (CCL5/RANTES)(*310*) which are essential for drawing leukocytes into brain capillaries where pRBCs have adhered to the endothelium. Since EphA2 has been implicated in activation of the NF-κB pathway(*311*), a critical signaling cascade that mediates inflammation, we investigated if *EphA2-/-* derived MBMECs had reduced NF-κB signaling and inflammatory responses. Stimulation of *EphA2+/+* MBMECs with *Pb*A pRBCs induced phosphorylation of NFκB p65 and IKKα/β, but this effect was abolished in the absence of EphA2 (**Fig 6C**). The reduced phosphorylation of these members of the NF-κB signaling pathway was associated with significantly reduced TNF-α secretion from *EphA2-/-* MBMECs (**Fig 6D**) as well as a clear reduction in transcript levels **(Fig 6E)** and secreted protein **(Fig 6F)** of CXCL10, CCL2 and RANTES in MBMECs stimulated with *Pb*A pRBCs. Together, the reduced cytokine and chemokine production from brain endothelial cells in the absence

of EphA2 explain the lack of CD8+ T cells found in the brains of *EphA2*-/- mice during *Pb*A infection and the resulting improvement in survival.

EphA2 contributes to destabilization of tight and adherens junctions

Since EphA2 was found to be involved in CD8+ T cell retention in the brain during ECM along with BBB breakdown, we next examined the mechanism by which EphA2 could be contributing to BBB destabilization. In comparison to *EphA2*-/- mice, *EphA2*+/+ littermate control mice infected with *Pb*A had significantly reduced transcription of several tight junction proteins (**Fig 7A**) but not the adherens junction protein vascular endothelial cadherin (VE-cadherin). This suggests that the maintenance of an intact BBB in *EphA2*-/- mice was the result of preserved tight junction protein expression. A link between EphA2 activation and dysregulation of adherens and tight junctions in the BBB has been previously shown in other homeostatic and disease contexts (*284, 312, 313*). Additional immunofluorescence analyses of MBMECs isolated from *EphA2*-/- and *EphA2*+/+ mice and stimulated with ephrin-A1 ligand along with the inflammatory cytokine LT-α revealed significantly reduced expression of both adherens junction **(Fig 7B)** and tight junction **(Fig 7C)** proteins in EphA2 sufficient endothelial cells upon stimulation. On the contrary, expression of these junction proteins was fully maintained in stimulated *EphA2*-/- MBMECs. Using a transwell system we found that in the absence of EphA2, baseline MBMEC barrier integrity appeared more robust than in the presence of EphA2 (**Fig 7D, left**) presumably as a result of enhanced adherens and tight junction protein expression. Activation of EphA2 on MBMECs with ephrin-A1 ligand resulted in the disruption of endothelial barrier integrity (**Fig 7D, right**) with a trend towards decreased permeability in *EphA2*-/- MBMEC cultures. The permeability observed in *EphA2*-/- cultures stimulated with ephrin-A1 ligand could be due to the expression of several other

EphA receptors in the brains of *EphA2-/-* mice **(Fig 1F)** that have the potential to bind ephrin-A1 ligand with lower affinity. A similar phenomenon was also observed in HBMECs stimulated with human TNF-α and ephrin-A1 ligand which showed a significant reduction of VE-cadherin expression upon stimulation with both TNF-α and ephrin-A1 ligand (**Fig 7E)**. It is possible that activation of EphA2 upon ephrin-A1 binding leads to either internalization and recycling of junction proteins or EphA2-induced ADAM- and MMP-mediated shedding of junction proteins **(Fig 4D and Fig S5A-B**). However, plasma levels of the adherens junction proteins VE-cadherin and epithelial cadherin (E-cadherin) are equivalent or lower in *Pb*A-infected mice compared to naïve mice **(Fig S5C)**. These findings favor the hypothesis that destabilization of junctions occurs through protein internalization either as a direct or indirect (e.g. via suppression of RhoA (*284*)) result of EphA2 signaling.

Blocking of the EphA2/ephrin-A ligand pathway confers protection against BBB breakdown

Having shown a pivotal role for EphA2 in mediating BBB disruption during ECM, we assessed whether EphA2 could serve as a novel therapeutic target in an adjunctive therapy for ECM. Treatment of *Pb*A-infected C57BL/6J mice beginning at day 4 post-infection with the receptor tyrosine kinase inhibitor Nilotinib, which has been shown to inhibit multiple receptor tyrosine kinases including EphA2 (*314*) and can cross the BBB unlike related compounds (*315, 316*), significantly prevented BBB breakdown in comparison to vehicle control treated mice with no effect on peripheral parasitemia **(Fig 7F)**. Given that Nilotinib is not an EphA2-specific inhibitor, we next utilized a strategy aimed at preventing activation of EphA2 through interfering with ephrin-A ligand binding. We treated mice beginning at day 4 post-infection with a recombinant EphA2-Fc protein which has the potential to act as a decoy receptor

through binding soluble and cell-bound ephrin-A ligands and preventing their binding to cell-bound EphA2. This treatment also resulted in significantly improved BBB integrity during *Pb*A infection compared to vehicle control treated mice (**Fig 7G)**. These results are notable given that the treatments were only administered beginning at day 4 post-infection, rather than prophylactically, and were still able to prevent the typical onset of BBB breakdown at day 6 post-infection. While neither of these strategies is entirely specific to inhibiting or blocking EphA2 as Nilotinib can act on other receptor tyrosine kinases and recombinant EphA2-Fc treatment will also prevent ephrin ligands from binding to other EphA receptors, these data demonstrate that blocking EphA2 signaling or interaction with its cognate ephrin ligands is a feasible strategy for preventing BBB breakdown during malaria. Given the involvement of Eph receptors and EphA2 in particular in other highly prevalent diseases including several cancers, more targeted therapeutics aimed at blocking binding to and inhibiting activation of EphA2 in a highly specific manner are being developed (*148, 317, 318*). These are avenues that should also be investigated further in the context of ECM adjunctive therapy.

Discussion

Here we demonstrate that EphA2 is a molecule that mediates BBB breakdown during ECM. Although we have previously shown a critical role for the related Eph receptor, EphB2, in the development of malaria-associated liver fibrosis (*72*), this study constitutes the first time that any member of this family of Eph receptors has been linked to neurological manifestations of malaria. A critical role for CD8+ T cells in increasing vascular permeability of the BBB in ECM has been repeatedly shown using the *Pb*A mouse model. However, the hypothesis that this occurs predominantly via induction of apoptosis in peptide-MHC I-expressing endothelial cells has little support given the distinct absence of any significant apoptosis in the brain during

ECM (*207, 240, 288, 319*). Contrary to a pro-apoptotic role for CD8+ T cells and their lytic proteins, our hypotheses that EphA2 upregulation during *Pb*A infection contributes to adherens and tight junction protein dysfunction resulting in increased BBB permeability and that ECM development involves the interaction between EphA2 and CD8+ T cells **(Fig 8)** are consistent with the results of this study.

Indeed, EphA2 has been shown in a variety of contexts to coordinate with and regulate various junction proteins. Through interactions with cadherins (*320*), EphA2 upregulation and activation appears to destabilize cell-cell contacts (*284*). Similarly in the case of tight junction proteins, EphA2 plays a role in the dissolution of tight junctions between endothelial cells which can be prevented through EphA2 inactivation or silencing (*243, 321, 322*). It is not clear whether brain endothelial cells lacking EphA2 have higher cellular expression of junction proteins or if *EphA2*-/- mice have a greater density of endothelial cells in the brain. However, our data demonstrates that these EphA2 deficient endothelial cells maintain robust expression of numerous components of tight and adherens junctions which results in a preserved BBB and enhanced survival at a time when *EphA2*+/+ mice experience rapid BBB permeability and death. While our data support a critical role for EphA2 expression on brain endothelial cells in mediating BBB breakdown and ECM development, EphA2 is also expressed on CD31 negative cell types known to contribute to BBB maintenance, including pericytes, astrocytes, and neurons (*313, 323-326*). As such, future studies should aim to determine the contribution of EphA2 expression on other cellular components of the neurovascular unit to *Plasmodium*-induced BBB junction dysfunction as data on the contribution of these cell types to ECM development is currently very limited (*327, 328*).

Of particular interest to us are the key differences we observed in EphA2 involvement between *Pb*A infection, which causes ECM, and *Pb*NK65 infection, which does not cause BBB breakdown or cerebral pathology (*329, 330*). While these strains are highly conserved, there is not a clear understanding of why infection with *Pb*A, but not *Pb*NK65, leads to ECM development although there is evidence suggesting the existence of differential responses of endothelial cells to the parasites (*223*). Given that CD8+ T cells found in the brains of mice infected with *Pb*A and *Pb*NK65 appear to be comparable in terms of their activation status and expression of effector molecules (*207*), it seems likely that the stark differences in cerebral pathogenesis observed between these two models involve their differential effects on the brain microvasculature. Our finding that EphA2 is uniquely upregulated in brains of mice infected with *Pb*A and not *Pb*NK65 or another non-ECM causing strain (*Pc*AS) highlights EphA2 expression in the brain as a critical correlate of BBB breakdown. Although ephrin-A1 ligand is upregulated on CD8+ T cells and released into the circulation during both *Pb*A and *Pb*NK65 infections, this occurred to the same extent in both infections. Further, the lack of ephrin-A1 ligand upregulation in the brain in both models points to the importance of brain EphA2, not ephrin-A1, in inducing BBB breakdown and ECM development.

Therapeutic options for CM are currently limited to anti-parasitic drugs and supportive care. Our observation that children suffering from neurological manifestations of *P. falciparum* infection have elevated levels of ephrin-A1 ligand in the bloodstream demonstrates clinical relevance of our findings. Future studies will aim to determine if EphA2 modulation is present in brains of individuals who succumb to CM as data from our mouse model suggests that this would likely be the primary manner by which Eph receptors could contribute to the BBB dysfunction that has been identified in patients with CM (*271-274*). CD8+ T cells along with

other cells known to express ephrin ligands including platelets (*63*) and leukocytes (*73*) have been found in post-mortem brain histology sections of humans who died of CM (*217, 251, 254, 331, 332*). Given the known expression of EphA2 in human brain tissue (*59*) and mounting evidence that endothelial-expressed EphA2 is involved in brain endothelial junction disruption (*243, 313*), it is quite possible that interactions between EphA2 upregulated on human brain endothelial cells and ephrin-A ligands on other hematopoietic or non-hematopoietic cells could contribute to CM-associated BBB disruption in humans. Although more studies will be needed to elucidate the possible involvement of EphA2 in human CM as well as to determine the optimal method for EphA2 blocking/inactivation, a therapeutic strategy aimed at preventing EphA2-associated junction dysregulation at the BBB could have translational potential.

EphA2 has also recently been shown to serve as a hepatocyte entry receptor for *Plasmodium* sporozoites (*154*). While the necessity of this function is not entirely known (*194*), it further supports the involvement of the EphA2 receptor in *Plasmodium* pathogenesis. Along with the data presented in this study, it suggests that an approach aimed at blocking/inactivating EphA2 could have significant implications for targeting both liver-stage and blood-stage infections. Therapeutic strategies targeting Eph receptors and their ephrin ligands, such as development of antagonistic blocking peptides, are continuously being developed for a number of highly prevalent diseases (*333*). Given the growing appreciation for the involvement of Eph receptors, including EphA2, in a variety of infectious diseases (*150, 152, 192, 334*), a better understanding of the optimal strategies for specifically inhibiting a particular Eph receptor while minimizing off-target effects would have broad implications for a number of infectious and non-infectious diseases.

Abbreviations

ADAM: A disintegrin and metalloproteinase domain-containing protein

BBB: Blood-brain barrier

CM: Cerebral malaria

ECM: Experimental cerebral malaria

Eph: Erythropoietin-producing hepatocellular receptors

Ephrin: Eph receptor interacting ligands

F4: Replication protein A1, epitope 199-206

GAP50: Glideosome-associated protein 50, epitope 40-48

HBMEC: Human primary brain microvascular endothelial cells

LT-α: Lymphotoxin-alpha

MMP: Matrix metalloproteinase

MBMEC: Mouse primary brain microvascular endothelial cells

*Pb*A: *Plasmodium berghei* ANKA, a rodent *Plasmodium* parasite strain

*Pb*NK65: *Plasmodium berghei* NK65, a rodent *Plasmodium* parasite strain

*Pc*AS: *Plasmodium chabaudi* AS, a rodent *Plasmodium* parasite strain

Pf: *Plasmodium falciparum*, a human *Plasmodium* parasite strain

pRBCs: *Plasmodium*-infected red blood cells

TNFR2: Tumor necrosis factor receptor 2

VE-cadherin: Vascular endothelial cadherin

Materials and Methods

Ethics statement

Blood from healthy controls was obtained from volunteers at Emory University under approval from the Emory University Institutional Review Board (Protocol number 00045690). Ethical approval for the study in Cameroon was obtained from the Emory University (Protocol number 00076693) and University of Utah (Protocol Number 00098806) Institutional Review Boards and from the Cameroon National Ethics Committee (Protocol number 2015/08/622/CE/CNERSH/SP). Administrative authorization of the study was obtained from the Cameroon Ministry of Public Health (Number 6310716). Written informed consents were obtained from the parents or legal guardians of all participants.

Study population

This study was a cross-sectional study involving 175 children between the ages of 6 months and 17 years of age who presented at the Emergency Units or Outpatient departments of 3 district hospitals (Obala, Efoulan, Nkoleton) and 1 pediatrics reference hospital (Chantal Biya Foundation Hospital) in the Central Region of Cameroon between 2015-2017. The region has continuous transmission of *Plasmodium* peaking between March-May and August-October. The majority of infection (>96%) is caused by *Plasmodium falciparum*. Exclusion criteria included evidence or history of meningitis or encephalitis or a history of developmental delay or other neurological conditions. Individuals were initially tested for *Plasmodium* infection using *Plasmodium falciparum* histidine rich protein II (*Pf*HRPII) and pan-*Plasmodium* species-based rapid diagnostic tests (SD Bioline, S. Korea) followed by examination of thick and thin blood smears to confirm the presence of *Plasmodium*-infected red blood cells. Neurological complications were defined as patients admitted with altered mental status, convulsions, prostration or coma and with visible *Plasmodium*-pRBCs on thick blood smears. Uncomplicated malaria was defined as presence of fever, or history of fever in the last 48

hours with visible *Plasmodium*-pRBCs on thick blood smears with no other signs of severe malaria such as severe malarial anemia (ie. hemoglobin <5g/dL), acidotic breathing or loss of consciousness. Subjects with no visible parasites on thick smears and negative for *Plasmodium* infection by rapid diagnostic test were considered as uninfected endemic controls. All children received the standard clinical care as outpatients or inpatients as applicable. Venipuncture was performed into citrate saline tubes (Vacutainer CPT, BD Biosciences, San Jose, California) and blood samples were refrigerated and transported to the lab and processed within 24 hours. Plasma was frozen at -80^{0}C until used.

Rodent *Plasmodium* infection

Female C57BL/6J wild type (WT) mice aged 6-12 weeks were bred in-house or purchased from The Jackson Laboratory (Jax stock #000664) (Bar Harbor, ME, USA). *EphA2*-/- whole-body knockout mice on a mixed background (The Jackson Laboratory; JAX stock #006028) were re-derived and bred in-house under a heterozygous breeding system. *TNFRp75*-/- whole-body knockout mice (JAX stock #002620) and *LT-α*-/- whole-body knockout mice (JAX stock #002258) were obtained and used directly for experiments. All mice were given water and food (LabDiet, MO, USA: chow 5001) *ad libitum* and housed under standard conditions. Infections were initiated intraperitoneally with 0.5-1x10^6 *Pb*A pRBCs (clone15cy1 or reporter line1037cl WT-GFP-Luc^{schiz} mutant RMgm-32 (*335*)), 0.5-1x10^6 *Pb*NK65 pRBCs (New York Clone), or 1x10^5 *Pc*AS pRBCs obtained from donor C57BL/6J mice. Peripheral parasitemia was monitored by counting 300-500 RBCs on Diff-Quik (Siemens) stained thin blood smears. Mice were monitored at a minimum of two times a day during experimentation. Parasite burden in tissues was determined by quantitative PCR or using a Xenogen IVIS 100 Bioluminescent Imager after injecting mice with 100μL RediJect D-Luciferin bioluminescent

substrate (Perkin Elmer) 30 minutes prior to euthanization and organ dissection for subsequent bioluminescent imaging of parasites. All experiments were approved and carried out according to protocols approved by the Institutional Animal Care Use Committee at Emory University (Protocol number DAR-2000454-021114BN) and University of Utah (Protocol number 17-01001) and the biosafety committees of Emory University (Protocol number HAD01-2425-11R15-101915) and University of Utah (Protocol number 05-17).

In vivo anti-TNFR2 treatment

C57BL/6J mice were intraperitoneally injected with 20μg of either a purified anti-TNFR2 antibody (unconjugated, clone TR75-32.4, BioLegend) or a purified IgG isotype control antibody (unconjugated, clone HTK888, BioLegend) in a volume of 200μL/mouse (diluted in PBS) on days -1, 2, and 5 post-infected with *Pb*A. Mice were euthanized on day 6 post-infection and brains were prepared for RNA extraction and qPCR analyses as described in detail in below sections.

Plasmodium falciparum parasite culture

P. falciparum parasite lines 3D7 and W2 were cultured under standard conditions. Cultures were grown at a 2% haematocrit in 75-cm^2 tissue culture flasks at 37°C in medium consisting of human O+ red blood cells in RPMI-1640 (Invitrogen) supplemented with 10% pooled heat-inactivated human A+ serum, 6.0g/L HEPES, 1.8g/L $NaHCO_3$, 1.35mg/L hypoxanthine (All from Sigma-Aldrich). Cultures were gassed with a mixture of 3% CO_2, 1%O_2 and 96% N_2 (Airgas). These parasites lines were routinely synchronized by treatment with 5% D-sorbitol (Sigma-Aldrich) and schizont-stage parasites were enriched by centrifugation over a 60% Percoll (Sigma-Aldrich) gradient at 500g for 10min to a purity of ≥95%.

Isolation of *Pb*A schizonts

*Pb*A-infected mice were euthanized at day 6 post-infection and blood from five infected mice (~2.5mL total) was collected, pooled, and washed extensively with RPMI-1640. The infected RBCs were then transferred to two 75-cm^2 tissue culture flasks and cultured for 20 hours at a 2% haematocrit in a medium consisting of RPMI-1640, 25mM HEPES, 100μg/ml penicillin, 10U/ml streptomycin, 2mM L-glutamine, 1x sodium pyruvate (all from Sigma) and 10% FCS (Gibco). Cultures were gassed with a mixture of 90%N_2, 5%O_2, and 5%CO_2 (Airgas) prior to incubation at 37°C. *Pb*A schizont-stage parasites were enriched by centrifugation over a 68% Percoll (Sigma-Aldrich) gradient at 450g for 15min. Lysates of pRBCs were made by suspending pRBCs or naïve red blood cells in culture medium at 1x10^7cells/mL followed by two cycles of freezing and thawing before use.

PBMC isolation and stimulation

Peripheral blood mononuclear cells (PBMCs) from the blood of malaria-naïve healthy volunteers were isolated by density centrifugation through a Histopaque-1077 gradient (Sigma-Aldrich) and suspended in RPMI-1640 medium supplemented with 10% FCS (Gibco), 1mM sodium pyruvate, 1x penicillin/streptomycin, 2mM L-glutamine and 2-mercaptoethanol (Invitrogen). PBMCs were plated in a 24-well plate (Nunc) at 5x10^5 per well and incubated overnight in a 5% CO_2 incubator set at 37°C. The following day, the isolated PBMCs were exposed to *P. falciparum* (W2)-enriched schizonts for 48 hours at different ratios. Naïve RBCs were added as a negative control at a ratio of 40:1. In some experiments, isolated PBMCs were depleted of T cells using human CD3 microbeads following the manufacturer's instructions

(Miltenyi) after being exposed to *P. falciparum* (3D7) schizont-stage parasites. Stimulated PBMCs were stored in RNA Stat60 (Tel-Test Inc) at -20ºC until use.

In vivo Evans Blue blood-brain barrier permeability assay

Mice were injected intravenously with 200μL of 1% Evans Blue (Sigma) on day 6 post-infection and euthanized 1 hour after Evans Blue administration. Brains were removed and imaged using a MicroCapture digital microscope (Veho) and placed into vials containing 1mL formamide (Sigma) at 37°C for 4 days to allow for extraction of Evans Blue dye from whole brain tissue. The concentration of the extracted dye was then measured at an absorbance of 620nm using a plate reader (Biotek). For the treatment experiments, Nilotinib (Selleckchem) was dissolved in DMSO and recombinant mouse EphA2-Fc (rmEphA2) (R&D Systems) was dissolved in PBS. Nilotinib was diluted in water and provided to mice via oral gavage at a dose of 100mg/kg/day in 100μL on days 4-6 post-infection and control mice were given DMSO + water via oral gavage. Naïve control mice were also given Nilotinib and the vehicle control. rmEphA2 was diluted in PBS and intravenously injected into mice at a dose of 13.3μg/mouse/day in 200μL on days 4-6 post-infection and control mice were given PBS intravenously. Naïve control mice were also given rmEphA2 and the vehicle control.

Primary human brain microvascular endothelial cells

Primary human brain microvascular endothelial cells (HBMECs) used in this study were either gifted or obtained from a commercial source (Creative Dynamics Inc). HBMECs were cultured in SuperCult® endothelial cell growth medium following the supplier instructions (Creative Dynamics Inc). Endothelial cells (HBMEC) were used between passage 2 and 5.

Isolation and culture of primary murine brain microvascular endothelial cells

The technique for isolating primary murine brain microvascular endothelial cells (MBMECs) has been described elsewhere (*336*). Briefly, at least 5 mice (8-12 weeks old C57BL/6J or *EphA2*+/+ and *EphA2*-/-) were euthanized, the brain extracted, and the brain stems, cerebella, and thalami removed and discarded while the cerebra were transferred into a falcon tube containing DMEM-F12 medium (Gibco). The tissue was minced by pipetting up and down several times and digested with a mixture of collagenase D (10mg/mL) and DNAse (1mg/mL) (Roche) in DMEM-F12 medium for 1 hour at 37°C on an orbital shaker at 180rpm. DMEM-F12 (10mL) was added to the tissue suspension and the homogenate centrifuged at 1000g for 10 min at 4°C. De-myelination of brain homogenate was achieved by mixing the pellet in 25mL of 20% BSA-DMEM/F12, thoroughly pipetting several times, and centrifuging at 1000g for 20 min. at 4°C. The upper myelin layer was discarded and the pellet containing endothelial cells (ECs) was washed twice with DMEM-F12 supplemented with 1x MEM vitamin, 1x MEM amino acid, 1x antibiotic-antimycotic (Sigma-Aldrich), 1mM sodium pyruvate and 2-mercaptoethanol denoted "incomplete DMEM/F12" (iDMEM/F12). Next, the pellet was resuspended in red blood cell lysis buffer (eBioscience), incubated on ice for 5 min., and centrifuged for 5 min. at 1000g. The cells were then gently overlaid onto a 30% Percoll gradient and centrifuged for 10 minutes at 700g at 4°C with no acceleration or brake. The interface containing endothelial cells was carefully removed and washed with iDMEM/F12 twice and suspended in iDMEM/F12 supplemented with 20% FCS (Gibco), 100μg/mL endothelial cell growth supplement (BD Biosciences), 1 unit of Heparin (Hospira Inc.) (complete endothelial cell medium) and 10μg/mL puromycin (Sigma-Aldrich). Endothelial cells were then plated in a 6-well plate and incubated at 37°C in a 5% CO_2 incubator. After two days of culture, puromycin was removed from the endothelial cell

medium described above and ECs were cultured until they reached 90% confluency. The purity of the endothelial cell preparation was verified by immunofluorescence staining for the endothelial cell marker von Willebrand factor (VWF) and flow cytometry staining with an anti-CD31 antibody. Primary MBMEC were used between passage 2 and 5.

Stimulation of endothelial cells

Recombinant human and mouse tumor necrosis factor-alpha (TNF-α) and lymphotoxin-α (LT-α) were used at a concentration of 10ng/mL (R&D Systems). EphA2 (Catalog # 639-A2) and ephrin-A1 (Catalog # 602-A1) ectodomain-human IgG1 Fc fusion proteins were from R&D Systems. Purified human IgG-Fc protein was from Calbiochem (EMD Millipore Catalog # 401104). EphA2-Fc, Ephrin-A1-Fc, and IgG proteins were used at a concentration of 5μg/mL and were clustered by mixing with anti-human IgG-Fc in a 2:1 w/w ratio and incubated at 22ºC for 1 hour or overnight at 4ºC. This treatment allows the soluble Fc proteins to reproduce the clustering that occurs on cell membranes necessary for the initiation of biologically relevant signaling. Endothelial cells were also stimulated with 50μL of either naïve RBC or *Pb*A-infected RBC lysates.

Brain sectioning

Brain sections prepared for immunofluorescence staining were collected from 5-9 week old *EphA2*-/-, *EphA2*+/+, or C57BL/6J mice at day 6 post-infection with *Pb*A or Krebs saline for naïve control mice. Extracted brains were bisected to separate the left and right hemispheres and incubated in 4% paraformaldehyde (PFA) overnight at 4°C. Afterwards, brains were transferred to a 30% sucrose and 70% of 4% PFA solution and incubated for seven days at 4°C. To embed in preparation for slicing, brains were placed in embedding molds

and subsequently submerged in Tissue-Tek O.C.T. compound (Sakura Finetek) before freezing with dry ice. Once frozen, the molds were stored in -80°C for a maximum of two weeks prior to sectioning. 8 micron thick sagittal sections were obtained using a cryostat maintained at -20°C working temperature. Sections were collected on Shandon Colorfrost Plus microscope slides (ThermoScientific) and stored at -20°C until used for immunofluorescence staining.

Immunofluorescence staining

For staining of endothelial cell cultures, cells were seeded on gelatin-coated chamber slides (Lab-Tek, 8 wells, glass) and grown to confluence before being serum starved for 4 hours in iDMEM/F12 containing 1% BSA prior to stimulation. After stimulation, cells were washed with PBS, fixed with 2% paraformaldehyde (PFA) (Sigma-Aldrich) solution for 30 min. at room temperature, and permeabilized using 0.5% Triton X-100/Tris-HCl (Sigma-Aldrich) (100mM) for 10 min. at room temperature, blocked with 5% donkey serum (Abcam) for 1 hour and incubated overnight at 4ºC with the following primary antibodies: rabbit polyclonal to von Willebrand factor (1:500, ab9378, Abcam), rabbit polyclonal to VE-cadherin (1:50; ab33168, Abcam), goat polyclonal to VE-cadherin (1:50, AF1002, R&D Systems), ZO-2 (1:50; Cell Signaling Technology), FITC-conjugated lectin from *Lycopersicon esculentum* (tomato) (1:100, L0401, Sigma), and mouse monoclonal to EphA2 (1:50, 1C11A12, Thermo Fisher). Cells were then stained with NorthernLights 493® or NorthernLights 577® conjugated secondary antibodies for 1 hour (1:500; R&D Systems). Nuclei were counterstained with mounting medium containing DAPI (VectorShield). Brain sections were processed and stained using the same protocol. Images were taken at room temperature using a Nikon A1 confocal microscope with either a 20X (numerical aperture: 0.75) or 60X (numerical aperture:

1.4) objective lens using NIS-Elements acquisition software. ImageJ software (NIH) was used for image processing post-acquisition and at least ten random fields were analysed for quantification.

Transmission electron microscopy

For TEM examination of endothelial cell cultures, the samples were fixed with 2.5% glutaraldehyde in 0.1 M sodium cacodylate (pH 7.4). Samples were then washed with the same buffer twice and post-fixed with 1% osmium tetroxide and 1.5% potassium ferrocyanide, dehydrated through a graded ethanol series to 100%, and embedded in Eponate 12 resin (Ted Pella Inc., Redding, CA). Ultrathin sections were cut on a Leica UltraCut S ultramicrotome (Leica Microsystems Inc., Buffalo Grove, IL) at 70 nm, and counter-stained with 4% aqueous uranyl acetate and 2% lead citrate. Sections were examined using a 120 kV JEOL JEM-1400 LaB6 transmission electron microscope (JEOL, Ltd., Japan).

ELISA

Mouse ephrin-A1 (R&D Systems), VE-cadherin (Abcam), and E-cadherin (Abcam) ELISA kits were used to detect the presence of soluble ephrin-A1 ligand, VE-cadherin, and E-cadherin, respectively, in the plasma of mice. Mouse ephrin-A1 ELISA kits were also used to detect soluble ephrin-A1 present in MBMEC culture supernatants post-stimulation as described in detail in a previous section. Mice were euthanized with isoflurane and whole blood was collected into heparinized tubes and centrifuged at 1000g for 15 minutes at 4°C to isolate plasma. Plasma was diluted 1:10 for ELISA analysis of ephrin-A1 ligand, 1:800 for ELISA analysis of VE-cadherin, and 1:2000 for ELISA analysis of E-cadherin. Absorbance was measured at 450nm using a plate reader (Biotek) and plasma concentrations were determined

using standard curves as per the manufacturer's instructions. Human ephrin-A1 (Sino Biological) and human EphA2 (R&D Systems) ELISA kits were used to detect the presence of soluble ephrin-A1 ligand and soluble EphA2, respectively, in the plasma of humans and carried out according to the manufacturer's instructions.

Luminex of endothelial cell culture supernatants

Cytokine and chemokine analysis from EC culture supernatant was performed using Singleplex Luminex® kits for each analyte tested according to the manufacturer's instructions (eBioscience and ThermoFisher Scientific).

***In vitro* endothelial cell permeability assay**

Transendothelial electrical resistance (TEER) was measured by Electric Cell-substrate Impedance Sensing (ECIS). An 8W10E+ electrode 96-well culture array (Applied Biophysics) was coated with 0.1% gelatin (Sigma) and 10 μg/mL human fibronectin. 1 x 10^4 primary MBMECs isolated from *EphA2*+/+ and *EphA2*-/- mice per well were seeded in complete media onto the electrode culture array and monitored until a stable monolayer formed. Once a stable measurement of resistance from MBMECs was achieved, resistance changes were further monitored in real time for up to 48 hours. Data were analyzed using the X-CELLigence experiment report software.

To assess paracellular permeability, primary MBMECs from *EphA2*+/+ and *EphA2*-/- mice were seeded on gelatin-coated transwell filter plates (Costar 3413, 0.4μm pore size; Corning) and grown to confluence. For stimulation, MBMECs were serum starved for 4 hours in iDMEM/F12 containing 1% BSA, then pre-incubated with the lysates of naïve RBCs and

*Pb*A-schizonts (pRBCs), 5μg/mL of cluster-activated ephrin-A1-Fc and EphA2-Fc (for 2 hours) parallel to the diffusion of 25μg/mL FITC-dextran (250kD; Sigma-Aldrich) at 37°C and 5%CO_2. Fluorescence in the lower chamber was measured with a plate reader (BioTek) at 490nm.

RNA extraction and cDNA synthesis

Cells or tissue were homogenized in RNA-Stat60® (Tel-Test Inc) and total RNA was extracted using standard phenol-chloroform protocols followed by DNAse treatment of the RNA extracted using RNA-II purification kit (Nachery-Nagel). A total of 100ng of RNA per sample was converted into cDNA using Superscript II (Life Technologies) at 42°C for 50 min., 70°C for 15 min., in the presence of 5uM oligo $(dT)_{16\text{-}18}$, 5mM Dithiothreitol (DTT), 0.5mM dNTPs (all from Life Technologies), 8U RNAsin (Promega), 50mM Tris-HCl pH8.3, 75mM KCl and 3mM $MgCl_2$. The cDNA was treated with 2.5U RNAse H (Affymetrix) at 37°C for 20min to remove any remaining RNA residues.

Quantitative PCR

Real-time qPCR reactions were performed using Quantitect SYBR Green PCR reagent (Qiagen). PCR amplification was performed with 5μL cDNA per sample (diluted 1:10), 2μM of each primer, and 7μl of QPCR SYBR green mix. Plates were then run using Applied BioSystems FAST 7000 Sequence detection system (ABI Prism FAST 7000). Mouse primer sequences are shown in Supporting Table S1 and human primer sequences are shown in Supporting Table S2. Transcripts were normalized to a housekeeping gene (Ubiquitin or β-actin) and expression levels calculated using the $2^{-\Delta\Delta Ct}$ method (*337*). The fold change of

transcription for individual infected animals was calculated in relation to the average expression in naïve mice for each group at each time point.

Tissue processing for flow cytometry

Spleens were pressed through a 40μm cell strainer and suspended in Iscove's Modified Dulbecco's Medium (IMDM) containing 100units/mL penicillin, 100μg/mL streptomycin, 1μM L-glutamine, 12mM HEPES, 0.5mM sodium pyruvate, 5 X 10^{-5}M 2-mercaptoethanol (all Gibco) (cIMDM). Single cell suspensions of splenocytes were centrifuged at 1500rpm for 8 minutes at 4°C prior to RBC lysis of the pellet using an NH_4Cl-based RBC lysis buffer (BioLegend). Splenocytes were centrifuged again before resuspension in cIMDM with the addition of 10% heat-inactivated fetal calf serum (FCS) (PAA Laboratories) for downstream flow cytometric analysis. Brains were pressed through a 100μm cell strainer and resuspended in a 30% Percoll solution before overlaying onto a 70% Percoll gradient. Brain samples were centrifuged at 600g for 20 minutes at room temperature with no brake. The peripheral blood mononuclear cell (PBMC) interface was collected and washed with cIMDM + 10% heat-inactivated FCS before resuspension in cIMDM + 10% heat-inactivated FCS for downstream flow cytometric analysis. Lungs were pressed through a 40μm cell strainer, resuspended in cIMDM containing Liberase-TL synthetic collagenase (Roche) at a final concentration of 0.3mg/mL and dispase (Invitrogen) at final concentration 2mg/mL and further incubated for 45 min. at 37°C. The suspension was overlaid on a 30% Percoll gradient and centrifuged at 1800g for 10min. The pellet was collected and RBCs were removed from suspensions by incubation in an NH_4Cl-based RBC lysis buffer (BioLegend).

For flow cytometry, samples were incubated with Fc-blocking antibodies (anti-mouse CD16/CD32, clone 2.4G2, BioLegend) followed by various combinations of the following antibodies: CD3 (PE-Cy5, clone 145-2C11, BioLegend), CD4 (PerCP-Cy5.5, clone GK1.5, BioLegend), CD8 (BV711, clone 53-6.7, BioLegend), CD44 (Alexa 700, clone IM7, eBioscience) Zombie NIR viability dye (BioLegend), and EphA2 (PE, clone 233720, R&D Systems). For detection of *Plamodium*-specific CD8+ T cells, previously identified tetramers recognizing the glideosome-associated protein 50 epitope 40-48 (GAP50-PE) (*223*) and the replication protein A1 epitope 199-206 (F4-APC) (*287*) were generated by the NIH Tetramer Core Facility and incorporated into the flow panels. For detection of surface ephrin-A1 ligand expression, samples were first incubated with 2μg/mL recombinant mouse EphA2-Fc protein (R&D Systems) for 1 hour at room temperature prior to incubation with a secondary anti-human IgG-Fc antibody (PE or FITC, clone HP6017, BioLegend). Intracellular cytokine staining on splenocytes was undertaken after incubation for 6 hours at 37°C in a 96-well plate containing immobilized anti-CD3 (50μL/well at 5μg/mL) (clone 17A2) and soluble CD28 (2μg/mL) (clone 37.51) (eBioscience) in the presence of 10μg/mL brefeldin A (BioLegend). After surface staining, cells were fixed with a paraformaldehyde-based fixation buffer (BioLegend), permeabilized with a permeabilization buffer (BioLegend), and stained with anti-IFN-γ-PE (clone XMG1.2, BioLegend) and anti-Granzyme B-Alexa 647 (clone GB11, BioLegend). Flow cytometric acquisition was performed on BD LSRII and BD LSRFortessa flow cytometers (BD Biosciences) and data analyzed using FlowJo software (TreeStar).

Fluorescence activated cell sorting of splenocytes

For sorting of splenic T cells, B cells were first removed using CD19+ positive selection beads (Miltenyi Biotech) and populations were sorted from CD19 negative splenocytes. CD4+ T

cells (CD3+CD4+CD8-) and CD8+ T cells (CD3+ CD4-CD8+CD11c-) were sorted on a FACS Aria II (BD Biosciences) before being stored in RNA Stat-60 at -80°C until processed for RT-qPCR as described in detail in a previous section.

Western blot

Endothelial cell lysates were prepared with RIPA buffer containing 1x EDTA/proteinase-phosphatase inhibitor cocktail (Pierce). Protein concentration was determined using a BCA kit (Thermo Scientific). The supernatant lysate was stored at -80°C until used for immunoblotting. Protein extracts were separated by SDS-PAGE electrophoresis and blotted onto nitrocellulose membranes. Blots were incubated overnight with the following primary detection antibodies: anti-mouse pNFκBp65 (clone 93H1), NFκBp65 (clone D14E12), pIKKαβ (clone 16A6) (all from Cell Signalling Technology and used at a 1:1000 dilution), anti-mouse IKKαβ (clone 42D1) at a 1:500 dilution (Pierce), or β-actin (clone AC-15) at a 1:10,000 dilution (Pierce). Blots were then stained for 1 hour with mouse or rabbit HRP-conjugated secondary antibodies used at a 1:2000 dilution (R&D Systems). Finally, blots were developed using ECL substrate per the manufacturer's instructions (Pierce) and quantified using densitometry measurements on ImageJ software.

Statistical analyses

Using Prism software, differences between two groups of animals were assessed using a non-parametric 2-tailed Mann Whitney test or a 2-tailed parametric t-test as stated. Paired samples were tested using a non-parametric 2-tailed Wilcoxon matched pairs signed rank test or a paired t-test. Survival analysis was performed using a Log-rank Mantel-Cox test. Comparisons of more than two groups were assessed using non-parametric Kruskal-Wallis test followed by

Dunn's multiple comparisons test. General Linear Modelling (GLM), a variant of analysis of variance (ANOVA) including all 1st order interactions, was performed using Minitab software (Minitab, Inc.) to determine the statistical significance of soluble ephrin-A1 or EphA2 in patient samples taking into account age, area of residence, and peripheral parasitemia levels. Residual variation was assessed for normality using Anderson-Darling test and heterogeneity of variance using the F-test. To meet the requirements of parametric testing, both soluble EphA2 and ephrin-A1 data were logarithmically transformed prior to analysis. F values quoted are from the minimal model of the data with all insignificant terms removed. In all cases, P values are stated in the figures and $P<0.05$ was considered statistically significant. Only significant differences are shown as stated.

Acknowledgments

We thank the following individuals: Taryn Stewart for excellent animal husbandry; Esmeralda Meyer and Mary Galinski for technical assistance; Mary Galinski for the W2 and 3D7 *P. falciparum* clones; Cathy Stevens at Emory University Department of Pediatrics and medical staff at the Obala, Efoulan, Nkoletan District Hospitals and Chantal Biya Foundation Hospital for diagnostic and phlebotomy assistance; Aaron Rae and the Emory Department of Pediatrics Flow Core for FACS sorting; Neil Anthony at the Emory Integrated Imaging Facility and Michael Bridge and Christopher Rodesch at the University of Utah Cell Imaging Core for microscopy assistance; Elizabeth Wright at Emory University for transmission electron microscopy services; Chris Janse for the luciferase-expressing *P. berghei* ANKA AMA-1 strain; Mahalia Desruisseaux for the *P. berghei* NK65 New York clone; Monique Stins for HBMECs; and Robert Fujinami for the *LT-a-/-* mice. We also thank the clinical staff, patients, and their guardians at Obala, Efoulan, Nkoletan District Hospitals and Chantal Biya Foundation

Hospital for their participation in this study. All animal work was conducted with permission from the Emory University and the University of Utah IACUC boards. Ethical approval was obtained from the Emory University and University of Utah IRB committees. **Funding:** This work was funded by grants from National Institute for Neurological Disorders and Strokes (R21NS085382 and R01NS097819), the Emory Egleston Children's Research Fund, and Royal Society to TJL. TKD was supported by training grants T32AI007610, T32AI106699, and individual fellowship F31NS098736; **Author contributions:** TD and PM devised the experiments, performed the experiments, analyzed data, and drafted the paper; CB, BU, LB, CS, AT, and TL performed experiments; CEEM and LA devised experiments and analyzed data; TL devised the experiments, supervised the experiments, analyzed data, and wrote the paper; **Competing interests:** Authors declare no competing interests; **Data and materials availability:** All data is available in the main text or the supplementary materials.

Fig. 1

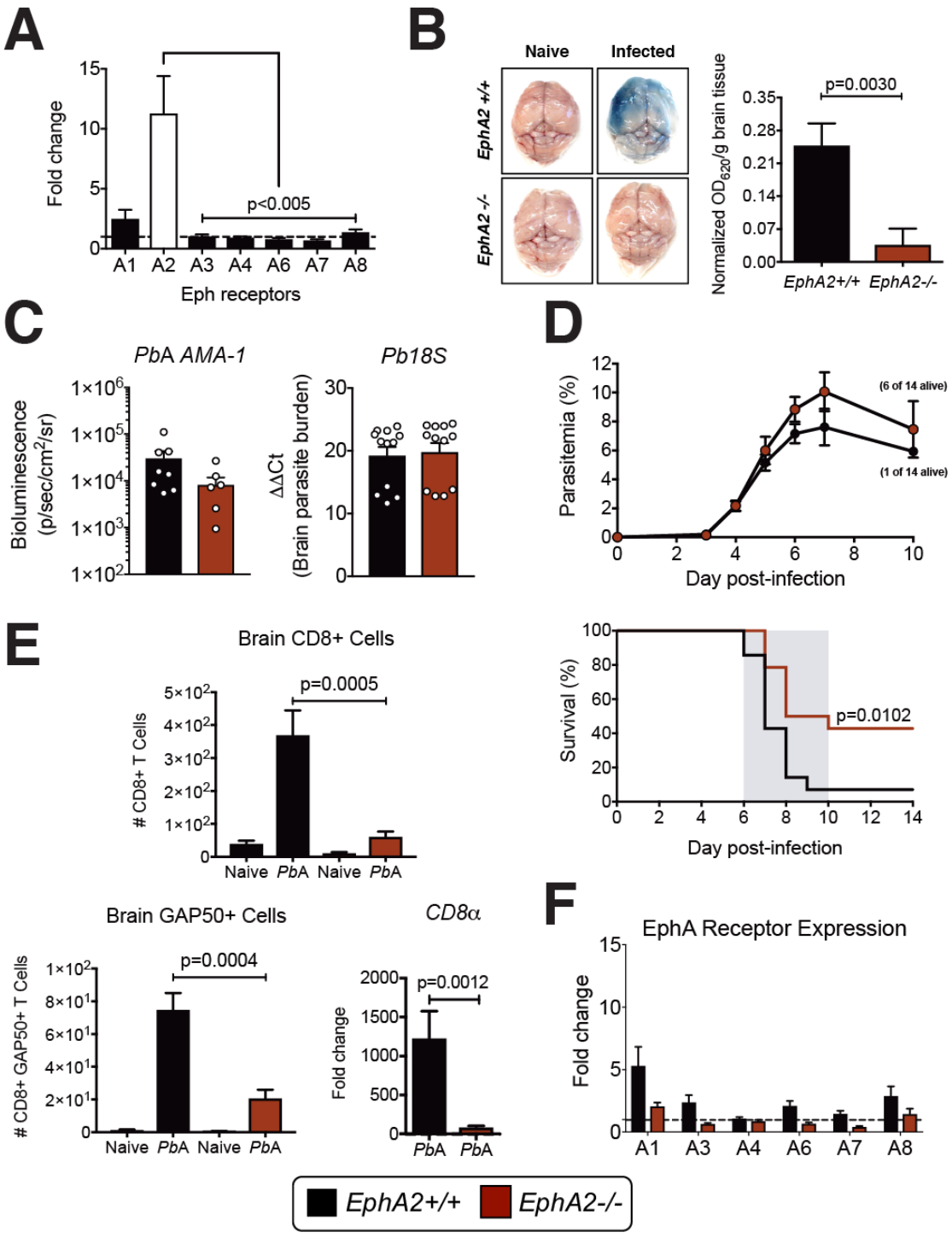
A
Fold change
15
10
5
0
p<0.005
A1 A2 A3 A4 A6 A7 A8
Eph receptors
B
Naive
Infected
EphA2 +/+
EphA2 -/-
Normalized OD620/g brain tissue
0.35
0.28
0.21
0.14
0.07
0.00
p=0.0030
EphA2+/+ EphA2-/-
C
PbA AMA-1
Pb18S
Bioluminescence (p/sec/cm2/sr)
1×10^6
1×10^5
1×10^4
1×10^3
1×10^2
ΔΔCt (Brain parasite burden)
30
20
10
0
D
Parasitemia (%)
12
10
8
6
4
2
0
(6 of 14 alive)
(1 of 14 alive)
0 2 4 6 8 10
Day post-infection
E
Brain CD8+ Cells
CD8+ T Cells
5×10^2
4×10^2
3×10^2
2×10^2
1×10^2
0
p=0.0005
Naive PbA Naive PbA
Survival (%)
100
80
60
40
20
0
p=0.0102
0 2 4 6 8 10 12 14
Day post-infection
Brain GAP50+ Cells
CD8+ GAP50+ T Cells
1×10^2
8×10^1
6×10^1
4×10^1
2×10^1
0
p=0.0004
Naive PbA Naive PbA
CD8α
Fold change
2000
1500
1000
500
0
p=0.0012
PbA PbA
F
EphA Receptor Expression
Fold change
15
10
5
0
A1 A3 A4 A6 A7 A8
EphA2+/+
EphA2-/-

Fig 1. EphA2 is required for blood-brain barrier breakdown and the development of ECM. (A) Transcription of EphA receptors relative to naïve mice (dashed line) in whole brains of C57BL/6J mice (n=16/group) at day 6 post-infection with *Pb*A. **(B)** Brain permeability in *EphA2*-/- and littermate control mice injected intravenously with 1% Evan's Blue at day 6 post-infection with *Pb*A. Representative images and quantification of dye extracted from whole brains is shown (n=9-10/group). OD values are normalized to naïve mice from each respective group. **(C)** Quantification of sequestered *Pb*A schizonts expressing luciferase under the *AMA-1* promoter (n=7-8/group) and 18S parasite DNA transcript (n=12/group) in whole brains of *EphA2*-/- and littermate control mice at day 6 post-infection. **(D)** Peripheral parasitemia and survival of *EphA2*-/- and littermate control mice infected with *Pb*A (n=14/group). **(E)** Total CD8+ T cells (top left; n=12-14/group), GAP50+CD8+ T cells (bottom left; n=7-10/group), and transcription of CD8α relative to naïve mice (dashed line) (bottom right; n=9/group) in brains of *EphA2*-/- and littermate control mice at day 6 post-infection with *Pb*A. Naïve and *Pb*A-infected groups are significantly different within each genotype. **(F)** Transcription of EphA receptors relative to naïve mice (dashed line) in whole brains of *EphA2*-/- and littermate control mice (n=12-13/group) at day 6 post-infection with *Pb*A. Bars in all graphs represent the mean ± SEM. Statistical analyses: Kruskal-Wallis and Dunn's multiple comparisons tests (A), Mann-Whitney test (B, C, E) and Log-rank Mantel-Cox test (D). Only statistically significant ($p<0.05$) values are shown unless otherwise noted in the legend. Figures represent combined data from 2 (B, C-left panel, D, E-bottom left panel), 3 (C-right panel, E-top and bottom right panels, F), or 4 (A) independent experiments.

Fig. 2

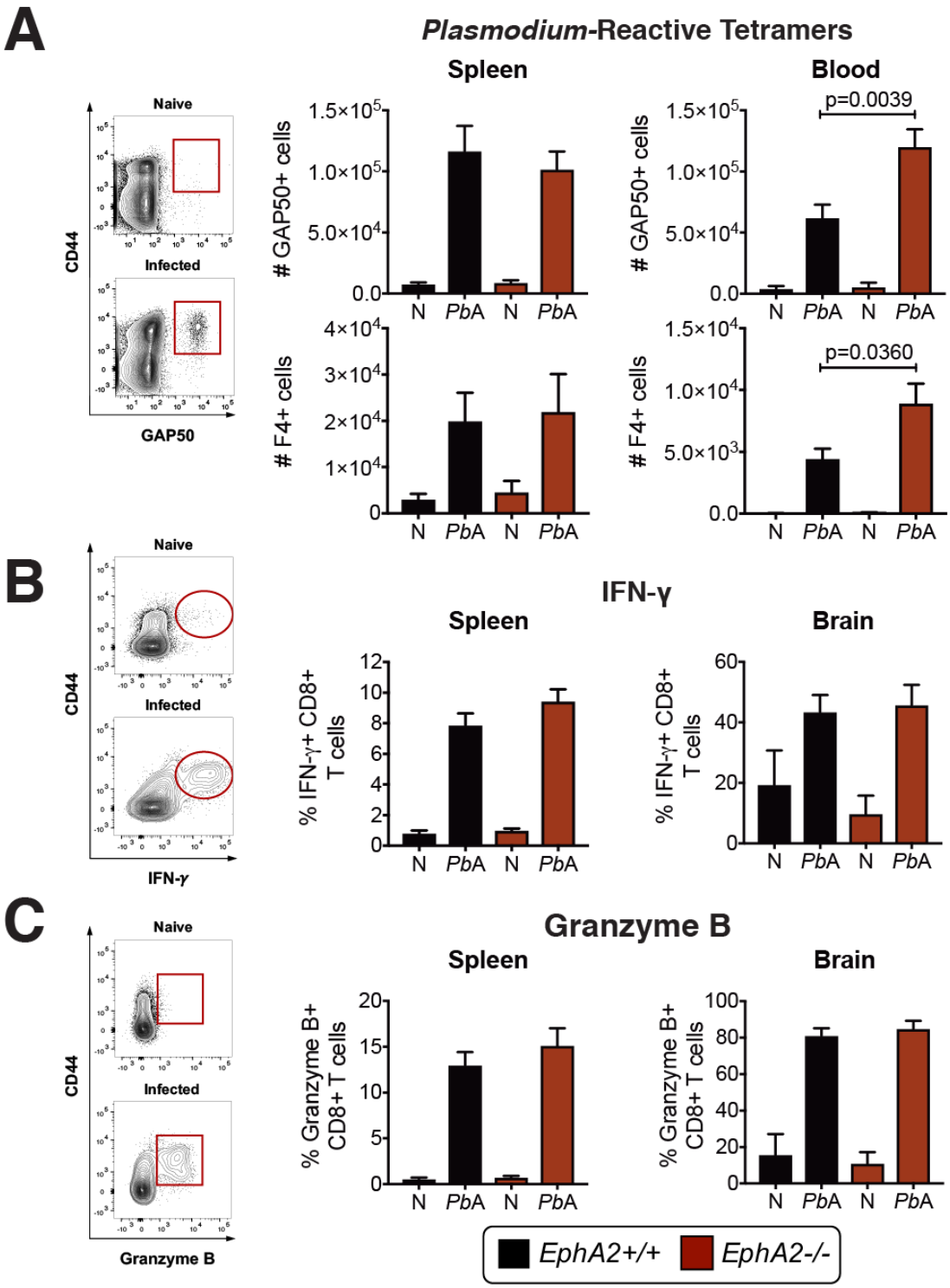
A
Plasmodium-Reactive Tetramers
Spleen
Blood
Naive
Infected
CD44
GAP50
GAP50+ cells
1.5×10^5
1.0×10^5
5.0×10^4
0.0
p=0.0039
# F4+ cells
4×10^4
3×10^4
2×10^4
1×10^4
0
1.5×10^4
1.0×10^4
5.0×10^3
p=0.0360
N PbA N PbA
B
IFN-γ
Spleen
Brain
IFN-γ
% IFN-γ+ CD8+ T cells
12
10
8
6
4
2
60
40
20
C
Granzyme B
Granzyme B
% Granzyme B+ CD8+ T cells
20
15
10
5
100
80
60
EphA2+/+
EphA2-/-

Fig 2. CD8+ T cell expansion and functionality is not affected by EphA2 deficiency. **(A)** Representative staining and total numbers of *Plasmodium* GAP50-reactive (n=11-18/group) and F4-reactive (n=8-9/group) CD8+T cells present in the spleen (left) and bloodstream (right) of *EphA2*-/- and littermate control mice at day 6 post-infection with *Pb*A compared to naïve (N) mice (n=4-8/group). Naïve and *Pb*A-infected groups are significantly different within each genotype for all graphs except bottom left. **(B-C)** Frequency of IFN-γ+ **(B)** or Granzyme B+ **(C)** CD8+ T cells in the spleen (n=10-15/group) and brain (n=7-10/group) of *EphA2*-/- and littermate control mice at day 6 post-infection with *Pb*A compared to naïve (N) mice (n=4/group). Naïve and *Pb*A-infected groups are significantly different within each genotype for all graphs except *EphA2*+/+ in B-right panel. Bars in all graphs represent the mean ± SEM. Statistical analysis: Mann-Whitney test (A-C). Only statistically significant ($p<0.05$) values are shown unless otherwise noted in the legend. Figures represent combined data from 2 (A-bottom left and right panels, B-right panel, C-right panel), 3 (A-top right panel, B-left panel, C-left panel), or 4 (A-top left panel) independent experiments.

Fig. 3

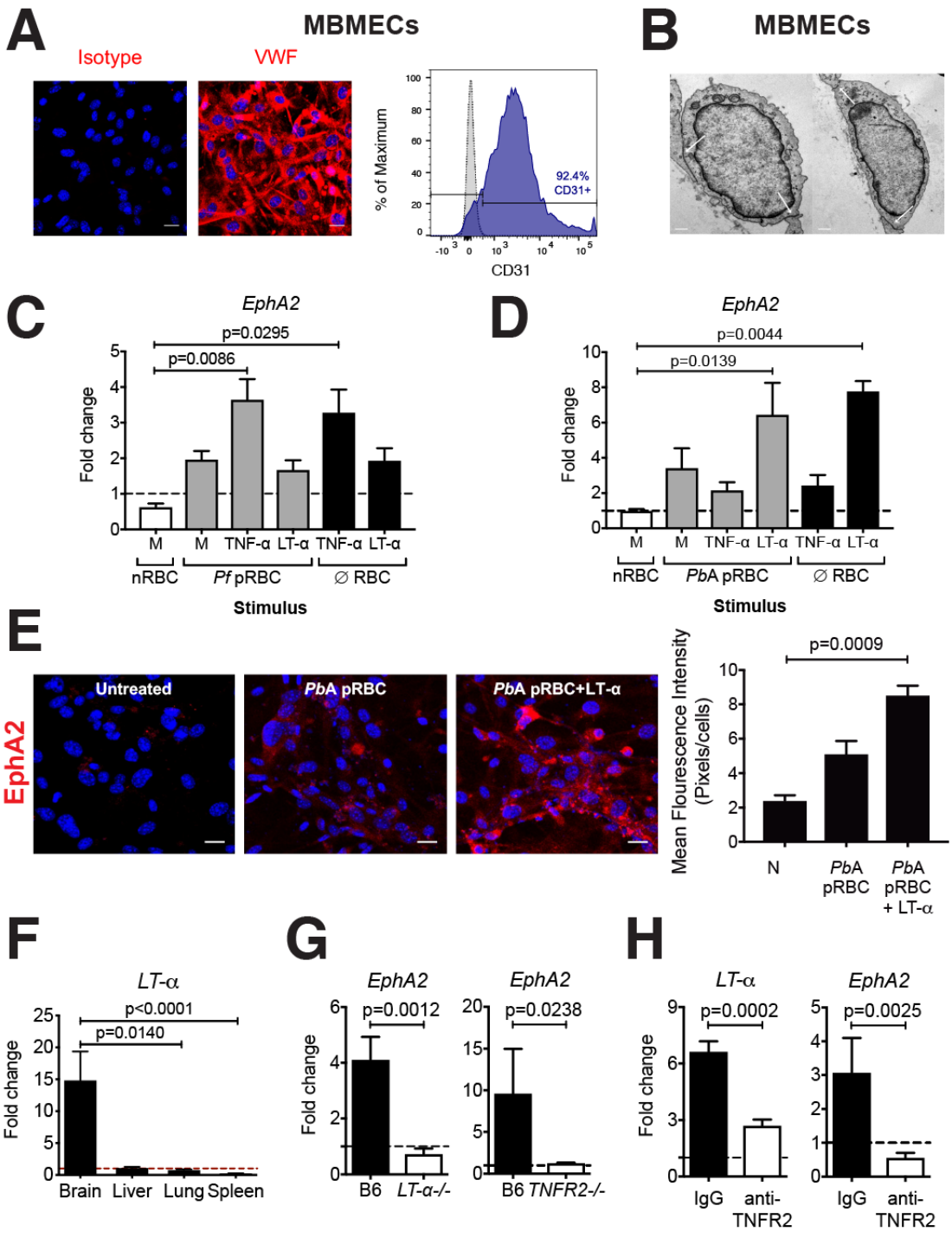
A
MBMECs
Isotype
VWF
% of Maximum
92.4%
CD31+
CD31
B
MBMECs
C
EphA2
p=0.0295
p=0.0086
Fold change
M
M
TNF-α
LT-α
TNF-α
LT-α
nRBC
Pf pRBC
∅ RBC
Stimulus
D
EphA2
p=0.0044
p=0.0139
Fold change
M
M
TNF-α
LT-α
TNF-α
LT-α
nRBC
PbA pRBC
∅ RBC
Stimulus
E
EphA2
Untreated
PbA pRBC
PbA pRBC+LT-α
Mean Flourescence Intensity (Pixels/cells)
p=0.0009
N
PbA pRBC
PbA pRBC + LT-α
F
LT-α
p<0.0001
p=0.0140
Fold change
Brain
Liver
Lung
Spleen
G
EphA2
p=0.0012
Fold change
B6
LT-α-/-
EphA2
p=0.0238
B6
TNFR2-/-
H
LT-α
p=0.0002
Fold change
IgG
anti-TNFR2
EphA2
p=0.0025
IgG
anti-TNFR2

Fig 3. *EphA2* is upregulated in human and mouse primary brain endothelial cells in response to inflammatory cytokines. Representative data showing von Willebrand factor (VWF) immunofluorescence staining (cell nuclei stained with DAPI-blue) **(A, left)**, CD31 flow cytometry staining (gray histogram: isotype control, blue histogram: anti-CD31) **(A, right)**, and transmission electron microscopy **(B)** of cultured MBMECs isolated from C57BL/6J mice. White arrows in **(B)** indicate endothelial cell contact points. Scale bars represent 25μm **(A)** and 0.5μm **(B)**. **(C-D)** *EphA2* transcription in human **(C)** and mouse **(D)** BMECs incubated for 24 hours with naïve RBC lysates (nRBC), *P. falciparum* 3D7-infected RBC lysates (*Pf* pRBC), *Pb*A-infected RBC lysates (*Pb*A pRBC), or no RBC lysate (∅ RBC) plus human **(C)** or mouse **(D)** LT-α, TNF-α, or media (M) (n=3-6 endothelial preparations/group). Values are normalized to untreated cells. **(E)** Immunofluorescence images and fluorescence quantification of EphA2 (red) on MBMECs unstimulated or stimulated with *Pb*A-infected RBC lysates (*Pb*A pRBC) in the presence of absence of LT-α for 24 hours. Cell nuclei stained with DAPI (blue). Scale bars represent 25μm. Images representative of two endothelial preparations. **(F)** *LT-a* transcription relative to naïve mice (dashed line) in whole brains, livers, lungs, and spleens of C57BL/6J mice (n=8-9/group) at day 6 post-infection with *Pb*A. **(G)** *EphA2* transcription relative to naïve mice (dashed line) in brains of *LT-a-/-* (n=7) and *TNFR2-/-* (n=3) mice at day 6 post-infection with *Pb*A compared to wild-type C57BL/6J mice (n=6-11). **(H)** *LT-a* and *EphA2* transcription relative to naïve mice (dashed line) in brains of isotype control (n=9) and anti-TNFR2 (n=8) treated mice at day 6 post-infection with *Pb*A. Bars in all graphs represent the mean ± SEM. Statistical analyses: Kruskal-Wallis and Dunn's multiple comparisons tests (C, D, E, F) and Mann-Whitney test (G, H). Only statistically significant ($p<0.05$) values are shown. Figures **Fig. 3**

(continued) represent combined data from 1 (G-right panel), 2 (E, F, G-left panel, H), or 3 (C, D) independent experiments.

Fig. 4

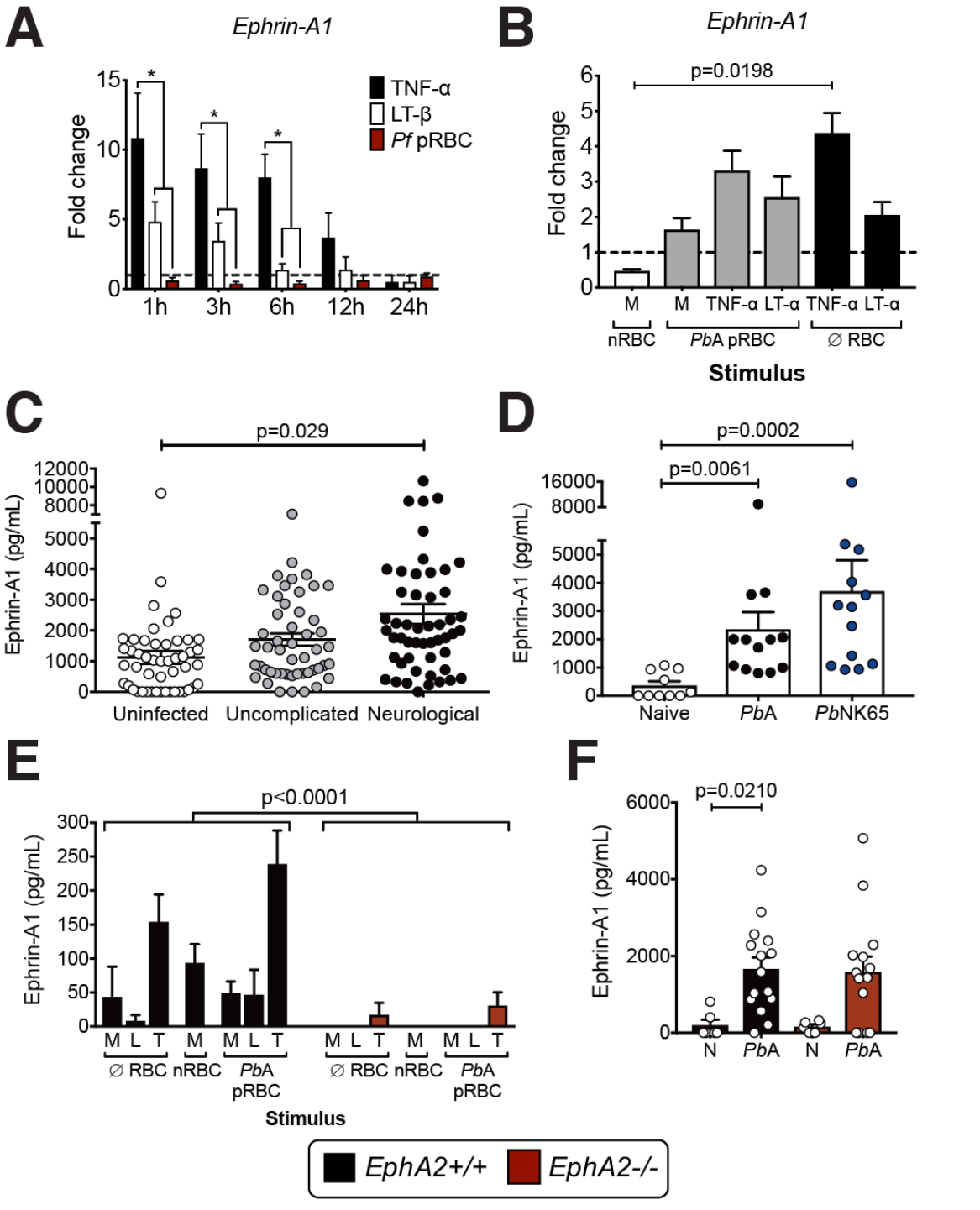
A
Ephrin-A1
Fold change
TNF-α
LT-β
Pf pRBC
1h
3h
6h
12h
24h
B
Ephrin-A1
p=0.0198
Fold change
M
M
TNF-α
LT-α
TNF-α
LT-α
nRBC
PbA pRBC
∅ RBC
Stimulus
C
p=0.029
Ephrin-A1 (pg/mL)
Uninfected
Uncomplicated
Neurological
D
p=0.0002
p=0.0061
Ephrin-A1 (pg/mL)
Naive
PbA
PbNK65
E
p<0.0001
Ephrin-A1 (pg/mL)
M L T
M
M L T
M L T
M
M L T
∅ RBC
nRBC
PbA pRBC
∅ RBC
nRBC
PbA pRBC
Stimulus
F
p=0.0210
Ephrin-A1 (pg/mL)
N
PbA
N
PbA
EphA2+/+
EphA2-/-

Fig 4. Ephrin-A ligands are upregulated and cleaved as a result of *Plasmodium* infection. (A) *Ephrin-A1* ligand transcription in HBMECs incubated for 1-24 hours with human TNF-α, LT-β, or *P. falciparum* 3D7-infected RBC lysates (*Pf* pRBC) (n=3 endothelial preparations/group/time point). Values are normalized to untreated cells. Asterisk indicates $p<0.05$. **(B)** *Ephrin-A1* ligand transcription in MBMECs incubated for 24 hours with naïve RBC lysates (nRBC), *Pb*A-infected RBC lysates (*Pb*A pRBC), or no RBC lysate (∅ RBC) plus mouse LT-α, TNF-α, or media (M)) (n=3 endothelial preparations/group). **(C)** Levels of soluble ephrin-A1 ligand in the plasma of children living in an area in Cameroon endemic for *P. falciparum* malaria. Patients were categorized by admission to the hospital for neurological complications (n=51), uncomplicated malaria (n=50), or uninfected and presenting for routine pediatric tests (n=49). Each dot represents an individual patient. **(D)** Levels of soluble ephrin-A1 ligand in the plasma of C57BL/6J mice infected with with *Pb*A (n=13) or *Pb*NK65 (n=13) at day 6 post-infection compared with naïve mice (n=10). **(E)** Ephrin-A1 ligands released from MBMECs derived from *EphA2-/-* or littermate control mice and incubated for 24 hours with no RBC lysate (∅ RBC), naïve RBC lysate (nRBC), and *Pb*A-infected RBC lysate (*Pb*A pRBC) with the addition of media (M), recombinant mouse LT-α (L), or TNF-α (T) (n=4 endothelial preparations). **(F)** Ephrin-A1 ligands in the plasma of *EphA2-/-* or littermate control mice at day 6 post-infection with *Pb*A (n=14-15/group) compared to naïve mice (N) (n=6/group). Bars in all graphs represent the mean ± SEM. Statistical analyses: Two-way ANOVA (A, E), Kruskal-Wallis and Dunn's multiple comparisons tests (B, D, F), and General linear modeling and Tukey's pairwise comparison post-ANOVA (C). Only statistically significant ($p<0.05$) values are shown. Figures represent combined data from 3 (A, B, D, F), or 4 (E) independent experiments.

Fig. 5

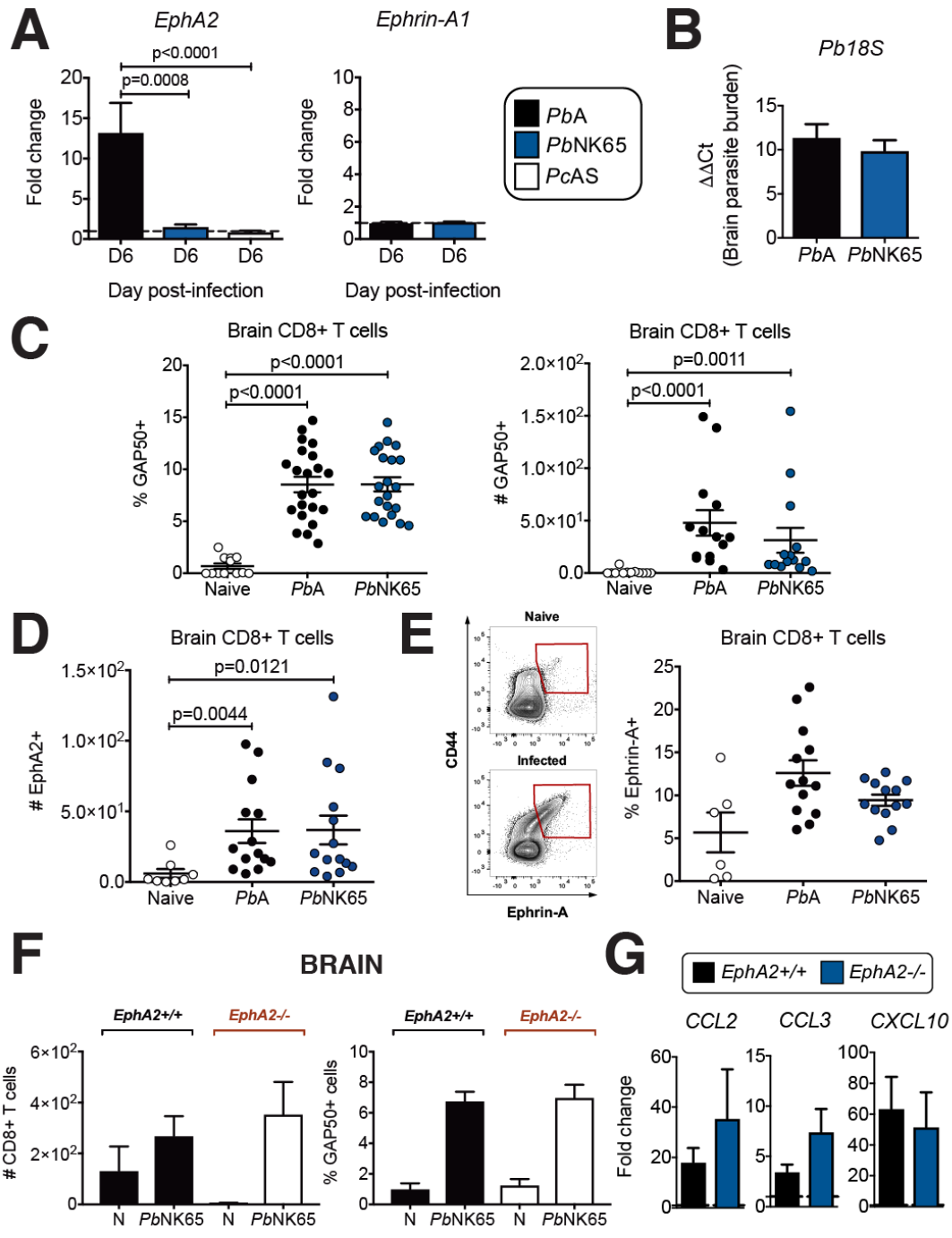
A
EphA2
Ephrin-A1
p<0.0001
p=0.0008
Fold change
D6
Day post-infection
PbA
PbNK65
PcAS
B
Pb18S
ΔΔCt
(Brain parasite burden)
C
Brain CD8+ T cells
% GAP50+
# GAP50+
p<0.0001
p=0.0011
Naive
D
# EphA2+
p=0.0121
p=0.0044
E
CD44
Infected
Ephrin-A
% Ephrin-A+
F
BRAIN
EphA2+/+
EphA2-/-
CD8+ T cells
% GAP50+ cells
N
G
CCL2
CCL3
CXCL10

Fig 5. EphA2 is not required for trafficking of CD8+ T cells in the brain during *Pb*NK65 infection. (A) Transcription of *EphA2* (left) and *ephrin-A1* (right) in whole brain lysates of C57BL/6J mice infected with *Pb*A (n=12), *Pb*NK65 (n=12) or *Pc*AS (n=8) relative to naïve mice (dashed line). **(B)** Quantification of 18S parasite DNA transcript in whole brain lysates of *Pb*A- and *Pb*NK65-infected mice (n=12-13/group) at day 6 post-infection. **(C)** Frequency and total number of *Plasmodium* GAP50-reactive CD8+ T cells in the brains of mice at day 6 post-infection with *Pb*A (n=14-22), *Pb*NK65 (n=14-21), or naïve (n=12). **(D)** Total number of EphA2+ CD8+ T cells in the brains of mice at day 6 post-infection with *Pb*A (n=14), *Pb*NK65 (n=14), or naïve (n=8). **(E)** Frequency of ephrin-A+ CD8+ T cells in the brains of mice at day 6 post-infection with *Pb*A (n=13), *Pb*NK65 (n=13), or naïve (n=6). **(F)** Total number of CD8+T cells and frequency of *Plasmodium* GAP50-reactive CD8+ T cells in the brains of *EphA2*-/- and littermate control mice at day 6 post-infection with *Pb*NK65 (n=9/group) compared to naïve mice (N) (n=4/group). Naïve and *Pb*NK65-infected groups are significantly different within each genotype for all graphs except *EphA2*+/+ in left panel. **(G)** Transcription of inflammatory chemokines in whole brain lysates of *EphA2*-/- and littermate control mice at day 6 post-infection with *Pb*NK65 (n=7-10/group) relative to naïve mice (dashed lines). Bars in all graphs represent the mean ± SEM. Statistical analyses: Kruskal-Wallis and Dunn's multiple comparisons tests (A-left panel, C, D, E, F) and Mann-Whitney test (A-right panel, B, G). Only statistically significant ($p<0.05$) values are shown unless otherwise noted in the legend. Figures represent combined data from 2 (E, F, G), 3 (A, B, D), or 4 (C) independent experiments.

Fig. 6

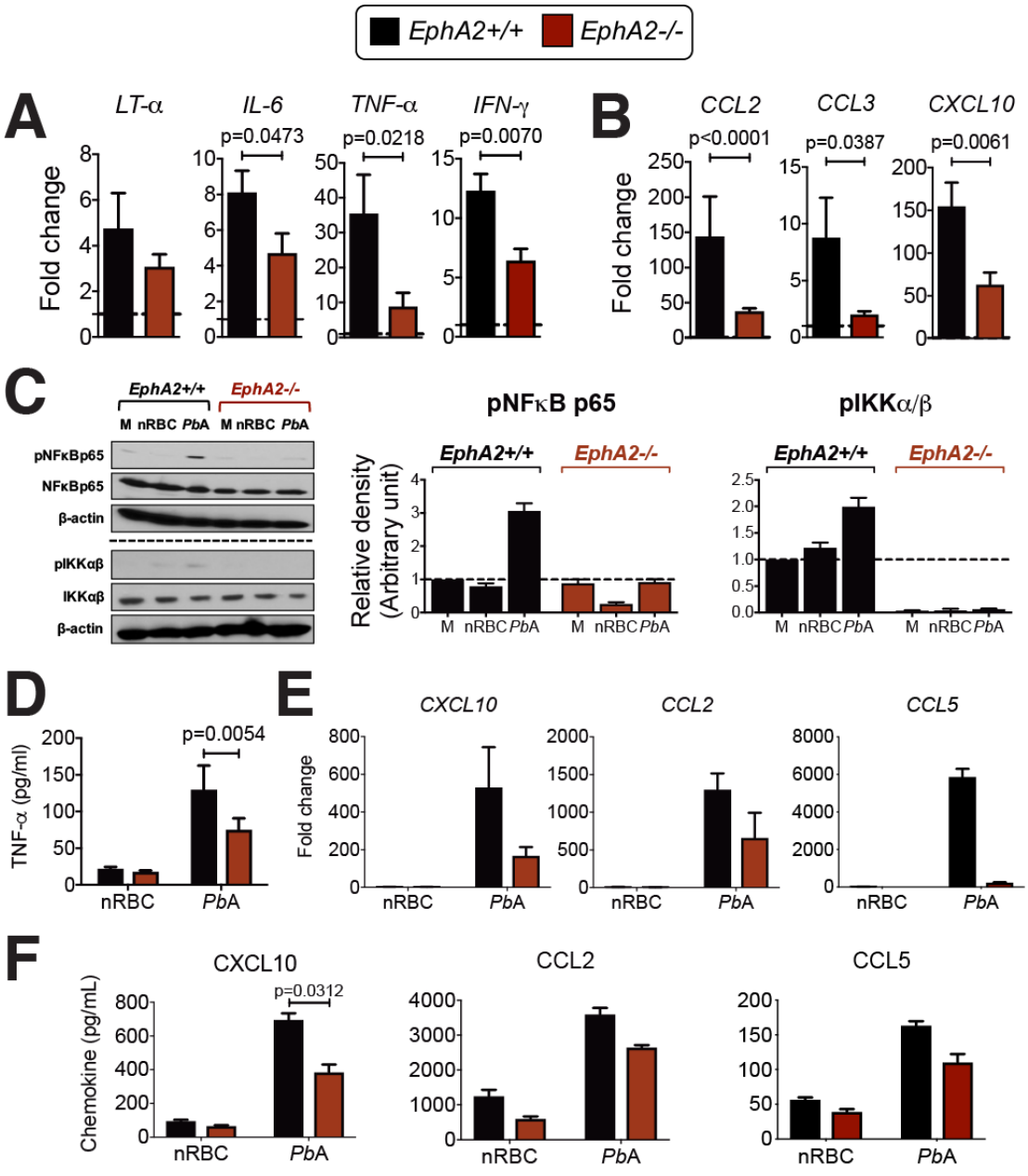
EphA2+/+
EphA2-/-
A
LT-α
IL-6
TNF-α
IFN-γ
p=0.0473
p=0.0218
p=0.0070
Fold change
B
CCL2
CCL3
CXCL10
p<0.0001
p=0.0387
p=0.0061
Fold change
C
EphA2+/+
EphA2-/-
M nRBC PbA M nRBC PbA
pNFκBp65
NFκBp65
β-actin
pIKKαβ
IKKαβ
β-actin
pNFκB p65
pIKKα/β
Relative density (Arbitrary unit)
M nRBC PbA M nRBC PbA
D
TNF-α (pg/ml)
p=0.0054
nRBC
PbA
E
CXCL10
CCL2
CCL5
Fold change
nRBC
PbA
F
CXCL10
CCL2
CCL5
Chemokine (pg/mL)
p=0.0312
nRBC
PbA

Fig 6. Brain inflammatory response is reduced in *Pb*A-infected *EphA2-/-* mice. Transcription of inflammatory cytokines **(A)** and chemokines **(B)** in whole brain lysates of *EphA2-/-* and littermate control mice at day 6 post-infection with *Pb*A (n=11-13/group) relative to naïve mice (dashed lines). **(C)** Western blots and densitometry quantification of MBMECs derived from *EphA2-/-* or littermate control mice and incubated with media (M), naïve red blood cell lysate (nRBC), or *Pb*A-infected red blood cell lysate (*Pb*A) for 30 minutes. Blots are representative of 3 endothelial preparations. The horizontal dashed line indicates two separate Western blots. **(D)** TNF-α secreted from identical culture conditions as described in C after 24 hours incubation (n=4 endothelial preparations). **(E)** Mouse primary brain endothelial cells derived from *EphA2-/-* or littermate control mice were incubated with naïve red blood cell (nRBC) or *Pb*A-infected red blood cell lysate (*Pb*A) for 24 hours and the fold change in the transcription of chemokines relative to unstimulated controls is shown (n=2 endothelial cultures/group). Chemokines secreted from identical culture conditions are shown in **(F)** (n=4-6 endothelial preparations/group). Bars in all graphs represent the mean ± SEM. Only statistically significant ($p<0.05$) values are shown. Statistical analyses: Mann-Whitney test (A-B) and Wilcoxon matched-pairs test (D-F). Only statistically significant ($p<0.05$) values are shown. Figures represent combined data from 2 (E), 3 (A-C), 4 (D, F-middle and right panels), or 6 (F-left panel) independent experiments.

Fig. 7

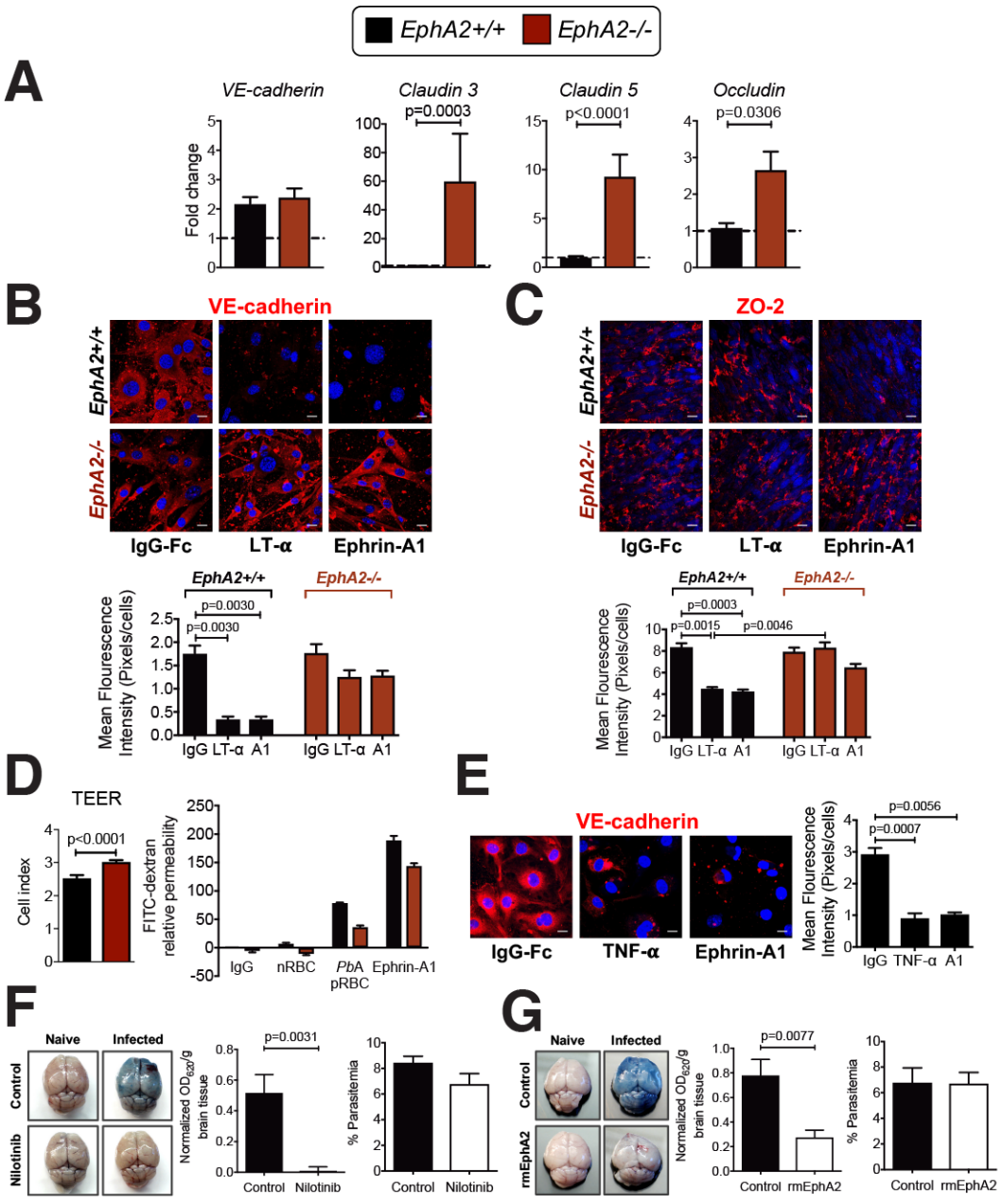
EphA2+/+
EphA2-/-
A
VE-cadherin
Claudin 3
p=0.0003
Claudin 5
p<0.0001
Occludin
p=0.0306
Fold change
B
VE-cadherin
EphA2+/+
EphA2-/-
IgG-Fc
LT-α
Ephrin-A1
Mean Flourescence Intensity (Pixels/cells)
p=0.0030
p=0.0030
IgG LT-α A1
C
ZO-2
p=0.0003
p=0.0015
p=0.0046
D
TEER
p<0.0001
Cell index
FITC-dextran relative permeability
IgG
nRBC
PbA pRBC
Ephrin-A1
E
VE-cadherin
TNF-α
p=0.0056
p=0.0007
IgG TNF-α A1
F
Naive
Infected
Control
Nilotinib
p=0.0031
Normalized OD620/g brain tissue
% Parasitemia
Control Nilotinib
G
rmEphA2
p=0.0077
Control rmEphA2

Fig 7. Endothelial cell barrier integrity is enhanced in the absence of EphA2. (**A)** Transcription levels of adherens and tight junction proteins in whole brains of *EphA2*-/- and *EphA2*+/+ mice at day 6 post-infection with *Pb*A (n=8-10/group) relative to naïve mice (dashed line). **(B-C)** Immunofluorescence images and fluorescence quantification of mouse primary brain endothelial cells derived from *EphA2*-/- or littermate control mice showing expression of adherens junction protein vascular endothelial cadherin (VE-cadherin, red) **(B)** and tight junction protein zonula occludens-2 (ZO-2, red) **(C)** after stimulation for 24 hours with recombinant mouse LT-α, recombinant mouse ephrin-A1-Fc, or IgG-Fc as a negative control. Cell nuclei are stained with DAPI (blue). Scale bars represent 25μm. **(D)** Baseline MBMEC transendothelial electrical resistance (TEER, left) and relative permeability (right) of MBMECs from *EphA2*-/- and *EphA2*+/+ mice. On right, transwell cultures were incubated for 2 hours with naïve RBC lysate (nRBC), *Pb*A-infected RBC lysate (*Pb*A pRBC), or mouse ephrin-A1-Fc ligand. Permeability is relative to IgG-stimulated *EphA2*+/+ endothelial cultures (n=3 endothelial preparations/group). **(E)** Immunofluorescence images and fluorescence quantification of human primary brain endothelial cells showing expression of VE-cadherin (red) after stimulation for 24 hours with recombinant human TNF-α, recombinant human ephrin-A1-Fc, or IgG-Fc as a negative control. Cell nuclei are stained with DAPI (blue). Scale bars represent 10μm. **(F-G)** Brain permeability in C57BL/6J mice either orally gavaged with 100μL Nilotinib or vehicle control (100 mg/kg/day; n=8-10/group) **(F)** or injected intraperitoneally with 200μL recombinant EphA2-Fc or vehicle control on days 4-6 post-infection (13.3 μg/mouse/day; n=4-12/group) **(G)**. Mice were injected intravenously with 200μL of 1% Evan's Blue at day 6 post-infection with *Pb*A. OD values are normalized to naïve mice from each respective treatment group. Bars in all graphs **Fig 7.**

(continued) represent the mean ± SEM. Statistical analyses: Mann-Whitney test (A, D - left, F, G) and Kruskal-Wallis and Dunn's multiple comparisons tests (B, C, E). Only statistically significant ($p<0.05$) values are shown. All figures are representative of 2 (A, B, C, E-G) or 3 (D) independent experiments.

Fig. 8

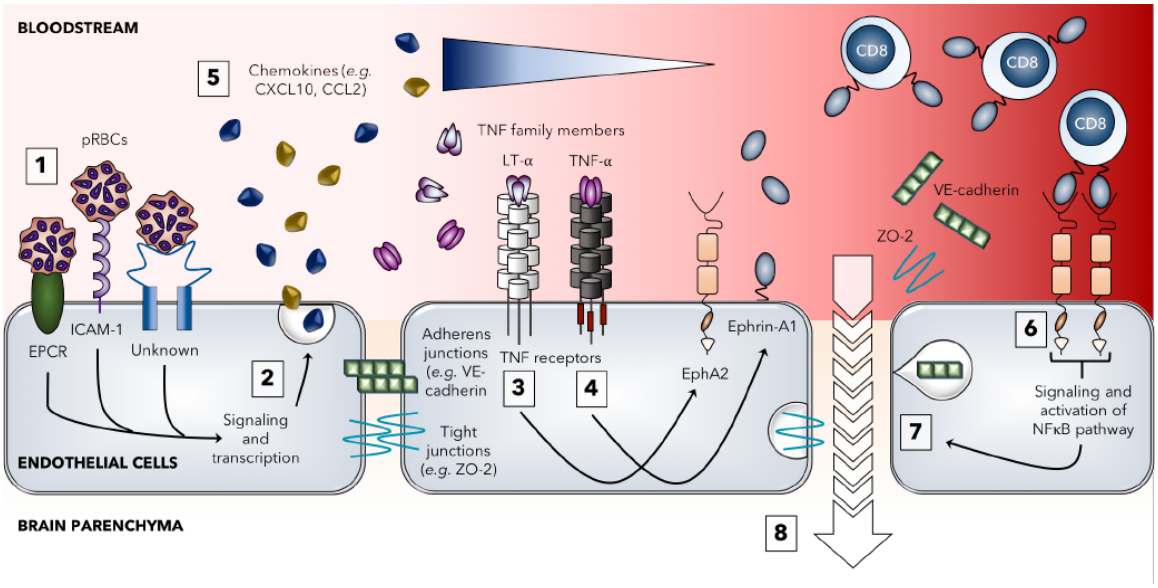
BLOODSTREAM
5
Chemokines (e.g. CXCL10, CCL2)
TNF family members
LT-α
TNF-α
CD8
CD8
CD8
VE-cadherin
ZO-2
1
pRBCs
ICAM-1
EPCR
Unknown
2
Signaling and transcription
ENDOTHELIAL CELLS
Adherens junctions (e.g. VE-cadherin
Tight junctions (e.g. ZO-2)
TNF receptors
3
4
Ephrin-A1
EphA2
6
Signaling and activation of NFκB pathway
7
8
BRAIN PARENCHYMA

Fig 8. Model for the role of EphA2 in the development of experimental cerebral malaria. The breakdown of the blood-brain barrier during blood-stage *Pb*A infection begins with parasitized red blood cells (pRBCs) in the schizont stage traveling through the bloodstream and adhering to various receptors expressed on brain microvascular endothelial cells including EPCR, ICAM-1, and other unknown receptors that have yet to be identified **(1)**. Signaling through these receptors leads to endothelial activation **(2)** and release of various pro-inflammatory cytokines and chemokines. The cytokine LT-α can act on proximal endothelial cells to induce upregulation of the receptor EphA2 **(3)** while TNF-α induces upregulation of ephrin-A1 ligand **(4)** which can be cleaved by metalloproteinases and released into the bloodstream (although this monomeric form is not believed to signal). Chemokines such as CXCL10 and CCL2 recruit circulating immune cells, including CD8+ T cells, to the brain to the site of inflammation **(5)**. Upon entry into the brain microvasculature, CD8+ T cells expressing ephrin-A1 ligand bind to EphA2 expressed on brain endothelial cells leading to clustering and activation of EphA2. Forward signaling cascades from the EphA2 receptor lead to activation of the NFκB pathway **(6)** which results in various downstream consequences including disruption of endothelial cell junctions due to both internalization and shedding of different adherens and tight junction protein components **(7)**. Once brain endothelial cell junctions are disrupted, contents of the vasculature can leak into the brain parenchyma **(8)** leading to vascular leakage, brain edema, and the development of other neurological symptoms associated with *Pb*A infection. In the absence of EphA2 upregulation or activation (*i.e.* EphA2 deficiency, PbNK65 infection, therapeutic targeting), this endothelial junction disruption does not occur and the blood-brain barrier remains intact.

Supplementary Materials for

EphA2 contributes to disruption of the blood-brain barrier in cerebral malaria

Thayer K. Darling, Patrice N. Mimche, Christian F. Bray, Banlanjo Umaru, Lauren M. Brady, Colleen Stone, Carole Else Eboumbou Moukoko, Thomas Lane, Lawrence S. Ayong, and Tracey J. Lamb*.

*Correspondence to: tracey.lamb@path.utah.edu

This section includes:

Figures S1 to S5
Tables 1-2: Mouse and human primer sequences

Fig. S1

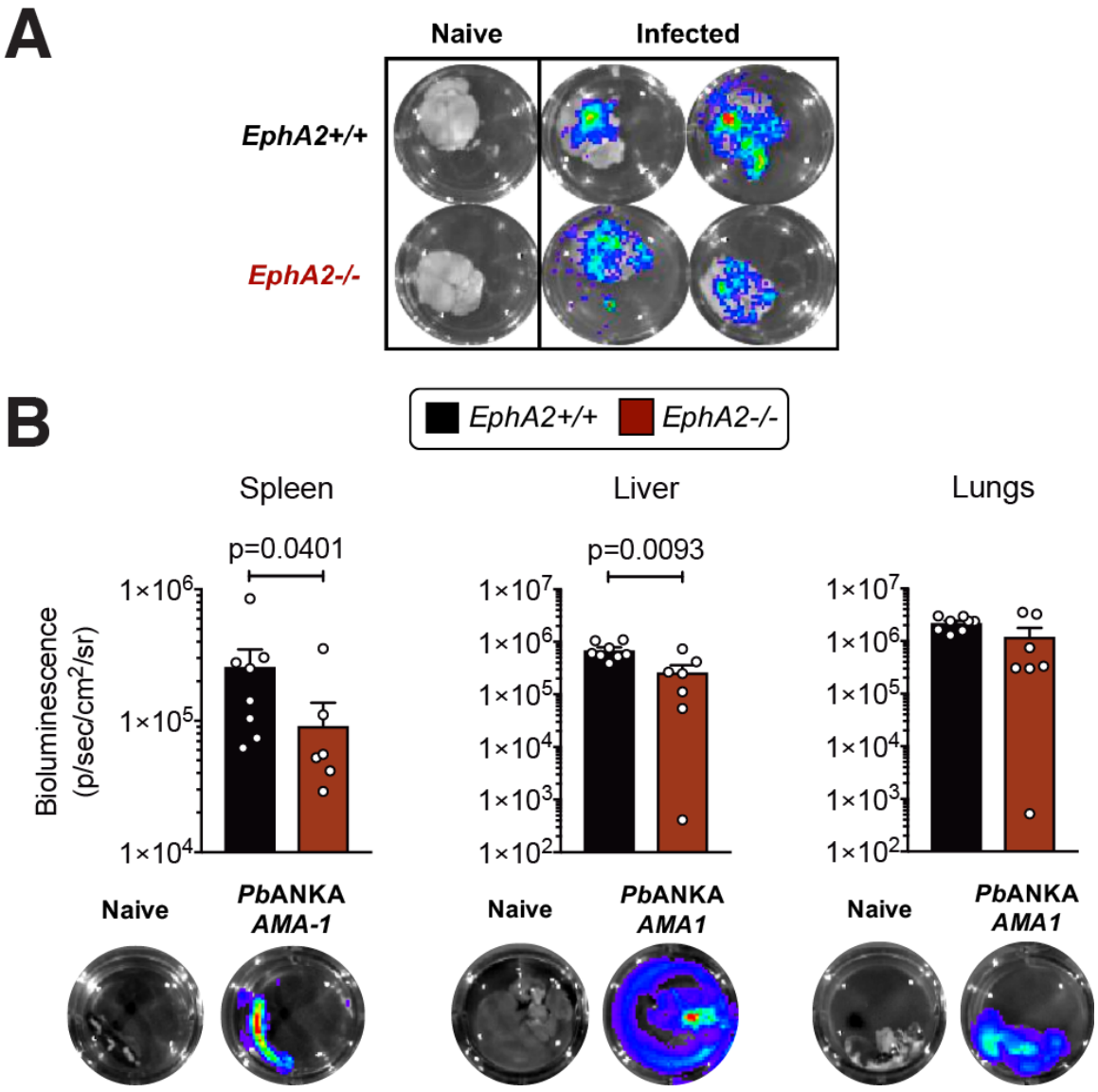
A
Naive
Infected
EphA2+/+
EphA2-/-
B
EphA2+/+
EphA2-/-
Spleen
Liver
Lungs
p=0.0401
p=0.0093
Bioluminescence (p/sec/cm²/sr)
1×10⁶
1×10⁵
1×10⁴
1×10⁷
1×10³
1×10²
Naive
PbANKA AMA-1
PbANKA AMA1

Fig S1. Parasite sequestration differs in spleen and liver, but not lung or brain, of *EphA2-/-* mice. (A) Representative images of *Pb*A schizonts expressing luciferase under the AMA-1 promoter sequestered in brains isolated from *EphA2-/-* and littermate control mice at day 6 post-infection in comparison to brains from naïve mice. **(B)** Quantification and representative images of *Pb*A schizonts expressing luciferase under the AMA-1 promoter (n=7-8/group) sequestered in spleen, liver, and lung tissue of *EphA2-/-* and littermate control mice at day 6 post-infection. Bioluminescence values are normalized to naïve mice from each respective group. Bars in all graphs represent the mean ± SEM. Statistical analyses: Mann-Whitney test (B). Only statistically significant ($p<0.05$) values are shown. Figures are representative of 2 (A-B) independent experiments.

Fig. S2

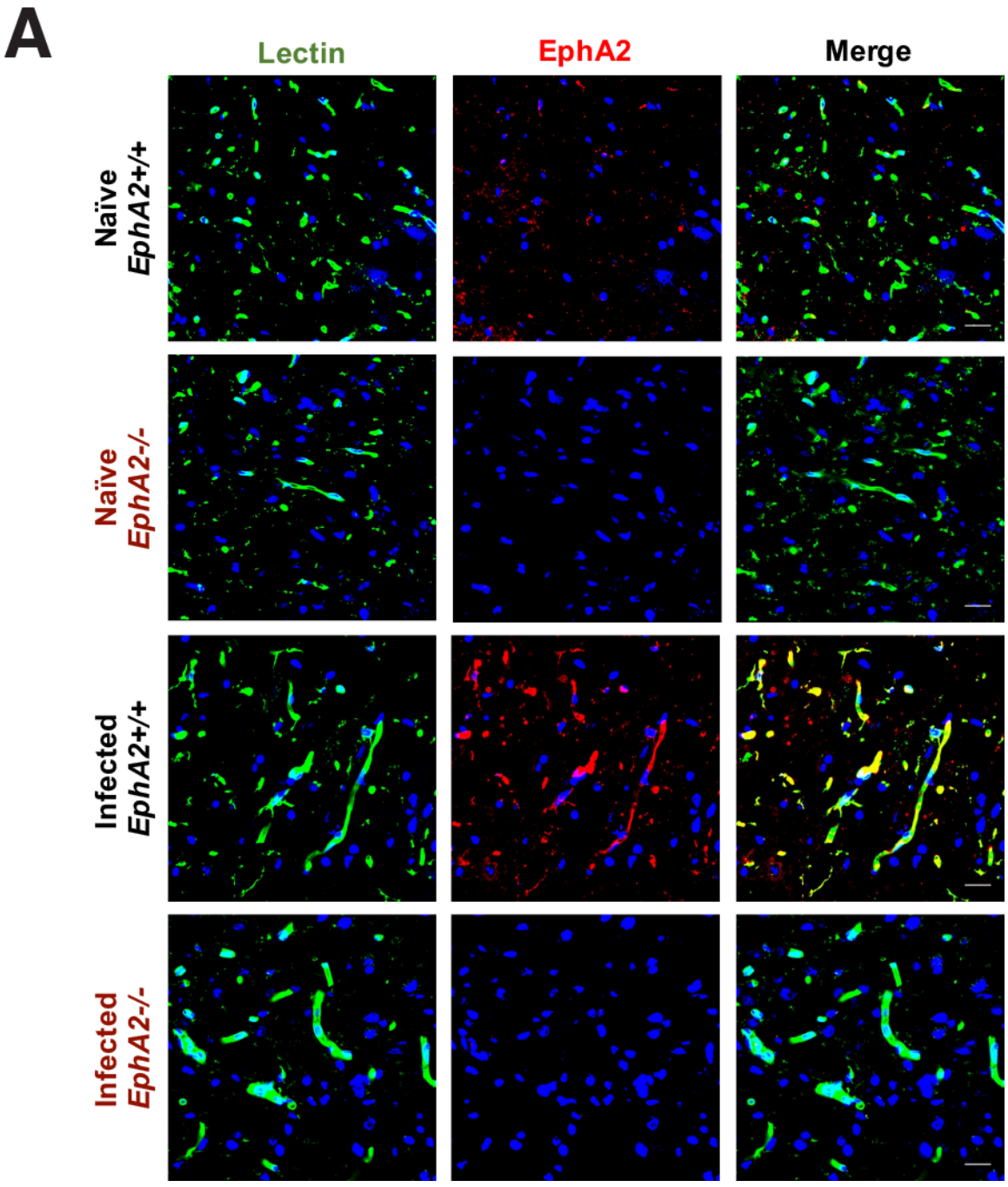
A
Lectin
EphA2
Merge
Naïve EphA2+/+
Naïve EphA2-/-
Infected EphA2+/+
Infected EphA2-/-

Fig S2. EphA2 protein is expressed on brain endothelial cells and upregulated during *Pb*A infection. (A) Immunofluorescence images demonstrating co-expression of the lectin-labeled vasculature (green) and EphA2 (red) in the cortex of sagittal slices from brains of *EphA2*-/- and *EphA2*+/+ mice isolated at day 6 post-infection with *Pb*A compared to naïve mice. Cell nuclei stained with DAPI (blue). Scale bars represent 25μm. Images representative of 2 independent experiments.

Fig. S3

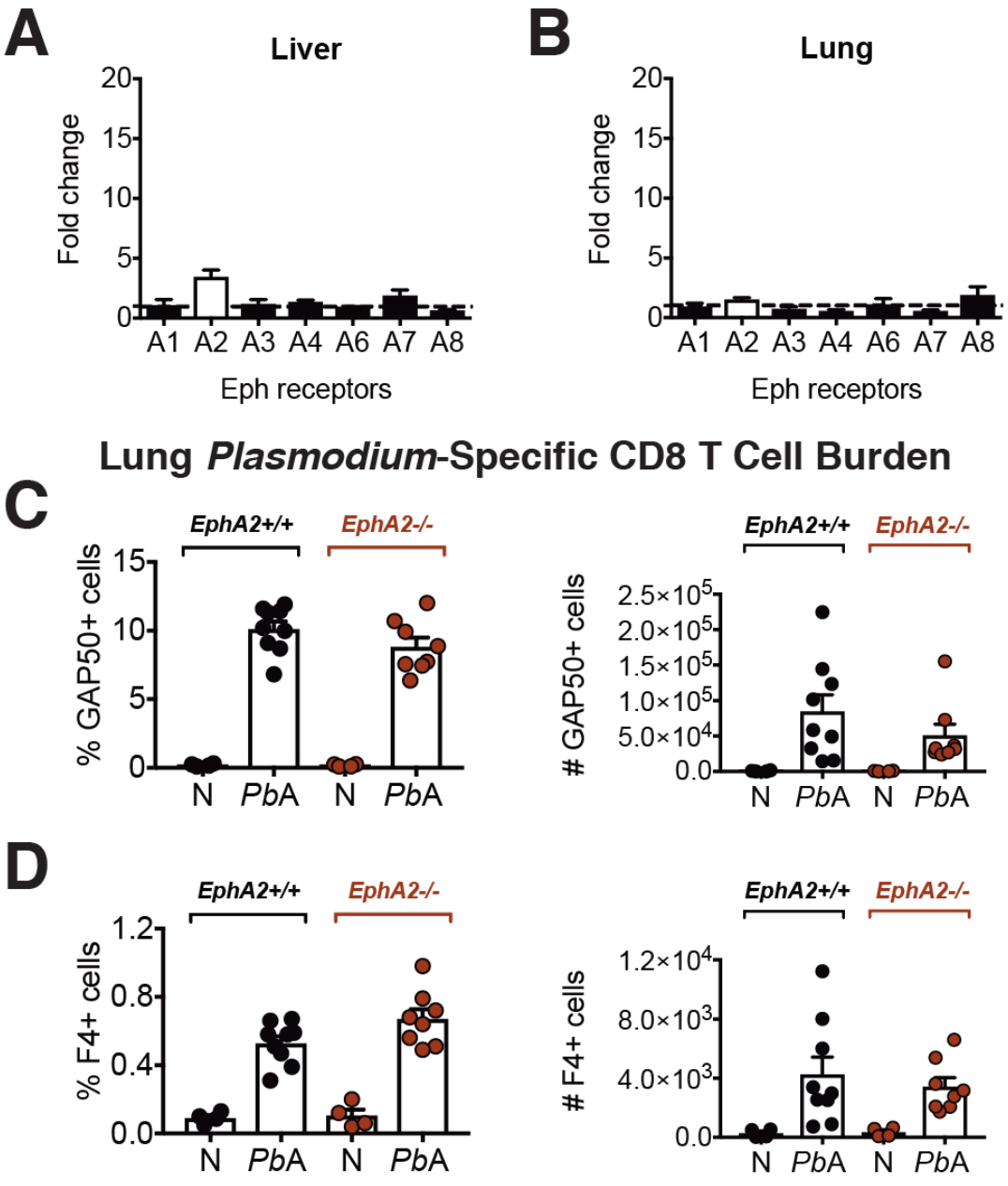
A
Liver
Fold change
20
15
10
5
0
A1 A2 A3 A4 A6 A7 A8
Eph receptors
B
Lung
Fold change
20
15
10
5
0
A1 A2 A3 A4 A6 A7 A8
Eph receptors
Lung Plasmodium-Specific CD8 T Cell Burden
C
EphA2+/+
EphA2-/-
% GAP50+ cells
15
10
5
0
N PbA N PbA
EphA2+/+
EphA2-/-
GAP50+ cells
2.5×10^5
2.0×10^5
1.5×10^5
1.0×10^5
5.0×10^4
0.0
N PbA N PbA
D
EphA2+/+
EphA2-/-
% F4+ cells
1.2
0.8
0.4
0.0
N PbA N PbA
EphA2+/+
EphA2-/-
F4+ cells
1.2×10^4
8.0×10^3
4.0×10^3
0.0
N PbA N PbA

Fig S3. *EphA2* expression is not upregulated in the liver and lung and EphA2 is not required for CD8+ T cell migration to the lung during *Pb*A infection. Transcription of EphA receptors relative to naïve mice (dashed line) in liver (n=8/group) **(A)** and lung (n=7-11/group) **(B)** lysates of C57BL/6J mice at day 6 post-infection with *Pb*A. **(C-D)** Frequency (left) and total number (right) of *Plasmodium* GAP50-reactive (n=8-9/group) **(C)** and *Plasmodium* F4-reactive (n=8-9/group) **(D)** CD8+ T cells present in the lungs of *EphA2*-/- and littermate control mice at day 6 post-infection with *Pb*A compared to naïve mice (N) (n=4/group). Naïve and *Pb*A-infected groups are significantly different within each genotype for all graphs. Bars in all graphs represent the mean ± SEM. Statistical analyses: Mann-Whitney tests (C-D). Only statistically significant ($p<0.05$) values are shown unless otherwise noted in the legend. Figures are representative of 2 (A-D) independent experiments.

Fig. S4

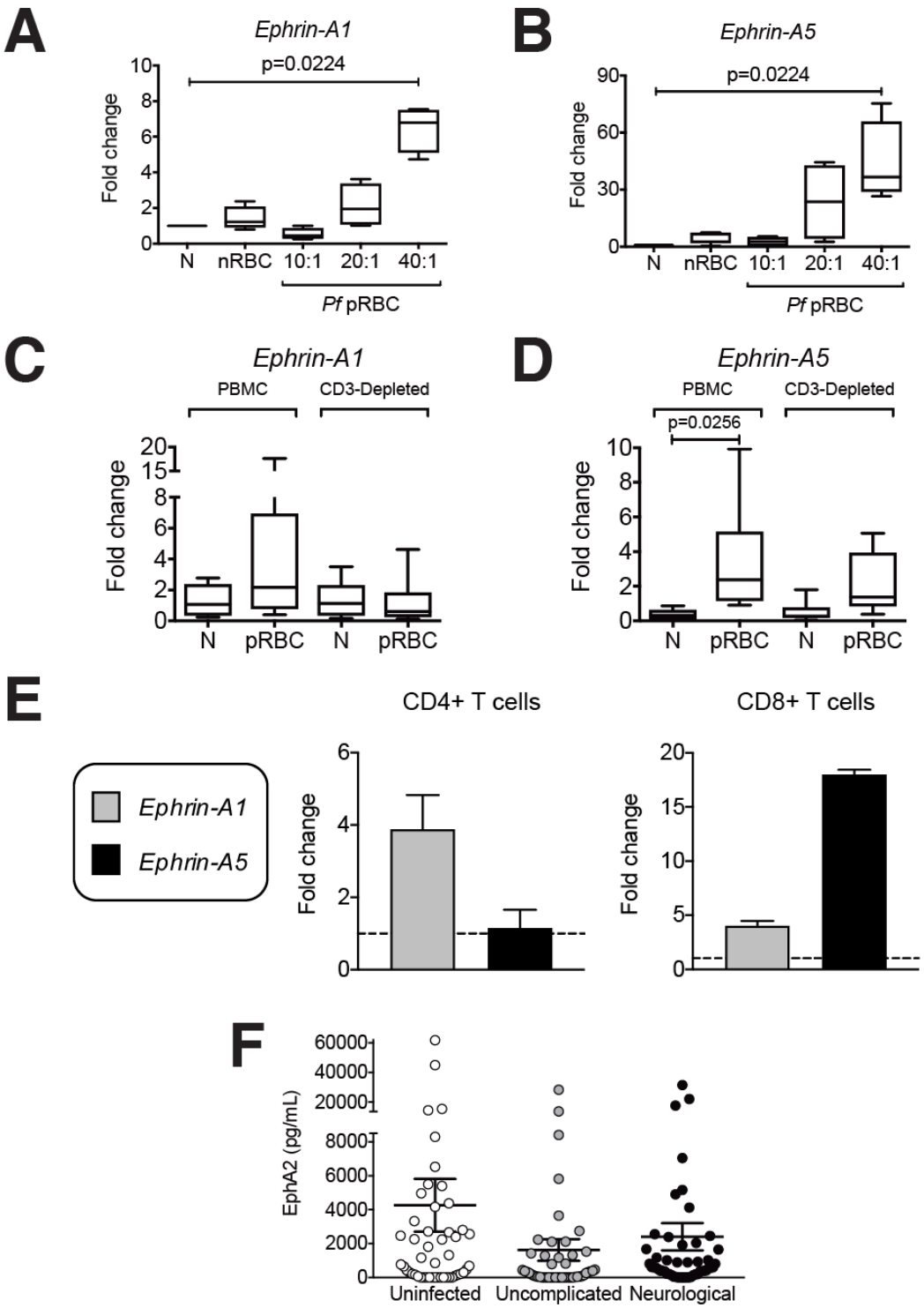
A
Ephrin-A1
p=0.0224
Fold change
N
nRBC
10:1
20:1
40:1
Pf pRBC
B
Ephrin-A5
p=0.0224
Fold change
N
nRBC
10:1
20:1
40:1
Pf pRBC
C
Ephrin-A1
PBMC
CD3-Depleted
Fold change
N
pRBC
N
pRBC
D
Ephrin-A5
PBMC
CD3-Depleted
p=0.0256
Fold change
N
pRBC
N
pRBC
E
Ephrin-A1
Ephrin-A5
CD4+ T cells
Fold change
CD8+ T cells
Fold change
F
EphA2 (pg/mL)
Uninfected
Uncomplicated
Neurological

Fig S4. Exposure to *Plasmodium* increases transcription of ephrin-A ligands in human PBMCs, particularly CD3+ T cells, and mouse CD4+ and CD8+ T cells. (A-B) Transcription of ephrin-A1 and ephrin-A4, ligands known to bind with high affinity to EphA2, in PBMCs isolated from healthy human donors incubated with naïve red blood cell lysates (nRBC) or *P. falciparum*-infected red blood cell lysates (*Pf* pRBC) (clone W2) at different ratios for 48 hours. **(C-D)** Transcription of ephrin-A1 and ephrin-A5 ligands in PBMCs isolated from healthy human donors incubated with naïve red blood cells lysates (nRBC) or *P. falciparum*-infected red blood cell lysates (pRBC) (clone 3D7) at a ratio of 40:1 for 48 hours before and after CD3+ T cell magnetic depletion. Boxes in A-D represent the median ±25th and 75th percentiles with minimum/maximum whiskers and transcription is relative to unstimulated PBMCs (N). **(E)** Transcription of ephrin-A1 and ephrin-A5 ligands on CD4+ and CD8+ T cells sorted from the spleens of C57BL/6J mice at day 5 post-infection with *Pb*A (n=8) relative to naïve mice (dashed line). **(F)** Levels of soluble EphA2 in the plasma of children living in an area in Cameroon endemic for *P. falciparum* malaria. Patients were categorized by admission to the hospital for neurological complications (n=51), uncomplicated malaria (n=50), or uninfected and presenting for routine pediatric tests (n=49). Each dot represents an individual patient. Bars in E-G represent the mean ± SEM. Statistical analyses: Kruskal-Wallis and Dunn's multiple comparisons tests (A-D) and General linear modeling and Tukey's pairwise comparison post-ANOVA (G). Only statistically significant ($p<0.05$) values are shown. Figures are representative of 2 (E), 4 (A, B), or 6 (C, D) independent experiments.

Fig. S5

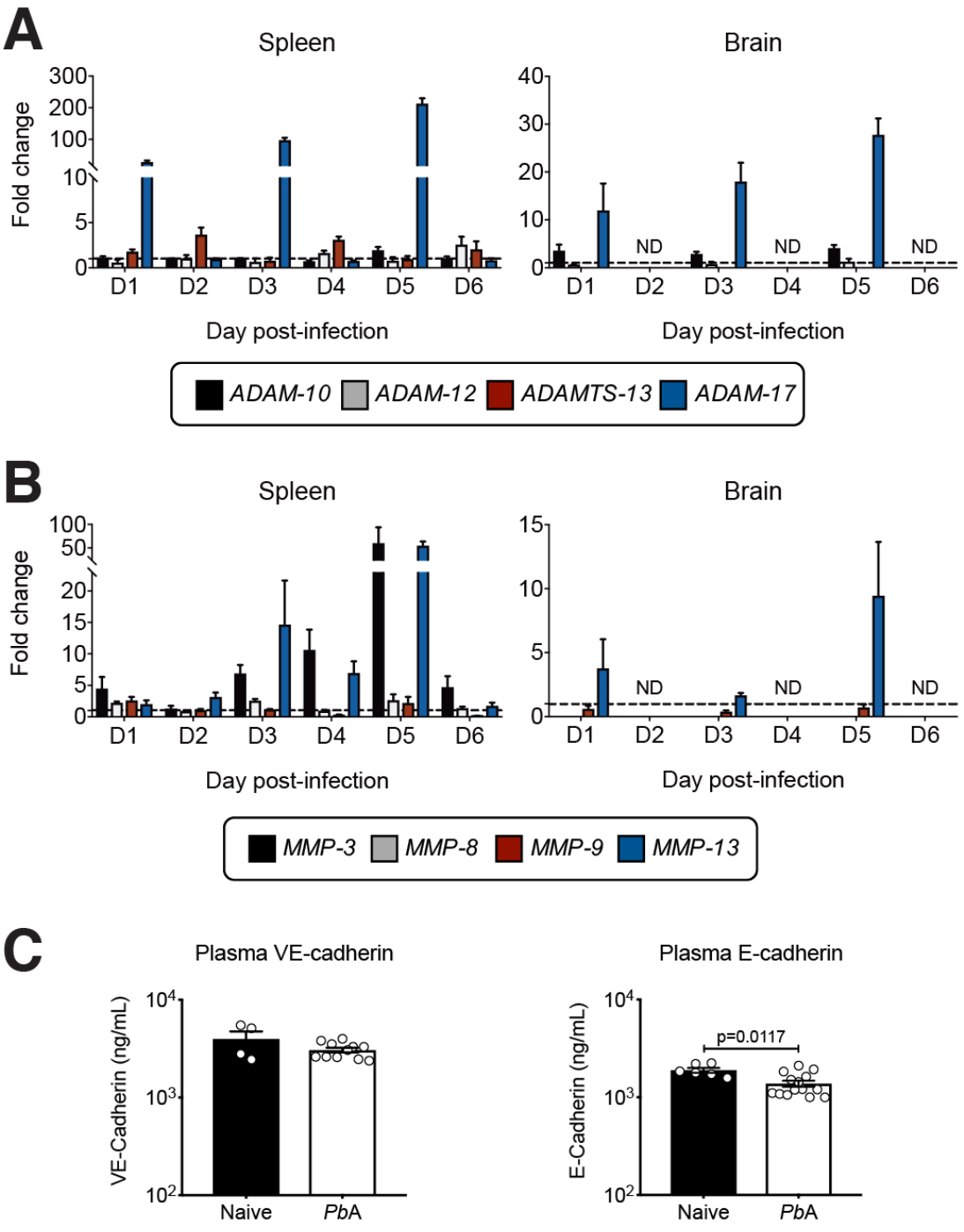
A
Spleen
Brain
Fold change
300
200
100
10
5
0
40
30
20
10
ND
D1
D2
D3
D4
D5
D6
Day post-infection
ADAM-10
ADAM-12
ADAMTS-13
ADAM-17
B
Spleen
Brain
Fold change
100
50
20
15
10
5
0
15
10
5
ND
Day post-infection
MMP-3
MMP-8
MMP-9
MMP-13
C
Plasma VE-cadherin
Plasma E-cadherin
VE-Cadherin (ng/mL)
E-Cadherin (ng/mL)
10^4
10^3
10^2
p=0.0117
Naive
PbA

Fig S5. Transcription of metalloproteinases is upregulated in the spleen and brain during the course of *Pb*A infection. Transcription of a disintegrin and metalloproteinase domain-containing proteins (ADAM-10, ADAM-12, ADAM-17) with thrombospondin motifs (ADAMTS-13) **(A)** and matrix metalloproteinases (MMP-3, MMP-8, MMP-9, MMP-13) **(B)** relative to naïve mice (dashed line) in spleen (n=4/day) and brain (n=4/day) lysates of C57BL/6J mice at different time points post-infection with *Pb*A. ND indicates no transcript was detected. **(C)** VE-cadherin (left) and E-cadherin (right) present in the plasma of C57BL/6J mice at day 6 post-infection with *Pb*A (n=11-14/group) compared to naïve mice (n=4-6/group). Bars in all graphs represent the mean ± SEM. Statistical analyses: Mann-Whitney test (C). Only statistically significant ($p<0.05$) values are shown. Figures are representative of 1 (A-B) or 2 (C) independent experiments.

Gene	Forward Primer	Reverse Primer
Ephrin-A1	CCTCAGGCCCATGACAATCCACAGG	CCTTCACGGGGTTTGCAGCAAGC
Ephrin-A5	CCAGGCGTGATGTTGCACGTGG	CCAGTAGACAGCGTAGCGGTCG
EphA1	ATCAGGGACTCAACTCTCCCT	TGCACACCTTTTCCACAGGGT
EphA2	TCCATTAAGGACTCGGGGCAGGAGG	CTCGCTCTCGGTCCGATCCCCC
EphA3	CCGCTCTGCTTCAGCGCACG	GGCTGCCTTTCCGCGAACCC
EphA4	GATGCCACCTGTGCCAAGTGCCC	TCAAGTTCAGGGGAGCAGATGGTGG
EphA6	ACTGTGGTGGATGCAATTCCCCTCG	TGCAGCTGCTTCGGAGGAGGACG
EphA7	CCAGAGGCTCTTCGCTGCTGT	CCGTGATGACTCCATTGGGAT
EphA8	CACCACGAACCAGGCAGCCC	CCACAGCAGCGAGACGCTGG
Pb18S	AAGCATTAAATAAAGCGAATACATCCT-TAC	GGAGATTGGTTTTGACGTTTATGTG
CD8α	GCTCAGTCATCAGCAACTCG	ATCACAGGCGAAGTCCAATC
LT-α	AGTCTGTGTATCCGGGACTTCAA	GGTCTCCCTTACTGAGCAGGAA
TNF-α	TCTCATTCCTGCTTGTGGC	CACTTGGTGGTTTGCTACG
IL-6	ACACATGTTCTCTGGGAAATCGT	AAGTGCATCATCGTTGTTCATACA
CCL2	GGCTCAGCCAGATGCAGTTAA	CCTACTCATTGGGATCATCTTGCT
CCL3/MIP-1α	CCATGACACTCTGCAACCAAGT	TCCGGCTGTAGGAGAAGCA

CCL5/RANTES	GCAAGTGCTCCAATCTTGCA	CTTCTCTGGGTTGGCACACA
CXCL10	GACGGTCCGCTGCAACTG	GCTTCCCTATGGCCCTCATT
IFN-γ	CGGCACAGTCATTGAAAGCCTA	GTTGCTGATGGCCTGATTGTC
VE-cadherin	CACTGCTTTGGGAGCCTTC	GGGGCAGCGATTCATTTTTCT
HPRT	GGCCCACCTAGTCAGATAAGAGTTCC	ATGGCTCAGAAACGCTGCCGG
GAPDH	TGTGTCCGTCGTGGATCTGA	TTGCTGTTGAAGTCGCAGGAG
UBIQUITIN	TGGCTATTAATTATTCGGTCTGCAT	GCAAGTGGCTAGAGTGCAGAGTAA
MMP-3	ACATGGAGACTTTGTCCCTTTTG	TTGGCTGAGTGGTAGAGTCCC
MMP-8	TCTTCCTCCACACACAGCTTG	CTGCAACCATCGTGGCATTC
MMP-9	CTGGACAGCCAGACACTAAAG	CTCGCGGCAAGTCTTCAGAG
MMP-13	CTTCTTCTTGTTGAGCTGGACTC	CTGTGGAGGTCACTGTAGACT
ADAM-10	TCATGGGTCTGTCATTGATGGA	TCAAAAACGGAGTGATCTGCAC
ADAM-12	TGGGACCAGAGAGGAGCTTAC	GTTGCACAGTCAGCACGTCT
ADAMTS-13	GAGGACACAGAACGCTACGTG	TTGGCCGTGATATTCGGAGTA
ADAM-17	GGAACACGTCGTGGGATAATG	GGCAGACTTTGGATGCTTCTT
CLAUDIN-3	GTACAAGACGAGACGGCCAA	CAGCCTAGCAAGCAGACTGT
CLAUDIN-5	GCAAGGTGTATGAATCTGTGCT	GTCAAGGTAACAAAGAGTGCCA

OCCLUDIN	TGAAAGTCCACCTC CTTACAGA	CCGGATAAAAAGAGT ACGCTGG

Supplementary Table 1. Comprehensive list of mouse primers. All mouse forward and reverse primer sequences used for mRNA amplification and RT-qPCR assays for the genes listed, including data found in both primary and supplemental figures, are included in this table.

Gene	Forward Primer	Reverse Primer
Ephrin-A1	CACAGTCCTCAGGC CCATGACAATCC	CGGGGTTTGCAGCA GCAGAAGTGG
Ephrin-A5	CCAGGCGTGATGTT GCACGTGG	CCAGTAGACAGCGT AGCGGTCG
GAPDH	GAGTCAACGGATTT GGTCGT	TTGATTTTGGAGGGA TCTCG
β-Actin	CACGAAACTACCTT CAACTCC	CATACTCCTGCTTGC TGATC

Supplementary Table 2. Comprehensive list of human primers. All human forward and reverse primer sequences used for mRNA amplification and RT-qPCR assays for the genes listed, including data found in both primary and supplemental figures, are included in this table.

CHAPTER III

Platelet α-granules contribute to organ-specific pathologies in a mouse model of severe malaria

Chapter adapted from:

Darling TK, Schenk M, Zhou C, Maloba F, Mimche PN, Gibbins J, Jobe S, and Lamb TJ (2019) Platelet α-granules contribute to organ-specific pathologies in a mouse model of severe malaria. *Blood Advances*. In press.

Figure attributions:

Figures 1-2 were contributed primarily by myself. Figure 1 contains data from M. Schenk and P. Mimche. C. Zhou and F. Maloba provided technical assistance. Supplementary figures 1-3 were contributed by myself.

Key Points

- *Nbeal2* deficiency leads to significantly reduced lung and brain pathology and enhanced survival in a mouse model of malaria
- Both antibody-dependent and antibody-independent platelet depletion in mice recapitulate the findings observed in *Nbeal2*-/- mice

Introduction

Cerebral malaria (CM) and malaria-associated acute lung injury/acute respiratory distress syndrome (MA-ALI/ARDS) are among the most severe complications of *Plasmodium* infection. While these disease manifestations are multifactorial, platelets have been described to play a role in the development of both syndromes in humans (*251, 252*) and mice (*338, 339*). Although the impact of platelets on malaria has been well-studied, questions remain with regard to their contribution to parasite control and immunopathogenesis. Studies have indicated that platelets can kill *Plasmodium*-infected red blood cells (iRBCs) (*255, 266-268*). However, there are contrasting reports that platelets do not exert any significant control over parasite growth but rather exacerbate malaria immunopathology (*246, 256, 264, 338, 340*). In this study, we address the role of platelets in the development of severe malaria in three different mouse models of platelet dysfunction/depletion. We show a key role for platelets, and particularly platelet alpha granules (α-granules), in mediating organ-specific pathologies during rodent *Plasmodium* infection.

Materials and methods

Rodent *Plasmodium* infection

Female C57BL/6J mice aged 6-12 weeks were bred in-house or purchased from The Jackson Laboratory. Homozygous *Nbeal2*-/- mice on a C57BL/6J background originated from the Di Paola laboratory and were obtained by Dr. Robert Campbell to be bred in-house. C57BL/6-Tg(Pf4-icre)Q3Rsko/J mice (PF4-Cre, Stock 008535) and C57BL/6-*Gt(ROSA)26Sor*$^{tm1(HBEGF)Awai}$/J mice (B6-iDTR, Stock 007900) were purchased from The Jackson Laboratory. Homozygous B6-iDTR mice were bred with PF4-Cre positive or negative mice to generate Pf4-Cre positive/iDTR and Pf4-Cre negative/iDTR mice. Infections were initiated intraperitoneally with 0.5x10^6 *Plasmodium berghei* ANKA *(Pb*A) iRBCs (clone15cy1, 1037cl1 WT-GFP-Luc$_{schiz}$; mutant RMgm-32, or a constitutive GFP-expressing clone) obtained from donor C57BL/6J mice. Peripheral parasitemia was monitored by counting 300-500 red blood cells (RBCs) on Diff-Quik (Siemens) stained thin blood smears. All experiments were carried out according to protocols approved by the Institutional Animal Care Use Committees and Biosafety Committees of Emory University (DAR-2000454-021114BN, HAD01-2425-11R15-101915) and the University of Utah (17-01001, 05-17).

Tissue preparation for flow cytometry

Spleens were pressed through a 40μm cell strainer and suspended in Iscove's Modified Dulbecco's Medium (IMDM) containing 100units/mL penicillin, 100μg/mL streptomycin, 1μM L-glutamine, 12mM HEPES, 0.5mM sodium pyruvate, 5 X 10^{-5}M 2-mercaptoethanol (all Gibco) (cIMDM). Single cell suspensions of splenocytes were centrifuged at 1500rpm for 8 minutes at 4°C prior to RBC lysis of the pellet using an RBC lysis buffer (BioLegend). Splenocytes were centrifuged again before resuspension in cIMDM with the addition of 10% heat-inactivated fetal calf serum (HI-FCS) (PAA Laboratories) for downstream flow cytometric analysis. Brains were pressed through a 100μm cell strainer and resuspended in a

30% Percoll solution before overlaying onto a 70% Percoll gradient. Brain samples were centrifuged at 600g for 20 minutes at room temperature with no brake. The peripheral blood mononuclear cell (PBMC) interface was collected and washed with cIMDM + HI-FCS before resuspension in cIMDM + HI-FCS for downstream flow cytometric analysis. Lungs were placed in a 6-well plate and minced with scissors prior to incubation in digestion media (RPMI + collagenase D (Roche) + DNase (Invitrogen)) at 37°C for 30 minutes in a shaking incubator. Cells were filtered through a 100μm cell strainer and centrifuged at 1500rpm for 8 minutes at 4°C. The pellet was then suspended in a 40% Percoll solution before overlaying onto an 80% Percoll gradient. Lung samples were centrifuged at 1600rpm for 25 minutes at room temperature with no brake. The interface was collected and washed prior to RBC lysis and resuspension in cIMDM + HI-FCS for downstream flow cytometric analysis.

Flow cytometry staining

Whole blood (5μL) was collected into Krebs saline containing antibodies of interest for staining. Platelet depletion efficacy was determined by size and granularity and CD41 expression (PE, Pacific Blue, or BV421, cl. MWReg30) via flow cytometry. For time course experiments monitoring platelet-iRBC aggregation and platelet activation, the following additional antibodies were used: TER-119 (APC/Cy7 or BV786, cl. TER-119), CD62P/P-selectin (PE or PE/Cy7, cl. RMP-1), CD63 (APC, cl. NVG-2), (all from BioLegend) and αIIbβ3 (PE, cl. JON/A) (EmFret). A *Pb*ANKA clone expressing constitutive GFP (*Pb*A-GFP) was used for infections in which parasites are detected via flow cytometry. For neutrophil sequestration experiments, the following antibodies were used: Ly-6G (PE, cl.

1A8), CD11b (BV605, cl. M1/70), CD19 (BV510, cl. 6D5), Ly-6C (PerCP/Cy5.5, cl. HK1.4), and Zombie NIR viability dye (all from BioLegend).

Imaging flow cytometry

Experiments were performed on an ImageStream^X Mk II imaging flow cytometer with INSPIRE acquisition software (Amnis) which allows for distinguishing coincident versus contact events. All images were captured with the 60x objective. Whole blood (5μL) was collected into Krebs saline containing antibodies of interest for staining. The following antibodies were used: CD41-BV421 (cl. MWReg30) to identify platelets and TER-119-AF647 (cl. TER-119) to identify red blood cells (both from BioLegend) in addition to the *Pb*A-GFP fluorescent parasite to identify infected red blood cells. BV421 was excited by the 405nm laser and emission captured in the range 435-505nm (Ch1), GFP was excited by the 488nm laser and emission captured in the range 505-560nm (Ch2), AF647 was excited by the 642nm laser and emission captured in the range 642-745nm (Ch5), and brightfield was captured in Ch3. Single stained controls were used to generate a compensation matrix. IDEAS v6.2 software (Amnis) was used for data analysis on compensated data.

ELISA

Mouse PF4, Elastase, and MPO ELISA kits (all from R&D Systems) were used to detect these molecules in plasma of mice according to the manufacturer's instructions.

Bioluminescent parasite imaging

Parasite burden in tissues was determined using an IVIS Spectrum Bioluminescent Imaging System (PerkinElmer). At either days 2, 4, or 6 post-infection with the *Pb*A schizont-specific

luciferase reporter line, mice were injected with 150μL RediJect D-Luciferin bioluminescent substrate (PerkinElmer) 30 minutes prior to euthanization, organ dissection, and imaging. Regions of intensity were quantified using IVIS Living Image software.

In vivo platelet/megakaryocyte depletion

C57BL/6J mice were intraperitoneally injected with 0.1mg purified anti-mouse CD41 antibody (clone MWReg30, BioLegend) or isotype control antibody (Rat IgG1, κ, BioLegend) one day post-infection with *Pb*A. Pf4-Cre positive/iDTR mice and Pf4-Cre negative/iDTR mice were intraperitoneally injected with 20ng diphtheria toxin (Sigma) on days -7, -4, and -1 prior to infection with *Pb*A.

In vivo Evans Blue permeability assay

Mice were injected intravenously with 200μL of 1% Evans Blue (Sigma) on day 6 post-infection with *Pb*A and sacrificed 1 hour later. Brains and lungs were removed and imaged using a MicroCapture digital microscope (Veho) and placed into vials containing 1mL formamide (Sigma) at 37°C for 4 days. The concentration of the dye extracted from the tissues was measured at an absorbance of 620nm using a plate reader (Biotek).

Results and discussion

Previous studies in mice have demonstrated the importance of platelets in the development of severe malaria pathology even as platelet counts decrease significantly over the course of *Plasmodium* infection (*246*) which is a phenomenon we also observe **(Figure 1A)**. In order to investigate how platelets and platelet α-granules may function to mediate severe malaria

pathogenesis, we utilized *Plasmodium berghei* ANKA (*Pb*A), a parasite strain which causes a well-established mouse model of experimental cerebral malaria (ECM) (*341*) and lung injury (*342, 343*), to infect wild-type C57BL/6J mice along with Neurobeachin-like 2 (*Nbeal2*) deficient mice which have severe defects in platelet α-granule formation (*344, 345*). Naïve *Nbeal2*-/- mice had a slight, but significant, reduction in platelets compared to naïve control mice **(Figure 1B)**. Upon infection with *Pb*A, we observed a significantly lower frequency of platelet-iRBC conjugates in whole blood isolated from *Nbeal2*-/- mice compared to C57BL/6J mice **(Figure 1C, left)** even though there were no significant differences in peripheral parasitemia between the two groups over the course of infection **(Figure 1C, right)**. Additionally, we confirmed using imaging flow cytometry that >90% of platelet-iRBC double positive events indeed represented platelets in contact with iRBCs **(Figure S1)**. While we cannot conclusively determine whether platelets become activated subsequent to contact with iRBCs or if activated platelets preferentially bind to iRBCs, these data indicate that platelet α-granules can impact the ability of platelets to interact with iRBCs. However, this interaction between platelets and iRBCs has no effect on overall peripheral parasite growth which supports previous findings (*246*).

P-selectin (CD62P) is present within platelet α-granules and is externalized upon platelet activation. Five days post-*Pb*A infection we observed a lower frequency of P-selectin+ platelets in blood from *Nbeal2*-/- mice compared to control mice as expected **(Figure 1D, left graph)**. To determine more broadly if *Nbeal2* deficiency affected overall platelet activation, we analyzed surface expression of two α-granule independent markers of platelet activation: CD63, which is present in dense granules and lysosomes and externalized upon platelet activation (*346*), and the high-affinity conformation of the integrin αIIbβ3 (CD41/CD61)

(*347*). Similar to our findings with P-selectin, we observed a significantly lower frequency of CD63+ and CD41/CD61+ platelets isolated from *Nbeal2*-/- mice at day 5 post-*Pb*A infection compared to control mice **(Figure 1D, middle graphs)** despite *Nbeal2*-/- mice containing more platelets at this time point **(Figure 1D, right graph).** The dysfunctional platelet α-granule secretion in *Nbeal2*-/- mice was further validated by the presence of significantly lower concentrations of platelet factor 4 (PF4) in *Nbeal2*-/- plasma compared to C57BL/6J control plasma in both naïve mice and in mice at day 6 post-infection with *Pb*A **(Figure 1E)**. Of note, *Pb*A-infected mice have significantly less plasma PF4 compared to naïve mice given the significant reduction in the platelet count that occurs by day 6 post-infection **(Figure 1A)**. Taken together, these data suggest that *Nbeal2* deficiency affects platelet activation as a whole in the context of severe malaria which may subsequently influence the ability of *Nbeal2*-/- platelets to interact with iRBCs.

Although we found that platelet α-granules do not inhibit *Pb*A blood-stage parasite growth **(Figure 1C, right)**, peripheral parasitemia does not reflect the quantity of iRBCs, specifically schizonts, that have sequestered in the microvasculature of organs. Therefore, we quantified iRBC sequestration in key organs of *Nbeal2*-/- mice as measured by bioluminescence of a schizont-specific luciferase-expressing *Pb*A strain. The spleen, which is responsible for iRBC clearance and activation of the immune response against iRBCs (*348*), contained significantly fewer iRBCs in *Nbeal2*-/- mice when compared to C57BL/6J mice **(Figure 1F)**. *Pb*A sequestration has been associated with acute lung injury (*343*), yet there was no significant effect of platelet dysfunction on lung parasite sequestration in the absence of *Nbeal2* **(Figure 1G)**. However, we did observe significant differences in brain parasite sequestration which has been associated with ECM (*329, 349*) as *Nbeal2*-/- mice harbored significantly fewer parasites

in the brain than control mice **(Figure 1H)**. Therefore, while platelets do not appear to alter blood-stage *Pb*A growth, platelet α-granules can potentiate *Pb*A organ sequestration.

*Pb*A-induced lung and brain damage are associated with ECM (*350*) although the contribution of platelets to these events has not been fully elucidated. Since parasite sequestration does not always correlate with ECM development (*351*), we determined whether reduced parasite sequestration was accompanied by reduced pathology in these key organs. Malaria-induced vascular permeability was significantly abrogated in both the lungs **(Figure 1I)** and brains **(Figure 1J)** of *Nbeal2-/-* mice compared to control mice at day 6 post-infection with *Pb*A. Strikingly, this protection from lung and brain damage correlated with nearly complete protection from ECM-associated death in *Nbeal2-/-* mice **(Figure 1K)**. Thus, platelet α-granules appear to impact parasite sequestration and contribute to fatal *Plasmodium*-associated organ damage during ECM.

Several recent studies have described abnormalities in neutrophils and monocytes in *Nbeal2-/-* mice in response to different pathogenic infections (*352, 353*). We also observed differences in neutrophil and monocyte trafficking in *Pb*A-infected mice with *Nbeal2-/-* mice harboring significantly more neutrophils and inflammatory monocytes in the spleen when compared to *Pb*A-infected C57BL/6J control mice **(Figure S2A)**. However, the numbers of neutrophils present in the lungs and brains of *Pb*A-infected *Nbeal2-/-* and C57BL/6J mice were similar **(Figure S2B-C, left graphs)**. *Pb*A-infected *Nbeal2-/-* mice had a significantly higher frequency and number of inflammatory monocytes in their lungs compared to *Pb*A-infected C57BL/6J control mice **(Figure S2B, right graphs)**. Previous studies have shown that inflammatory monocytes play a key role in the clearance of organ-sequestered *Pb*A-iRBCs

which can help minimize organ damage (*342*). Thus, it is possible that the increase in inflammatory monocytes in the spleens of *Nbeal2*-/- mice could participate in reducing parasite sequestration although this does not appear to be the case in the lungs where parasite sequestration was not significantly affected by *Nbeal2* deficiency. Furthermore, *Nbeal2*-/- mice also experienced significantly reduced brain parasite sequestration and pathology in the absence of any difference in brain inflammatory monocyte numbers **(Figure S2C, right graphs)**. It therefore seems unlikely that these observed differences in monocytes are responsible for the protective phenotype observed in the *Nbeal2*-/- mice. Similarly, although neutrophils have been shown in a few studies to potentially contribute to *Plasmodium*-associated lung and brain damage in severe malaria (*354, 355*), the fact that we observe no significant differences in neutrophil numbers in the lungs or brains of *Pb*A-infected *Nbeal2*-/- mice compared to C57BL/6J mice also suggests that the reduced organ damage is independent of any effects of *Nbeal2* deficiency on neutrophil function. In support of this, there are no significant differences in the levels of myeloperoxidase or elastase in the plasma of *Pb*A-infected *Nbeal2*-/- and C57BL/6J mice at day 6 post-infection **(Figures S2D-E).** This suggests similar systemic neutrophil activation at the onset of severe disease even though naïve *Nbeal2*-/- mice have significantly higher levels of both enzymes compared to naïve C57BL/6J mice as has been described previously (*353*).

Given the clearly reduced organ pathology and enhanced survival in *Pb*A-infected *Nbeal2*-/- mice, we next determined if we could recapitulate the impacts of *Nbeal2* deficiency using two different mouse models of platelet deficiency. The first involves administering an anti-CD41 antibody to deplete platelets which has been shown to protect against ECM (*264*). The second model, which has not been previously utilized in any *Plasmodium* studies, involves mice which

selectively express the diphtheria toxin receptor (DTR) on megakaryocytes allowing for diphtheria toxin-inducible (iDTR) megakaryocyte depletion and reduced platelet production (*356*). Flow cytometry confirmed that platelets are depleted equivalently in anti-CD41 (α-CD41) and Pf4-Cre positive/iDTR ((-) MK) mice **(Figure 2A)**. As in *Nbeal2*-/- mice, peripheral parasite growth at day 6 post-infection was unaffected by the absence of platelets **(Figure 2B)** further demonstrating the minimal role that platelets play in controlling *Pb*A peripheral parasite growth. Similar to *Nbeal2*-/- mice, platelet depleted mice had reduced splenic parasite accumulation **(Figure 2C)** although this trend was not significant in (-) MK mice. We found no significant differences in *Pb*A parasite burden in the lungs or brains of platelet depleted mice compared to their respective platelet intact control groups **(Figure 2D-E)**. Additionally, aside from a slight but significant difference in lung parasite burden at day 2 post-infection, we observed no clear effects of platelet depletion on parasite sequestration at earlier time points post-infection prior to day 6 **(Figure S3A-C)**. Along with the data shown in Figure 1, these data collectively suggest a more complex role for platelets in mediating parasite trafficking and/or sequestration during *Pb*A infection.

Despite similar parasite burdens, *Plasmodium*-induced vascular permeability in both the lungs **(Figure 2F)** and brain **(Figure 2G)** was significantly reduced in both models of induced thrombocytopenia. As with *Nbeal2* deficiency, platelet depleted mice also experienced significantly improved survival from ECM in both models **(Figure 2H-I)** although the magnitude of survival varied. This suggests that the method and timing of platelet depletion impacts ECM development.

In summary, our results show that *Nbeal2*-/- mice are robustly protected from the organ damage and death characteristic of *Pb*A infection suggesting the importance of platelet α-granules in contributing to severe malaria pathology. These effects of *Nbeal2* deficiency are largely recapitulated by platelet depletion. As *Nbeal2*-/- mice harbor dysfunctional platelets from birth while α-CD41 treated mice and diphtheria toxin treated (-) MK mice experience transient platelet depletion as adults, it is likely the differences among the three models of platelet dysfunction/depletion can potentially be attributed to the timing, magnitude, and/or mechanism of platelet depletion. The differing extents of brain parasite sequestration and survival in α-CD41 and (-) MK mice indicate that the methodology of platelet depletion itself may impact severe malaria pathology. Dysfunctional platelets in *Nbeal2*-/- mice may be able to recruit immune cells to sites of parasite sequestration during early *Pb*A infection in an α-granule-independent manner (*357*) benefitting the early response to infection. On the other hand, their lack of α-granules may render them unable to recruit pathogenic CD8 T cells to organs (*358*) which is required for ECM-associated pathology. Interestingly, the absence of any *in vivo* increase in peripheral parasitemia in any of our mouse models of platelet dysfunction/depletion contrasts with several studies that suggest platelets are a central mechanism responsible for killing iRBCs (*267, 359*). However, those studies primarily involve non-severe malaria models in which the kinetics of the parasite-induced inflammatory milieu likely have significant impacts on the timing of platelet activation and their subsequent response to infection. While additional research is required to continue to elucidate the complex roles of platelets in malaria, this study further supports a pathogenic role for platelets, particularly platelet α-granules, in the development of severe malaria.

Acknowledgments

We thank the following individuals: Taryn Stewart and Nicole Stokes for excellent animal husbandry; the Emory University Department of Pediatrics Flow Cytometry Core and the University of Utah Health Science Center Flow Cytometry Core for flow cytometry support; Jorge Di Paola and Robert Campbell for the *Nbeal2*-/- mice; Josh Andersen and Daniel Call at Brigham Young University for ImageStream use and technical assistance; and Chris Janse for the luciferase-expressing and GFP-expressing *Plasmodium berghei* ANKA parasite strains. This work was supported by grants from the National Institutes for Neurological Disorders and Stroke (F31NS098736) (T.K.D.), Kirschstein-NRSA training grants (T32AI007610 and T32AI106699) (T.K.D.), and the Institute for Cardiovascular Medicine and Research Seed Grant Fund (T.J.L.). T.K.D. is a PhD candidate at Emory University. This work is submitted in partial fulfillment of the requirement for the PhD degree.

Authorship Contributions

Contributions: T.K.D. devised and performed the experiments, analyzed the results, and wrote and edited the manuscript; M.P.S., C.Z., F.M.M. and P.N.M. performed the experiments; J.M.G. and S.M.J. contributed to designing the experiments; and T.J.L. devised and supervised the experiments and edited the manuscript.

Conflict-of-interest disclosure: The authors declare no competing financial interests.

Correspondence: Tracey J. Lamb, Department of Pathology, University of Utah, 15 North Medical Drive, Salt Lake City, UT 84112; e-mail: tracey.lamb@path.utah.edu.

Fig. 1

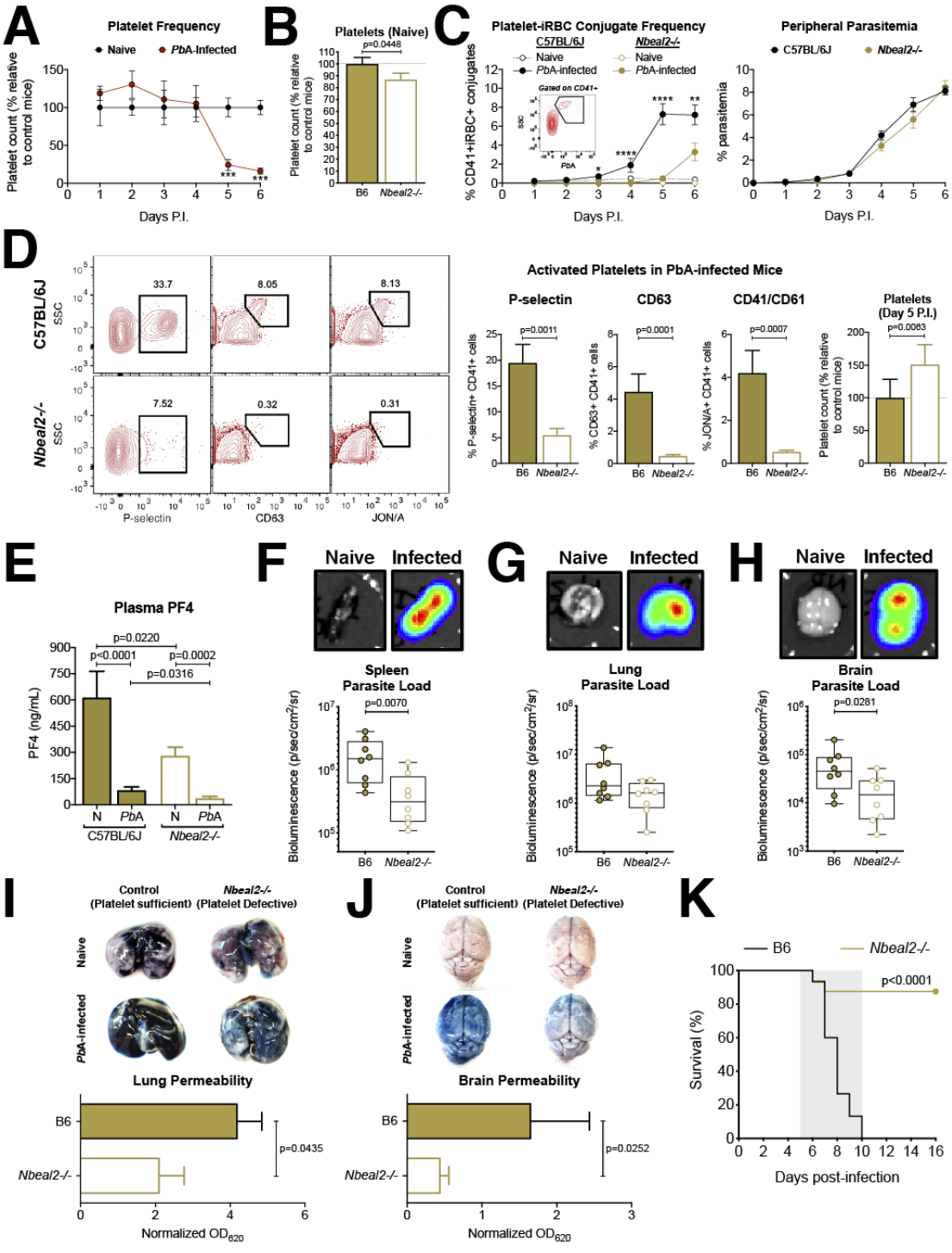
A
Platelet Frequency
Naive
PbA-Infected
Platelet count (% relative to control mice)
Days P.I.
B
Platelets (Naive)
p=0.0448
B6
Nbeal2-/-
C
Platelet-iRBC Conjugate Frequency
C57BL/6J
Nbeal2-/-
Naive
PbA-infected
% CD41+iRBC+ conjugates
Gated on CD41+
Peripheral Parasitemia
% parasitemia
D
C57BL/6J
Nbeal2-/-
SSC
P-selectin
CD63
JON/A
33.7
8.05
8.13
7.52
0.32
0.31
Activated Platelets in PbA-infected Mice
P-selectin
CD63
CD41/CD61
Platelets (Day 5 P.I.)
p=0.0011
p=0.0001
p=0.0007
p=0.0063
E
Plasma PF4
PF4 (ng/mL)
p=0.0220
p<0.0001
p=0.0002
p=0.0316
N
PbA
C57BL/6J
Nbeal2-/-
F
Naive
Infected
Spleen Parasite Load
p=0.0070
Bioluminescence (p/sec/cm²/sr)
G
Lung Parasite Load
H
Brain Parasite Load
p=0.0281
I
Control (Platelet sufficient)
Nbeal2-/- (Platelet Defective)
Lung Permeability
p=0.0435
Normalized OD620
J
Brain Permeability
p=0.0252
K
B6
Nbeal2-/-
p<0.0001
Survival (%)
Days post-infection

Figure 1. *Nbeal2* deficiency significantly alters parasite sequestration, lung and brain pathology, and survival in *Pb*A-infected mice. (A) Time-course of platelets in peripheral blood of C57BL/6J mice after *Pb*A infection compared to naïve control mice (n=7-10 mice/group) as determined by flow cytometry. (B) Platelets in whole blood of naive *Nbeal2*-/- mice normalized to naive C57BL/6J (B6) control mice as determined by flow cytometry (n=20-24 mice/group). (C) Frequency of platelet-infected red blood cell (iRBC) conjugates (left, n=10-20 mice/group) in whole blood of C57BL/6J and *Nbeal2*-/- mice after *Pb*A-GFP infection and time course of peripheral parasitemia as determined by staining and counting of thin blood smears (right, n=10 mice/group). (D) Representative flow cytometry plots and quantification of the frequency of P-selectin+, CD63+, and CD41/CD61+ platelets as well as total platelets normalized to control mice in whole blood isolated from C57BL/6J (B6) and *Nbeal2*-/- mice at day 5 post-infection with *Pb*A (n=10-26 mice/group). (E) Quantification of PF4 in the plasma of C57BL/6J and *Nbeal2*-/- mice at day 6 post-infection with *Pb*A (n=10-14 mice/group) or naïve (N) (n=9-10 mice/group) as determined by ELISA. (F-H) Representative images and bioluminescence quantification of sequestered *Pb*A schizonts expressing luciferase under the *AMA-1* promoter in spleens (F), lungs (G) and brains (H) of *Pb*A-infected C57BL/6J (B6) and *Nbeal2*-/- mice (n=8 mice/group). Values are normalized to naïve control mice from each respective group (n=4 mice/group). (I-J) Lung permeability (I) and brain permeability (J) in C57BL/6J (B6) and *Nbeal2*-/- mice injected intravenously with 200μL of 1% Evans Blue dye at day 6 post-infection with *Pb*A (n=9-13/group). Representative images and quantification of dye extracted from whole organs are shown. OD values are normalized to naïve control mice from each respective group (n=4 mice/group). (K) Survival curves of *Pb*A-infected *Nbeal2*-/- (gold line) and C57BL/6J (B6, black line) mice (n=15-16 mice/group). The gray shaded region represents the typical

Figure 1 (continued) timeframe of death from ECM. Graphs in A-E and I-J represent the mean ± SEM. Boxes in F-H represent the median ± the 25th and 75th percentiles with minimum/maximum whiskers. Statistical analyses: Mann-Whitney U test (A-J) and Log-rank Mantel-Cox test (K). Only statistically significant ($p<0.05$) values are shown. For graphs in A and C, * < 0.05, ** < 0.005, *** < 0.0005, and **** < 0.0001. Figures represent combined data from 2 (A, C-right, D-middle and right graphs, E-J) or 3 or more (B, C-left, D-left, K) independent experiments.

Fig. 2

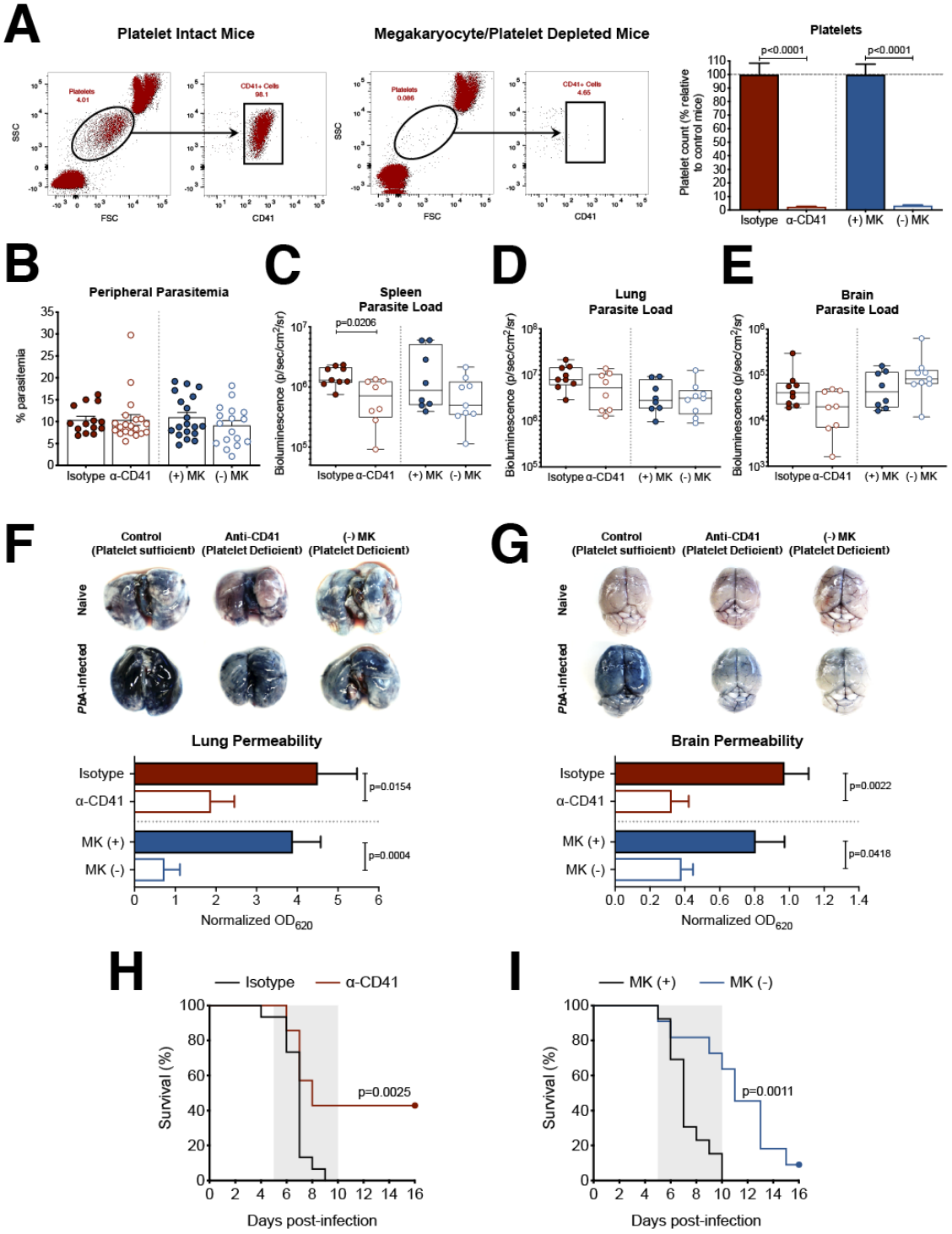
A
Platelet Intact Mice
Megakaryocyte/Platelet Depleted Mice
Platelets
p<0.0001
p<0.0001
Platelet count (% relative to control mice)
Isotype
α-CD41
(+) MK
(-) MK
B
Peripheral Parasitemia
% parasitemia
C
Spleen Parasite Load
p=0.0206
Bioluminescence (p/sec/cm²/sr)
D
Lung Parasite Load
E
Brain Parasite Load
F
Control (Platelet sufficient)
Anti-CD41 (Platelet Deficient)
(-) MK (Platelet Deficient)
Naive
PbA-infected
Lung Permeability
Isotype
α-CD41
MK (+)
MK (-)
p=0.0154
p=0.0004
Normalized OD620
G
Brain Permeability
p=0.0022
p=0.0418
H
Survival (%)
p=0.0025
Days post-infection
I
p=0.0011

Figure 2. Platelet depletion recapitulates the reduced organ pathology and increased survival observed in *Nbeal2-/-* mice. (A) Representative flow cytometry plots of platelets in mouse whole blood when platelets are present (left, platelet intact mice) or absent (right, megakaryocyte/platelet depleted mice). Platelets in whole blood of platelet depleted anti-CD41-treated C57BL/6J mice (α-CD41) and diphtheria toxin-treated Pf4-Cre positive/iDTR mice ((-) MK) normalized to their respective platelet intact control groups as quantified by flow cytometry (n=29-37 mice/group). C57BL/6J were intraperitoneally injected with 100μg of either an anti-CD41 or isotype control antibody on day 1 post-*Pb*A infection and platelets were measured on day 3 post-*Pb*A infection. Pf4-Cre negative/iDTR (megakaryocyte and platelet sufficient, *i.e.* (+) MK) and Pf4-Cre positive/iDTR (megakaryocyte and platelet deficient, *i.e.* (-) MK) mice were intraperitoneally injected with 20ng diphtheria toxin on days -7, -4, and -1 prior to *Pb*A infection and platelets were measured on day 0 of *Pb*A infection. (B) Frequency of infected red blood cells in peripheral blood of C57BL/6J mice given either an isotype control or anti-CD41 (α-CD41) antibody and diphtheria toxin-treated Pf4-Cre negative/iDTR ((+) MK) and Pf4-Cre positive/iDTR ((-) MK) mice at day 6 post-infection with *Pb*A as determined by staining and counting of thin blood smears (n=14-20 mice/group). (C-E) Representative images and bioluminescence quantification of sequestered *Pb*A schizonts expressing luciferase under the *AMA-1* promoter in spleens (C), lungs (D) and brains (E) of *Pb*A-infected mice in designated groups (n=8-9 mice/group). Values are normalized to naïve control mice from each respective group (n=4 mice/group). (F-G) Lung permeability (F) and brain permeability (G) in platelet intact and depleted mice as described in A injected intravenously with 200μL of 1% Evans Blue dye at day 6 post-infection with *Pb*A (n=7-11 mice/group). Representative images and quantification of dye extracted from whole organs are shown. OD values are normalized to **Figure 2 (continued)** naïve control mice from each

respective group (n=4-5 mice/group). (H) Survival curves of *Pb*A-infected C57BL/6J mice given an anti-CD41 (α-CD41, red line) or isotype control (black line) antibody on day 1 post-infection (n=15-21 mice/group). (I) Survival curves of *Pb*A-infected Pf4-Cre positive/iDTR ((-) MK, blue line) and Pf4-Cre negative/iDTR ((+) MK, black line) mice given diphtheria toxin on days -7, -4, and -1 prior to infection (n=11-13 mice/group). The gray shaded regions represent the typical timeframe of death from ECM. Bar graphs in A-B and F-G represent the mean ± SEM. Boxes in C-E represent the median ± the 25th and 75th percentiles with minimum/maximum whiskers. Statistical analyses: Mann-Whitney U test for isotype/α-CD41 and (+) MK/(-) MK groups, respectively (as separated by gray dotted line) (A-G) and Log-rank Mantel-Cox test (H-I). Only statistically significant ($p<0.05$) values are shown. Figures represent combined data from 2 (C-G, I) or 3 or more (A-B, H) independent experiments.

Supplementary Materials for

Platelet α-granules contribute to organ-specific pathologies in a mouse model of severe malaria

Thayer K. Darling, Michael P. Schenk, Chengjing C. Zhou, Franklin M. Maloba, Patrice N. Mimche, Jonathan M. Gibbins, Shawn M. Jobe, and Tracey J. Lamb*.

*Correspondence to: tracey.lamb@path.utah.edu

This section includes:

Figures S1 to S3

Fig. S1

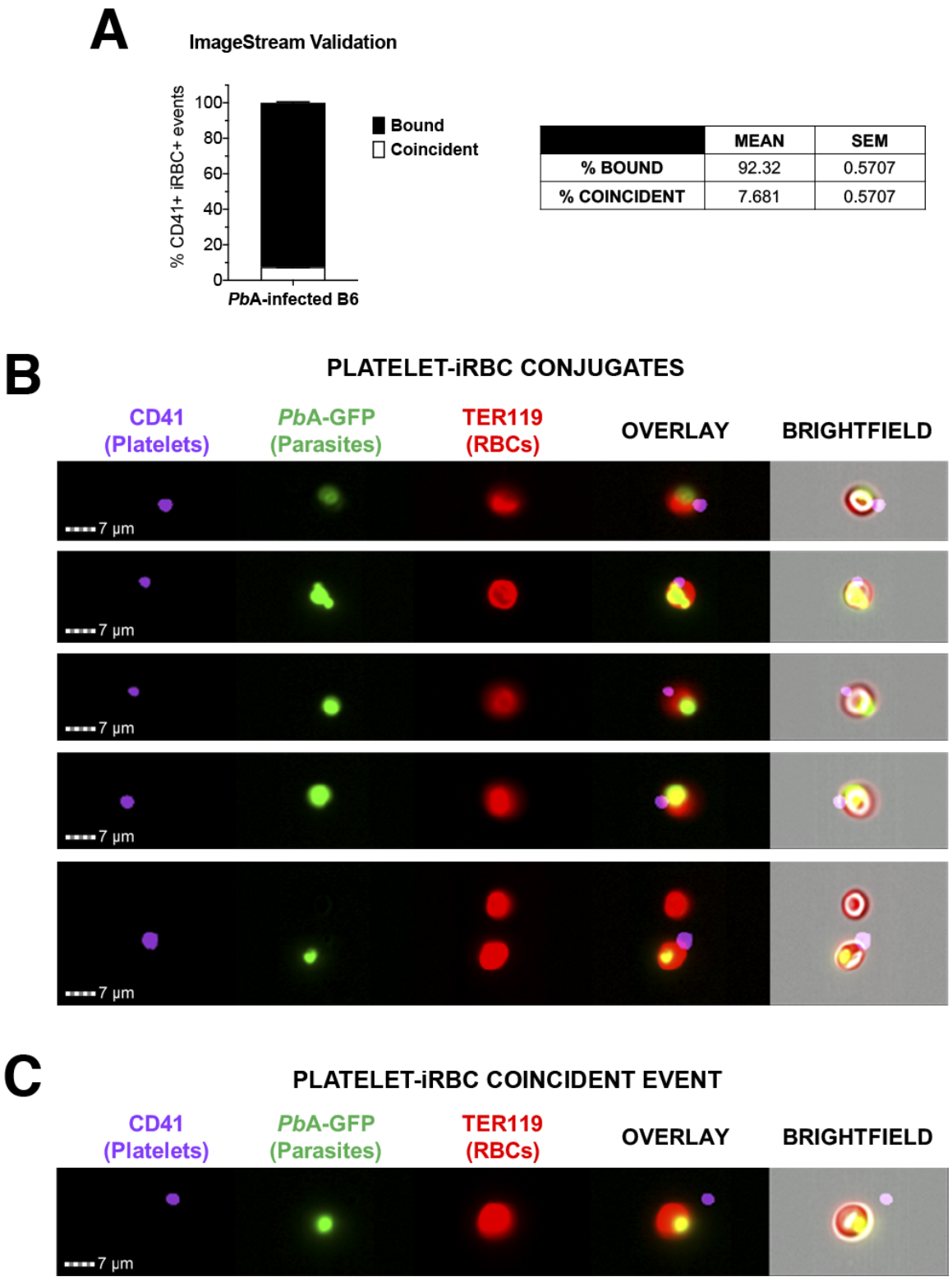

	MEAN	SEM
% BOUND	92.32	0.5707
% COINCIDENT	7.681	0.5707

Figure S1. Imaging flow cytometry confirms contact between platelets and *Pb*A-infected red blood cells. (A) Analysis of whole blood from C57BL/6J (B6) mice at day 6 post-infection with *Pb*A-GFP acquired on an ImageStream^X Mk II. Samples were stained with antibodies against CD41 and TER119 to identify platelets and red blood cells, respectively. Images from an average of ~200 CD41+iRBC+ events were examined for each sample (n=5 mice) to determine if they represented platelet-infected red blood cell (iRBC) conjugates (% Bound) or coincident events (% Coincident). Values for the mean and standard error for each category are shown. (B) Representative images of platelets (CD41+, purple) bound to *Pb*A-infected (GFP+ parasite, green) red blood cells (TER119+, red). (C) Representative image of a coincident event showing no contact between a platelet and an iRBC. Images were captured with a 60x objective. Bar graph in A represents the mean ± SEM. Figures represent combined data from 2 independent experiments.

Fig. S2

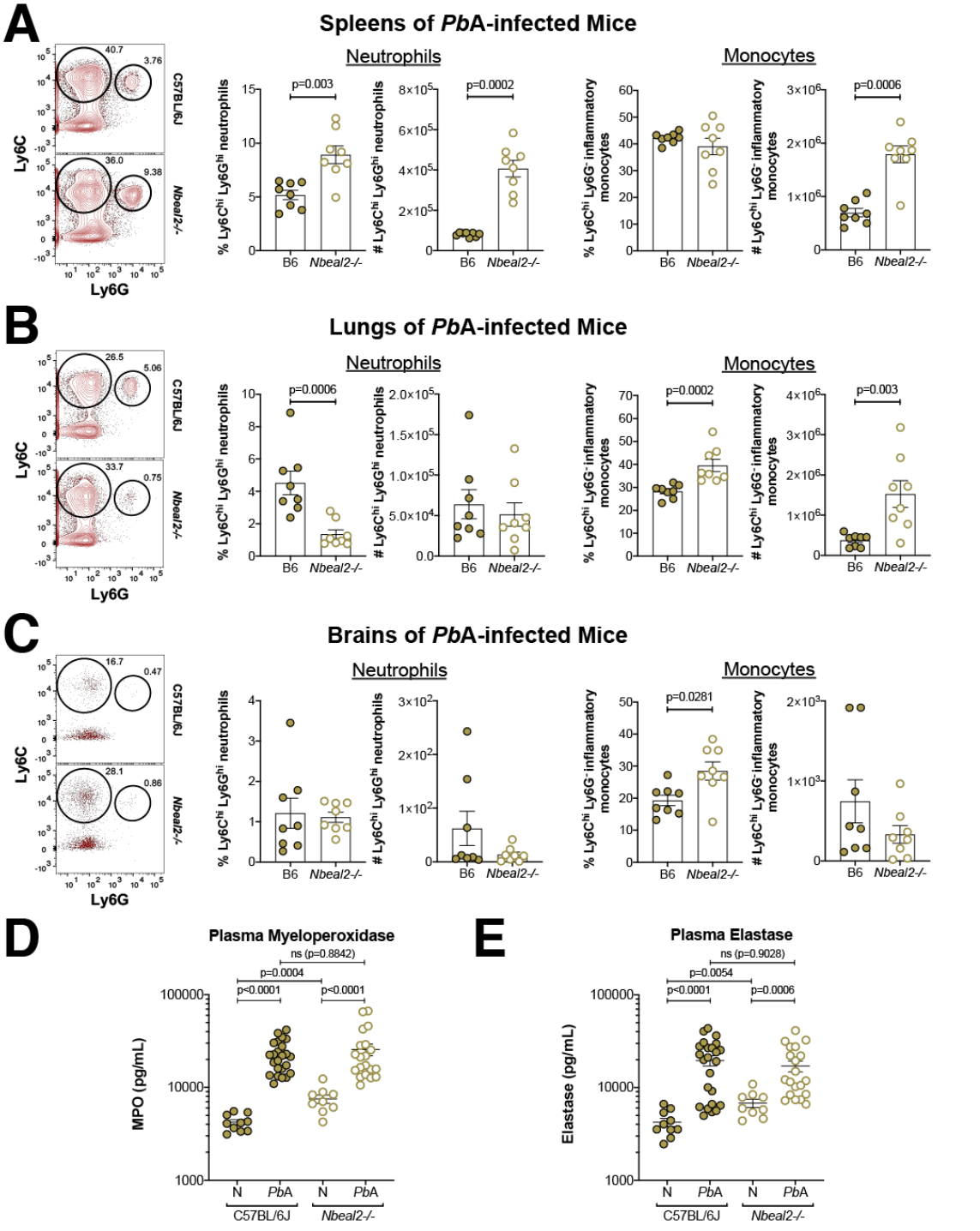
A
Spleens of PbA-infected Mice
Neutrophils
Monocytes
B
Lungs of PbA-infected Mice
C
Brains of PbA-infected Mice
Ly6C
Ly6G
C57BL/6J
Nbeal2-/-
% Ly6C^hi Ly6G^hi neutrophils
# Ly6C^hi Ly6G^hi neutrophils
% Ly6C^hi Ly6G^- inflammatory monocytes
# Ly6C^hi Ly6G^- inflammatory monocytes
B6
p=0.003
p=0.0002
p=0.0006
p=0.0002
p=0.003
p=0.0281
D
Plasma Myeloperoxidase
MPO (pg/mL)
ns (p=0.8842)
p=0.0004
p<0.0001
p<0.0001
E
Plasma Elastase
Elastase (pg/mL)
ns (p=0.9028)
p=0.0054
p<0.0001
p=0.0006
N
PbA
C57BL/6J
Nbeal2-/-

Figure S2. *Nbeal2* deficiency affects neutrophil and inflammatory monocyte sequestration in response to *Pb*A infection. (A-C) Representative flow cytometry plots and quantification of the frequency and absolute number of neutrophils ($Ly6C^{hi}Ly6G^{hi}$) and inflammatory monocytes ($Ly6C^{hi}Ly6G^{-}$) in the spleens (A), lungs (B), and brains (C) of C57BL/6J (B6) and *Nbeal2*-/- mice at day 6 post-infection with *Pb*A (n=8 mice/group). Cells were gated as following prior to Ly6C and Ly6G categorization: Lymphocytes, Singlets, Live, CD19-, CD11b+. (D-E) Quantification of myeloperoxidase (MPO) (D) and neutrophil elastase (E) in the plasma of C57BL/6J and *Nbeal2*-/- mice at day 6 post-infection with *Pb*A (n=20-24 mice/group) or naïve (N) (n=9-10 mice/group) as determined by ELISA. Graphs in A-E represent the mean ± SEM. Statistical analyses: Mann-Whitney U test (A-E). Only statistically significant ($p<0.05$) values are shown. Figures represent combined data from 2 (A-C) or 4 (D-E) independent experiments.

Fig. S3

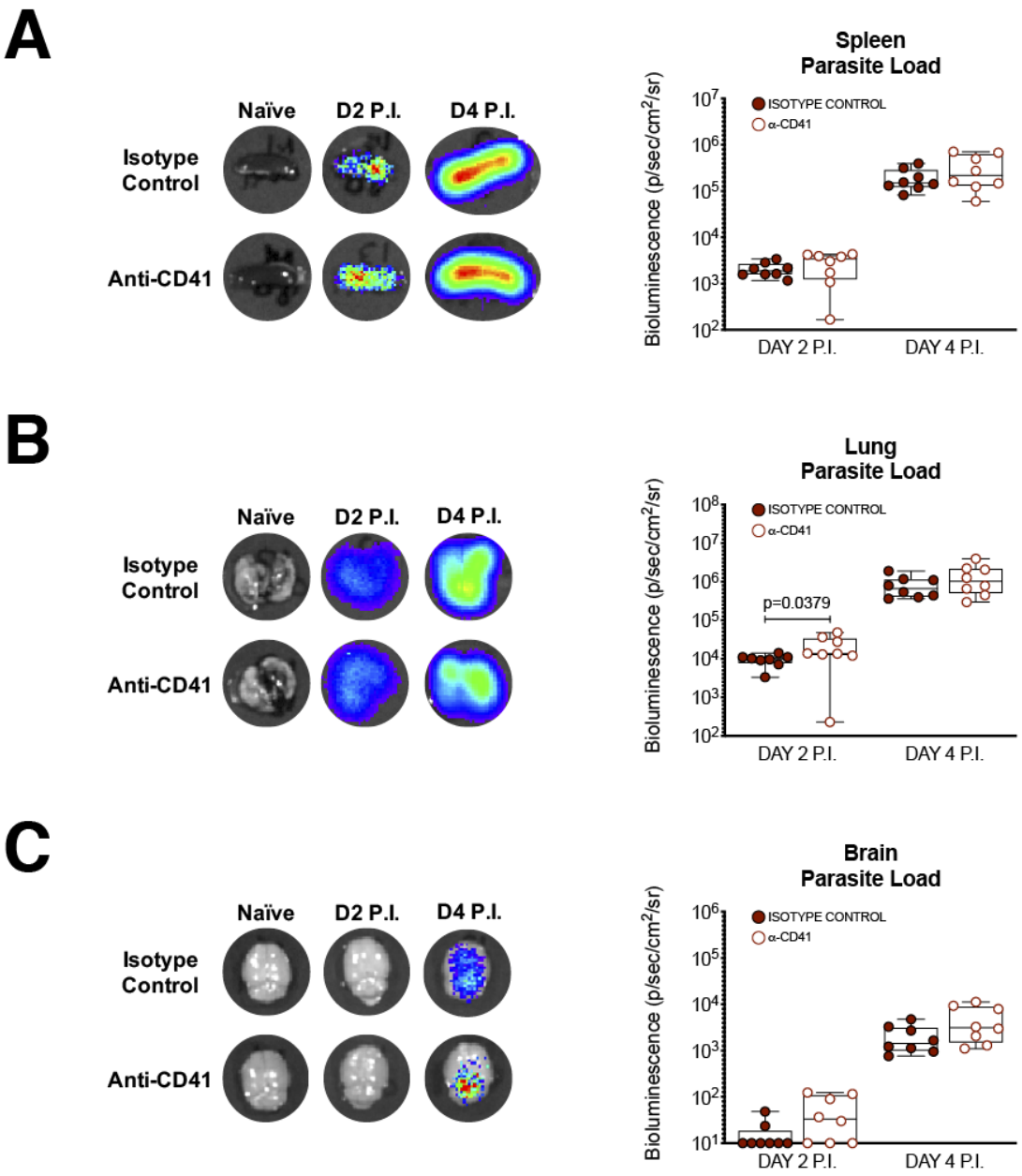
A
Naïve
D2 P.I.
D4 P.I.
Isotype Control
Anti-CD41
Spleen Parasite Load
ISOTYPE CONTROL
α-CD41
Bioluminescence (p/sec/cm²/sr)
DAY 2 P.I.
DAY 4 P.I.
B
Lung Parasite Load
p=0.0379
C
Brain Parasite Load

Figure S3. Antibody-mediated platelet depletion has minimal effects on parasite sequestration at early time points post-infection. (A-C) Representative images and bioluminescence quantification of sequestered *Pb*A schizonts expressing luciferase under the *AMA-1* promoter in spleens (A), lungs (B) and brains (C) of *Pb*A-infected C57BL/6J mice intraperitoneally injected with 100μg of either an anti-CD41 (α-CD41) or isotype control antibody on day 1 post-*Pb*A infection. Parasite sequestration was measured at days 2 and 4 post-infection (n=8 mice/group/day). Values are normalized to naïve control mice from each respective group (n=4 mice/group/day). Boxes in A-C represent the median ± the 25th and 75th percentiles with minimum/maximum whiskers. Statistical analyses: Mann-Whitney U test for isotype/α-CD41 for each respective day post-infection (A-C). Only statistically significant ($p<0.05$) values are shown. Figures represent combined data from 2 independent experiments.

CHAPTER IV

Discussion and Perspectives

CD8+ T cells and platelets are critical pathogenic immune cells in ECM

In this dissertation, we have demonstrated the critical importance of the receptor tyrosine kinase EphA2 and platelets to the development of ECM in mice. Collectively, these data significantly advance our understanding of several mechanisms underlying the development of cerebral malaria. While EphA2 has been linked to liver-stage *Plasmodium* infection (*154*), we demonstrate an additional relevance of EphA2 to blood-stage infection and, specifically, to blood-brain barrier disruption associated with cerebral malaria in mice. Our data strengthens the rationale for exploring therapeutics geared at inhibiting EphA2 activation which would have the potential to block successful parasite transmission as well as prevent the development of cerebral malaria if low-level transmission still occurs. We also identified EphA2 upregulation as a correlate of cerebral malaria in comparison with other non-severe and severe but non-cerebral forms of malaria which has long been a pressing question in the field. We have also described a mechanism by which platelets contribute to organ pathology and death in severe malaria. Specifically, platelet α-granules are involved in parasite organ sequestration and inducing lung and brain damage during *Plasmodium* infection which has never before been demonstrated. Platelets likely play an early role after infection in setting the trajectory for a pathological immune response while EphA2 and CD8+ T cells are critical at the onset of cerebral malaria, but Eph receptor/ephrin ligand expression and may link these processes together. We conclude this dissertation with a discussion of the ongoing directions of these two projects, how they are interconnected, and our goals to translate these findings to human disease in order to guide adjunctive therapies for cerebral malaria in the future.

Importance of EphA2 on other blood-brain barrier components

While we have demonstrated a clear importance of endothelial-expressed EphA2 to malaria-associated blood-brain barrier breakdown, it is also likely that expression of EphA2 on other cellular components of the neurovascular unit could be contribute to this process. Expression of EphA2 has been identified on other cell types that comprise the blood-brain barrier such as pericytes and astrocytes (*313, 323-326*). Given that both astrocytes and pericytes have been shown to play key roles in maintaining blood-brain barrier integrity (*360, 361*), it is possible that upregulation and activation of EphA2 on these cells serves a similar purpose to disrupt junctions and increase intercellular permeability. Alternatively, as astrocyte activation in response to brain injury has been shown to help prevent the spread of inflammation and aid in recovery from brain injury (*362*), it is also possible that EphA2 activation on astrocytes could serve to dampen the immunopathology that results from cerebral malaria. Activation of cells surrounding the brain endothelial vasculature could occur either through direct contact with infected red blood cells or indirectly in response to molecules secreted by activated endothelial cells. *Plasmodium* parasites are primarily thought to make contact with the vascular endothelium as they are obligate intracellular parasites in red blood cells, but they have also been shown to extravasate into the perivascular space which could induce pericyte and astrocyte activation (*207, 288*). We have observed increased frequencies and expression of both EphA2 and its high-affinity ligand ephrin-A1 on activated astrocytes at the onset of ECM in comparison with naive mice **(Appendix Figure 1)** providing evidence that *Plasmodium* infection induces increased expression of Eph receptors and their ligands on activated astrocytes. Future studies will aim to determine the importance of astrocyte and pericyte EphA2 expression and activation to ECM-associated blood-brain barrier breakdown by generating cell-specific EphA2 knockout and kinase-inactive mice and assessing the effects of astrocyte or pericyte specific EphA2 deletion or inactivation on measures of ECM

susceptibility. In doing so, we aim to fill in the remaining mechanistic gaps of how Eph and ephrin interactions between various cell types in the brain enhance endothelial junction disruption in the context of severe malaria.

Ephs and ephrins are expressed on platelets and could contribute to their pathogenicity during *Plasmodium* infection

As mentioned previously, different members of the Eph-ephrin family have been shown to be expressed on platelets. Platelet thrombi are present in the brain and lung microvasculature of patients who have died of complications from malaria (*251, 252*), and expression of Eph receptors and ephrin ligands such as EphA4 and ephrin-B1 on human platelets has been linked to the formation of stable thrombi at sites of vascular injury (*176*). Given the expression of Eph receptors and ephrin ligands on endothelial cells, it is possible that interactions between Ephs and ephrins on platelets and endothelial cells could contribute to platelet accumulation in the microvasculature during ECM. Surface expression of Ephs and ephrins increases on activated human platelets, and subsequent clustering results in secretion of platelet α-granules (*177*) which we have shown to be critical to lung and brain vascular permeability and *Plasmodium*-associated death in mice. Therefore, the fact that *EphA2*-/- mice are protected from ECM development could also involve effects of EphA2 deletion on platelets and platelet α-granule secretion. Platelet-derived growth factor (PDGF), which is synthesized in platelets and stored/released in platelet α-granules, has also been shown to induce phosphorylation of ephrin-B ligands (*363*) which represents an additional mechanism by which platelets and platelet α-granules could be linked to activation of EphA2 or ephrin-A ligands during *Plasmodium* infection. Although expression of EphA2 or its high affinity ephrin-A ligands has yet to be identified in mouse and human platelets, we intend to explore this possibility and

determine if platelet depletion or dysfunction influences *Pb*A-induced EphA2 brain upregulation in future studies.

In addition to the link between Eph receptor activation on platelets and thrombus formation, it also seems possible based on the current literature that platelets induce pathology during ECM in part through interactions with pathogenic CD8+ T cells. We have observed that platelets form conjugates with activated CD8+ T cells during *Pb*A infection, and formation of these platelet-activated CD8+ T cell conjugates is largely dependent on the presence of platelet α-granules **(Appendix Figure 2)**. Although the relevance of platelet-CD8+ T cell conjugates to human diseases has not been well studied, there are several recent reports that they may be associated with increased pathology in certain autoimmune and infectious disease contexts. Activated platelet-CD8+ T cell conjugates have been found at increased levels in the bloodstream of patients with other infectious and non-infectious diseases such as HIV and Systemic Lupus Erythematosus (*364, 365*) and it has been suggested that platelets may be serving to recruit antigen experienced CD8+ T cells to sites of inflammation and injury. In the context of severe malaria, platelets could be recruiting CD8+ T cells to the microvasculature of organs where parasites have sequestered. Therefore, part of the reduced pathology we observe in the lungs and brains of *Nbeal2*-/- mice could be due to lower frequencies of activated platelet-CD8+ T cell conjugates in the absence of platelet α-granules. Additionally, we have observed that *Nbeal2*-/- mice have significantly reduced frequencies of *Plasmodium*-reactive CD8+ T cells in the bloodstream **(Appendix Figure 3)** indicating that functional platelets are required not only for conjugation with CD8+ T cells but also for global CD8+ T cell expansion during *Plasmodium* infection. The intertwined roles of platelets and CD8+ T cells in the pathogenic immune response during severe malaria have not been explored in

detail. In the future, we aim to explore this link further by assessing expression of Eph receptors and ephrin ligands on platelets from wild-type and *Nbeal2*-/- mice to determine if expression of these proteins could be influencing the formation of platelet-CD8+ T cell conjugates and subsequent disease pathology.

Exploring links between Eph/ephrin expression and CD8+ T cell affinity

T cells are critical in orchestrating immune effector mechanisms involved in controlling infected red blood cells (iRBCs) (*366*) and understanding the features of protective T cell responses is critical for the rational design of blood-stage malaria vaccines. The features defining protective T cells in malaria are incompletely understood but likely depend on a combination of antigen reactivity, cytokine profile, lytic potential, and expression of surface receptors involved in T cell trafficking and adhesion. Of these features, very little is known regarding the antigen reactivity profile of T cells, in particular $CD8^+$ T cells, against blood-stage *Plasmodium*. Much of the field of immunology has previously supported the idea that high-affinity T cells predominantly survive and proliferate in polyclonal T cell responses (*367-369*). However, this concept is not supported by data demonstrating that low-affinity T cells can make up a significant proportion of the T cell population responding to a given epitope (*370, 371*). For example, it has recently been shown in several different disease models that low-affinity T cells also expand and are maintained during an immune response. In the experimental autoimmune encephalomyelitis (EAE) model of multiple sclerosis and in lymphocytic choriomeningitis virus (LCMV) infection, there is an abundance of low-affinity T cells in the polyclonal T-cell response, and these low-affinity T cells are equally functional as high-affinity T cells in terms of cytokine production (*370*). The role of low-affinity T cells in the immune response against malaria is currently completely unknown.

Tetramers containing *Plasmodium*-derived epitopes that recognize several immunodominant, high-affinity CD8+ T cell clones have been identified in recent years (*223, 287*). As tetramers only detect T cells above a specific affinity threshold (*370, 372*), they do not account for the expansion or participation of low-affinity CD8+ T cells in the immune response to *Plasmodium*. Using a two-dimensional micropipette adhesion frequency assay (*373*), we found that low-affinity CD8+ T cells actually comprise the majority of CD8+ T cells found in the brains of *Pb*A-infected mice. Using several fluorescent reporter mice, we also found that these low-affinity CD8+ T cells are capable of producing both IFN-γ and IL-10 **(Appendix Figure 4)** indicating that they not only traffic to the brain but also have the capacity to contribute functionally in the immune response to malaria. Given the known involvement of Eph receptors and ephrin ligands in various aspects of CD8+ T cell functionality (*93, 100, 103, 137*), it would be interesting to determine if expression of these molecules influences or is correlated in any way with CD8+ T cell affinity. For example, we could assess whether or not low-affinity and high-affinity *Plasmodium*-reactive CD8+ T cells have different expression levels or unique expression patterns of several Ephs and ephrins that they are known to express. If any specific receptors or ligands are identified, we could use cell-specific knockout mouse models to study the impact of T cell-specific Eph/ephrin deletion on the affinity profile generated in response to *Plasmodium* infection and whether the affinity profile of CD8+ T cells generated in response to *Pb*A infection, for example, is sufficient to cause experimental cerebral malaria. Additionally, part of the failure of existing malaria vaccine candidates that have advanced into phase II and III clinical trials (*6, 392-394*) is due to the evident gap in understanding what constitutes an effective immune response to malaria (*395*). Since it is completely unknown how TCR affinity impacts the antimalarial immune response, it is

important to explore the functions of these distinct low- and high-affinity T cell populations and how they may be linked to Eph receptor and ephrin ligand expression in order to determine the desirable response to elicit with antimalarial vaccines against blood-stage *Plasmodium*.

Therapeutic strategies for targeting Eph receptors and implications for malaria

Given their well-established involvement in cancer progression, Eph receptors and ephrin ligands have become promising new targets for cancer therapies whether aiming to suppress tumor-promoting effects or enhance tumor-suppressive effects. Several approaches currently exist to specifically target Ephs and ephrins in the context of cancer. One strategy involves interfering with Eph-ephrin signaling through the use of small molecule inhibitors. While several high-affinity Eph kinase inhibitors have been identified (*374*), it is also apparent that several existing inhibitors can inhibit Eph kinase activity as well as their intended targets. Dasatinib, for example, is already used to treat chronic myelogenous leukemia and appears to inhibit EphA2, EphB1, EphB2, and EphB4 (*375*) along with its primary targets Abl and Src family kinases, which likely improves its anti-cancer activity. Since EphA2 and ephrin-B2 appear to promote resistance to several therapies currently used to treat breast cancer (*376*) and glioblastoma, respectively, targeting the Eph or ephrin molecules themselves may overcome this resistance and associated treatment failure. Eph receptors have also been targeted with small interfering RNA delivered in liposomes, and this strategy has been used to silence Eph receptor expression, such as EphA2, and has been shown effective against ovarian cancer (*377*).

Another, more specific, strategy for targeting the Eph-ephrin members involves blocking Eph-ephrin interactions by administering soluble Eph or ephrin fusion proteins. For example, oncogenic EphA2-ephrin-A1 signaling can be inhibited using soluble EphA2-Fc or ephrin-A1-Fc proteins and have been shown effective at preventing tumor proliferation, vascularization, and invasiveness (*298*). These soluble chimeric proteins have the benefits of long half-life and broad effects on Eph/ephrin family members due to the promiscuous binding but negatively this also can lead to increased off-target side effects.

Peptide agonists and antagonists of Eph receptors have also been explored as potential therapeutics. These short peptides generally bind to the ephrin ligand binding site of the Eph receptors to prevent binding of cells expressing their cognate ligands. One interesting example is the 12 amino-acid KYL peptide which activates EphA2 while blocking ephrin ligand binding, and this receptor activation leads to EphA2 internalization (*378*) which is beneficial in this case given the oncogenic nature of EphA2. To expand on this strategy, peptides can also be conjugated to drugs, toxins, or nanoparticles for a highly-targeted delivery approach of therapeutics directly to tumors. In keeping with the previous example, another EphA2-specific agonistic peptide, YSA, was conjugated to the drug paclitaxel and administered in a mouse xenograft model leading to greatly increased efficacy of this chemotherapeutic drug that has poor bioavailability when administered alone (*379*). Using this strategy, Eph-specific peptides can also be conjugated to imaging agents to allow for targeted visualization of Eph-overexpressing tumor cells.

In terms of immunotherapy, the fact that many tumors overexpress Eph receptors and/or ephrin ligands provides the opportunity to boost the immune response to receptor or ligand

derived peptides. A current Phase I/II clinical trial for recurrent glioma indicated that a vaccination strategy using dendritic cells pulsed with glioma-associated antigens, including an $EphA2_{833-891}$ peptide, elicited a strong $CD8^+$ T cell response in approximately 58% of patients (*380*). Along with cancer vaccination strategies, other Eph-targeted immunotherapies are being explored. Monoclonal antibodies are a popular strategy for targeting Eph receptors given their high affinity and specificity for their cognate target, and both activating and inhibitory monoclonal antibodies against Ephs/ephrins are under development. EphA2 was the first receptor targeted for monoclonal antibody development, and several strongly agonistic antibodies were identified (*381*). Among these, a humanized version of mAb B233 was developed that had improved FcγRIII binding capacity and showed promising results in eliciting a strong antibody-dependent cell-mediated cytotoxicity antitumor response against several types of cancer including ovarian, lung, and breast cancer xenografts (*159*). Another study demonstrated that a single chain antibody capable of simultaneously binding both EphA2 and CD3 in the TCR complex led to T cell-mediated destruction of $EphA2^+$ tumor cells in a humanized mouse model (*382*).

Given the decline in funding for malaria research over the past decade (*383*), repurposing other approved drugs could be a more cost-effective way of identifying adjunctive therapies for cerebral malaria. Developing strategies to target Eph receptors in malaria will not be without major obstacles including specificity and balancing the costs versus benefits of immunosuppression. All of the aforementioned strategies have specific strengths and weaknesses, yet even with the inherent difficulty in targeting such a complex signaling system many of these treatment methods promise exciting new therapeutic avenues to treat this difficult disease.

Future goals in translating these studies to human malaria

The use of animal models for the studies included in this dissertation has been absolutely instrumental in identifying new mechanisms responsible for the development of immunopathology in severe and cerebral malaria. While we will continue to use mouse models for these reasons, our long-term goal is always to identify translatable features of our findings to human malaria. While we included several pieces of evidence supporting the correlation between ephrin ligands and malaria-associated neurological symptoms in humans in Chapter II, we have only just begun to expand upon and validate our data in mice with additional human studies. For example, we are working to implement the diagnosis of malarial retinopathy (*384*) in patients recruited for our studies in Yaoundé, Cameroon so that we can look specifically at differences in the concentration of ephrin-A ligands in plasma of patients with retinopathy-positive versus retinopathy-negative cerebral malaria. If retinopathy-positive patients have significantly higher levels of circulating ephrin-A1 in comparison to retinopathy-negative patients, this could potentially serve as an additional biomarker to confirm cerebral malaria in patients.

To further validate the relevance of endothelial-expressed EphA2 to human CM, we are exploring the options for examining EphA2 expression levels on brain sections collected at autopsy from patients who died of confirmed cerebral malaria. While there is considerable difficulty in obtaining these samples due to issues in obtaining family consent and often reduced capabilities in processing such tissue on-site (*212*), determining if EphA2 protein expression is increased in patients who have died of cerebral malaria in comparison to patients who have died of unrelated causes that are not associated with brain trauma or inflammation

will be absolutely essential in order to continue pursuing EphA2 inactivation/blocking strategies in the search for an adjunctive therapy for human CM.

In addition to our ongoing studies aimed at addressing the relevance of EphA2 and ephrins to human CM, we are also interested in expanding upon our findings in Chapter III by assessing differences in platelet characteristics and expression profiles in patients with uncomplicated versus severe malaria. While thrombocytopenia has long been appreciated as a feature of malaria in both mice and humans (*250, 385*), little is known about the specific platelet components and mechanisms by which platelets are involved in malaria pathogenesis. Given our findings in mice, we have current ongoing studies assessing the expression of different platelet α-granule and dense granules markers on platelets isolated from the peripheral blood of individuals with differing severities of malaria. In addition to looking at the granule content and activation status of patients with malaria, we could also incorporate platelet staining for Eph receptors and ephrin ligands in order to determine if there is any correlation between the expression levels of these molecules and malaria symptoms/severity in humans. While surface expression of several of these markers is indicative of platelet activation status, they do not necessarily represent the activation capacity or complete granular content of the platelets. We can supplement this analysis by stimulating platelets from malaria patients *ex vivo* with powerful platelet agonists such as thrombin (*386*) and determining if the platelet components released into the supernatant differ between patients with uncomplicated versus severe malaria. Finally, as platelet RNA sequencing is becoming more mainstream (*387-389*), our goal is to compare the transcriptomic profiles of platelets from patients with different malaria statuses to identify genes, such as potentially *Nbeal2*, that are differentially expressed and potentially correlate with either protection or disease severity. Since thrombocytopenia is

present in patients with both symptomatic and asymptomatic malaria (*390, 391*), defining characteristics of platelets that differ between different subsets of patients infected with *Plasmodium* could aid in understanding that qualities of platelets that are important for pathogenesis.

Concluding remarks

Overall, this dissertation significantly enhances our understanding of how components of the immune system such as CD8+ T cells and platelets mediate immunopathology in cerebral malaria. The discovery that the receptor EphA2 is critical for the process of malaria-associated blood-brain barrier breakdown in mice highlights a new mechanism by which *Plasmodium* infection alters the expression of host molecules that subsequently contribute to an aberrant and pathogenic immune response. The study of Eph receptors and ephrin ligands in immunology is an expanding area of research, and given the fact that the association with the immune system has only emerged in the past 15 years it is highly likely that more roles for this unique cell-cell communication system in the immune response to infectious disease have yet to be revealed. Ephs and ephrins represent promising therapeutic targets for several reasons. Given the high evolutionary conservation of this family of molecules, it is probable that the development and testing of therapeutics in animal models will be highly translatable in humans. Indeed, there are several Eph/ephrin-targeting strategies that are currently in various phases of clinical trials. It is also beneficial that there are several different strategies for targeting these interactions, all with promising leads, providing for a variety of mechanisms for attacking the same targets. Further, many currently existing drugs have been found to have activity against Eph receptors allowing for potential testing and repurposing of these drugs for new pathological conditions without the need for starting from the beginning of the drug

development process. Targeting Eph receptors has also been shown to overcome resistance to several existing therapies, particularly in cancer, and may enhance the effects of existing therapies, such as antimalarials, in a combination approach. It is possible that given the large number of members in the Eph family, certain Ephs or ephrins may be able to functionally compensate for other inhibited members which would be difficult to overcome therapeutically. Among the biggest challenges, the nearly ubiquitous expression of Ephs and ephrins, while all have different patterns of expression, almost guarantees detrimental side-effects from any targeted therapeutic strategy as Eph-ephrin interactions are also crucial for adult tissue homeostasis in various organs. However, in the case of such an acute and deadly complication as cerebral malaria the potential benefits of a short-term anti-Eph therapy may outweigh the risks.

While EphA2 presents itself as a promising therapeutic target for both liver-stage and blood-stage malaria, our findings in platelets are more important to understanding the basic biology and mechanisms behind malaria-associated immunopathology. Although depleting platelets in patients would clearly not be the goal in translating our results to humans, understanding that platelet α-granules are critical components in mediating pathology in malaria can help inform and potentially identify biomarkers for patients predisposed to developing severe malaria. Additionally, further studying the contribution of platelet-CD8+ T cell interactions to organ damage in malaria could inform strategies for potentially decoupling this interaction which may improve disease outcomes.

Malaria remains a severe global public health issue and will remain so for the foreseeable future. It is imperative that we continue to adjust our understanding of how the immune

system is involved in balancing both malaria control and pathogenesis in order to inform the development of novel therapeutic and vaccine strategies. By focusing our efforts on gaining a better mechanistic understanding of how CD8+ T cells and platelets contribute to organ pathology in severe and cerebral malaria, we have identified several key proteins, including EphA2 and Nbeal2, that are critical for the induction of malaria-associated immunopathology. These findings pave the way for many future studies that will aim to further dissect the interplay between CD8+ T cells, EphA2, and platelets in malaria and promise an exciting new chapter in the field of malaria immunology.

CHAPTER V

Bibliography

1. A. K. Rowe *et al.*, The burden of malaria mortality among African children in the year 2000. *International Journal of Epidemiology* **35**, 691-704 (2006).
2. R. W. Snow, C. A. Guerra, A. M. Noor, H. Y. Myint, S. I. Hay, The global distribution of clinical episodes of Plasmodium falciparum malaria. *Nature* **434**, 214-217 (2005).
3. L. J. Bruce-Chwatt, Alphonse Laveran's discovery 100 years ago and today's global fight against malaria. *Journal of the Royal Society of Medicine* **74**, 531-536 (1981).
4. J. Langhorne, F. M. Ndungu, A. M. Sponaas, K. Marsh, Immunity to malaria: more questions than answers. *Nat Immunol* **9**, 725-732 (2008).
5. S. Owusu-Agyei *et al.*, Incidence of symptomatic and asymptomatic Plasmodium falciparum infection following curative therapy in adult residents of northern Ghana. *The American Journal of Tropical Medicine and Hygiene* **65**, 197-203 (2001).
6. P. L. Alonso *et al.*, Efficacy of the RTS,S/AS02A vaccine against Plasmodium falciparum infection and disease in young African children: randomised controlled trial. *The Lancet* **364**, 1411-1420 (2004).
7. S. C. T. P. RTS, Efficacy and safety of RTS,S/AS01 malaria vaccine with or without a booster dose in infants and children in Africa: final results of a phase 3, individually randomised, controlled trial. *Lancet (London, England)* **386**, 31-45 (2015).

8. W. Jin, H. Luo, J. Wu, Effect of reduced EPHB4 expression in thymic epithelial cells on thymocyte development and peripheral T cell function. *Mol Immunol* **58**, 1-9 (2014).

9. A. Trampuz, M. Jereb, I. Muzlovic, R. M. Prabhu, Clinical review: Severe malaria. *Critical Care* **7**, 315-323 (2003).

10. H. H. Kyu, E. Fernández, Artemisinin derivatives versus quinine for cerebral malaria in African children: a systematic review. *Bulletin of the World Health Organization* **87**, 896-904 (2009).

11. N. L. Tuzi, W. J. Gullick, eph, the largest known family of putative growth factor receptors. *British journal of cancer* **69**, 417-421 (1994).

12. E. B. Pasquale, Eph receptor signalling casts a wide net on cell behaviour. *Nature reviews. Molecular cell biology* **6**, 462-475 (2005).

13. E. B. Pasquale, Eph-ephrin bidirectional signaling in physiology and disease. *Cell* **133**, 38-52 (2008).

14. E. Batlle, D. G. Wilkinson, Molecular mechanisms of cell segregation and boundary formation in development and tumorigenesis. *Cold Spring Harbor perspectives in biology* **4**, a008227 (2012).

15. E. M. Lisabeth, G. Falivelli, E. B. Pasquale, Eph receptor signaling and ephrins. *Cold Spring Harbor perspectives in biology* **5**, (2013).

16. H. Hirai, Y. Maru, K. Hagiwara, J. Nishida, F. Takaku, A novel putative tyrosine kinase receptor encoded by the eph gene. *Science (New York, N.Y.)* **238**, 1717-1720 (1987).

17. E. B. Pasquale, The Eph family of receptors. *Current opinion in cell biology* **9**, 608-615 (1997).

18. R. A. Lindberg, T. Hunter, cDNA cloning and characterization of eck, an epithelial cell receptor protein-tyrosine kinase in the eph/elk family of protein kinases. *Molecular and cellular biology* **10**, 6316-6324 (1990).

19. A. W. Boyd *et al.*, Isolation and characterization of a novel receptor-type protein tyrosine kinase (hek) from a human pre-B cell line. *J Biol Chem* **267**, 3262-3267 (1992).

20. P. Gilardi-Hebenstreit *et al.*, An Eph-related receptor protein tyrosine kinase gene segmentally expressed in the developing mouse hindbrain. *Oncogene* **7**, 2499-2506 (1992).

21. R. Zhou, T. D. Copeland, L. F. Kromer, N. T. Schulz, Isolation and characterization of Bsk, a growth factor receptor-like tyrosine kinase associated with the limbic system. *Journal of neuroscience research* **37**, 129-143 (1994).

22. P. C. Maisonpierre, N. X. Barrezueta, G. D. Yancopoulos, Ehk-1 and Ehk-2: two novel members of the Eph receptor-like tyrosine kinase family with distinctive structures and neuronal expression. *Oncogene* **8**, 3277-3288 (1993).

23. G. M. Fox *et al.*, cDNA cloning and tissue distribution of five human EPH-like receptor protein-tyrosine kinases. *Oncogene* **10**, 897-905 (1995).

24. J. Chan, V. M. Watt, eek and erk, new members of the eph subclass of receptor protein-tyrosine kinases. *Oncogene* **6**, 1057-1061 (1991).

25. H. C. Aasheim, S. Patzke, H. S. Hjorthaug, E. F. Finne, Characterization of a novel Eph receptor tyrosine kinase, EphA10, expressed in testis. *Biochimica et biophysica acta* **1723**, 1-7 (2005).

26. K. Letwin, S. P. Yee, T. Pawson, Novel protein-tyrosine kinase cDNAs related to fps/fes and eph cloned using anti-phosphotyrosine antibody. *Oncogene* **3**, 621-627 (1988).

27. B. Bohme *et al.*, PCR mediated detection of a new human receptor-tyrosine-kinase, HEK 2. *Oncogene* **8**, 2857-2862 (1993).

28. A. C. Andres *et al.*, Expression of two novel eph-related receptor protein tyrosine kinases in mammary gland development and carcinogenesis. *Oncogene* **9**, 1461-1467 (1994).

29. C. B. Gurniak, L. J. Berg, A new member of the Eph family of receptors that lacks protein tyrosine kinase activity. *Oncogene* **13**, 777-786 (1996).

30. R. Noberini, E. Rubio de la Torre, E. B. Pasquale, Profiling Eph receptor expression in cells and tissues: a targeted mass spectrometry approach. *Cell Adh Migr* **6**, 102-112 (2012).

31. G. Manning, D. B. Whyte, R. Martinez, T. Hunter, S. Sudarsanam, The protein kinase complement of the human genome. *Science* **298**, 1912-1934 (2002).

32. Y. Xia, C. Luo, S. Dai, D. Yao, Increased EphA/ephrinA expression in hippocampus of pilocarpine treated mouse. *Epilepsy research* **105**, 20-29 (2013).

33. D. J. Liebl, C. J. Morris, M. Henkemeyer, L. F. Parada, mRNA expression of ephrins and Eph receptor tyrosine kinases in the neonatal and adult mouse central nervous system. *Journal of neuroscience research* **71**, 7-22 (2003).

34. M. Henkemeyer, O. S. Itkis, M. Ngo, P. W. Hickmott, I. M. Ethell, Multiple EphB receptor tyrosine kinases shape dendritic spines in the hippocampus. *The Journal of cell biology* **163**, 1313-1326 (2003).

35. N. W. Gale *et al.*, Eph receptors and ligands comprise two major specificity subclasses and are reciprocally compartmentalized during embryogenesis. *Neuron* **17**, 9-19 (1996).

36. J. P. Himanen *et al.*, Repelling class discrimination: ephrin-A5 binds to and activates EphB2 receptor signaling. *Nat Neurosci* **7**, 501-509 (2004).

37. E. Munthe *et al.*, Ephrin-B2 is a candidate ligand for the Eph receptor, EphB6. *FEBS letters* **466**, 169-174 (2000).

38. A. Poliakov, M. Cotrina, D. G. Wilkinson, Diverse roles of eph receptors and ephrins in the regulation of cell migration and tissue assembly. *Developmental cell* **7**, 465-480 (2004).

39. T. K. Niethamer, J. O. Bush, Getting direction(s): The Eph/ephrin signaling system in cell positioning. *Developmental biology*, (2018).

40. J. P. Himanen, M. Henkemeyer, D. B. Nikolov, Crystal structure of the ligand-binding domain of the receptor tyrosine kinase EphB2. *Nature* **396**, 486-491 (1998).

41. E. B. Pasquale, Eph-ephrin promiscuity is now crystal clear. *Nature neuroscience* **7**, 417-418 (2004).

42. D. B. Nikolov, K. Xu, J. P. Himanen, Eph/ephrin recognition and the role of Eph/ephrin clusters in signaling initiation. *Biochimica et biophysica acta* **1834**, 2160-2165 (2013).

43. M. Takasugi *et al.*, Small extracellular vesicles secreted from senescent cells promote cancer cell proliferation through EphA2. *Nature communications* **8**, 15729 (2017).

44. K. K. Murai, E. B. Pasquale, 'Eph'ective signaling: forward, reverse and crosstalk. *Journal of cell science* **116**, 2823-2832 (2003).

45. S. J. Holland *et al.*, Bidirectional signalling through the EPH-family receptor Nuk and its transmembrane ligands. *Nature* **383**, 722-725 (1996).

46. K. Bruckner, E. B. Pasquale, R. Klein, Tyrosine phosphorylation of transmembrane ligands for Eph receptors. *Science* **275**, 1640-1643 (1997).

47. J. P. Himanen *et al.*, Architecture of Eph receptor clusters. *Proc Natl Acad Sci U S A* **107**, 10860-10865 (2010).

48. P. W. Janes *et al.*, Eph receptor function is modulated by heterooligomerization of A and B type Eph receptors. *The Journal of cell biology* **195**, 1033-1045 (2011).

49. D. J. Marston, S. Dickinson, C. D. Nobes, Rac-dependent trans-endocytosis of ephrinBs regulates Eph-ephrin contact repulsion. *Nature cell biology* **5**, 879-888 (2003).

50. M. Zimmer, A. Palmer, J. Kohler, R. Klein, EphB-ephrinB bi-directional endocytosis terminates adhesion allowing contact mediated repulsion. *Nature cell biology* **5**, 869-878 (2003).

51. T. N. Gaitanos, J. Koerner, R. Klein, Tiam-Rac signaling mediates trans-endocytosis of ephrin receptor EphB2 and is important for cell repulsion. *The Journal of cell biology* **214**, 735-752 (2016).

52. M. Hattori, M. Osterfield, J. G. Flanagan, Regulated cleavage of a contact-mediated axon repellent. *Science (New York, N.Y.)* **289**, 1360-1365 (2000).

53. P. W. Janes *et al.*, Adam meets Eph: an ADAM substrate recognition module acts as a molecular switch for ephrin cleavage in trans. *Cell* **123**, 291-304 (2005).

54. L. Atapattu, M. Lackmann, P. W. Janes, The role of proteases in regulating Eph/ephrin signaling. *Cell Adh Migr* **8**, 294-307 (2014).

55. M. C. Halloran, M. A. Wolman, Repulsion or adhesion: receptors make the call. *Current opinion in cell biology* **18**, 533-540 (2006).

56. J. Holmberg, D. L. Clarke, J. Frisen, Regulation of repulsion versus adhesion by different splice forms of an Eph receptor. *Nature* **408**, 203-206 (2000).

57. Y. Yin *et al.*, EphA receptor tyrosine kinases interact with co-expressed ephrin-A ligands in cis. *Neuroscience research* **48**, 285-296 (2004).

58. R. F. Carvalho *et al.*, Silencing of EphA3 through a cis interaction with ephrinA5. *Nat Neurosci* **9**, 322-330 (2006).

59. C. Hafner *et al.*, Differential gene expression of Eph receptors and ephrins in benign human tissues and cancers. *Clinical chemistry* **50**, 490-499 (2004).

60. R. Klein, Eph/ephrin signalling during development. *Development* **139**, 4105-4109 (2012).

61. B. Mosch, B. Reissenweber, C. Neuber, J. Pietzsch, Eph Receptors and Ephrin Ligands: Important Players in Angiogenesis and Tumor Angiogenesis. *Journal of Oncology* **2010**, 12 (2010).

62. E. Berrou *et al.*, A mutation of the human EPHB2 gene leads to a major platelet functional defect. *Blood*, (2018).

63. N. Prevost, D. Woulfe, T. Tanaka, L. F. Brass, Interactions between Eph kinases and ephrins provide a mechanism to support platelet aggregation once cell-to-cell contact has occurred. *Proceedings of the National Academy of Sciences of the United States of America* **99**, 9219-9224 (2002).

64. N. Prevost *et al.*, Eph kinases and ephrins support thrombus growth and stability by regulating integrin outside-in signaling in platelets. *Proc Natl Acad Sci U S A* **102**, 9820-9825 (2005).

65. N. Prevost *et al.*, Signaling by ephrinB1 and Eph kinases in platelets promotes Rap1 activation, platelet adhesion, and aggregation via effector pathways that do not require phosphorylation of ephrinB1. *Blood* **103**, 1348-1355 (2004).

66. S. Vaiyapuri *et al.*, EphB2 regulates contact-dependent and contact-independent signaling to control platelet function. *Blood* **125**, 720-730 (2015).

67. J. Braun *et al.*, Endothelial cell ephrinB2-dependent activation of monocytes in arteriosclerosis. *Arterioscler Thromb Vasc Biol* **31**, 297-305 (2011).

68. G. Ende *et al.*, TNF-alpha-mediated adhesion of monocytes to endothelial cells-The role of ephrinA1. *Journal of molecular and cellular cardiology* **77**, 125-135 (2014).

69. S. D. Funk, A. W. Orr, Ephs and ephrins resurface in inflammation, immunity, and atherosclerosis. *Pharmacological Research* **67**, 42-52 (2013).

70. S. Jellinghaus *et al.*, Ephrin-A1/EphA4-mediated adhesion of monocytes to endothelial cells. *Biochimica et Biophysica Acta (BBA) - Molecular Cell Research* **1833**, 2201-2211 (2013).

71. H. Liu *et al.*, EphrinB-mediated reverse signalling controls junctional integrity and pro-inflammatory differentiation of endothelial cells. *Thrombosis and haemostasis* **112**, 151-163 (2014).

72. P. N. Mimche *et al.*, The receptor tyrosine kinase EphB2 promotes hepatic fibrosis in mice. *Hepatology* **62**, 900-914 (2015).

73. M. Mukai, N. Suruga, N. Saeki, K. Ogawa, EphA receptors and ephrin-A ligands are upregulated by monocytic differentiation/maturation and promote cell adhesion and protrusion formation in HL60 monocytes. *BMC cell biology* **18**, 28 (2017).

74. D. Pfaff *et al.*, Involvement of endothelial ephrin-B2 in adhesion and transmigration of EphB-receptor-expressing monocytes. *Journal of Cell Science* **121**, 3842-3850 (2008).

75. D. M. Poitz *et al.*, EphrinB2/EphA4-mediated activation of endothelial cells increases monocyte adhesion. *Mol Immunol* **68**, 648-656 (2015).

76. N. Saeki, S. Nishino, T. Shimizu, K. Ogawa, EphA2 promotes cell adhesion and spreading of monocyte and monocyte/macrophage cell lines on integrin ligand-coated surfaces. *Cell Adh Migr* **9**, 469-482 (2015).

77. B. de Saint-Vis *et al.*, Human dendritic cells express neuronal Eph receptor tyrosine kinases: role of EphA2 in regulating adhesion to fibronectin. *Blood* **102**, 4431-4440 (2003).

78. P. N. Mimche *et al.*, Expression of the Receptor Tyrosine Kinase EphB2 on Dendritic Cells Is Modulated by Toll-Like Receptor Ligation but Is Not Required for T Cell Activation. *PLoS ONE* **10**, e0138835 (2015).

79. G. Rappocciolo *et al.*, Human Herpesvirus 8 Infects and Replicates in Langerhans Cells and Interstitial Dermal Dendritic Cells and Impairs Their Function. *Journal of virology* **91**, (2017).

80. M. C. Rissoan *et al.*, Subtractive hybridization reveals the expression of immunoglobulin-like transcript 7, Eph-B1, granzyme B, and 3 novel transcripts in human plasmacytoid dendritic cells. *Blood* **100**, 3295-3303 (2002).

81. C. L. Alonso *et al.*, Expression profile of Eph receptors and ephrin ligands in healthy human B lymphocytes and chronic lymphocytic leukemia B-cells. *Leuk Res* **33**, 395-406 (2009).

82. M. A. Flores *et al.*, EphrinA4 plays a critical role in alpha4 and alphaL mediated survival of human CLL cells during extravasation. *Oncotarget* **7**, 48481-48500 (2016).

83. Y. C. Huang *et al.*, Regulation of EBV LMP1-triggered EphA4 downregulation in EBV-associated B lymphoma and its impact on patients' survival. *Blood* **128**, 1578-1589 (2016).

84. B. J. Laidlaw *et al.*, The Eph-related tyrosine kinase ligand Ephrin-B1 marks germinal center and memory precursor B cells. *J Exp Med* **214**, 639-649 (2017).

85. P. Lu, C. Shih, H. Qi, Ephrin B1-mediated repulsion and signaling control germinal center T cell territoriality and function. *Science* **356**, (2017).

86. M. Yu *et al.*, EphB2 contributes to human naive B-cell activation and is regulated by miR-185. *FASEB journal : official publication of the Federation of American Societies for Experimental Biology* **28**, 3609-3617 (2014).

87. H. Nakanishi, T. Nakamura, E. Canaani, C. M. Croce, ALL1 fusion proteins induce deregulation of EphA7 and ERK phosphorylation in human acute leukemias. *Proc Natl Acad Sci U S A* **104**, 14442-14447 (2007).

88. I. P. Wicks, D. Wilkinson, E. Salvaris, A. W. Boyd, Molecular cloning of HEK, the gene encoding a receptor tyrosine kinase expressed by human lymphoid tumor cell lines. *Proc Natl Acad Sci U S A* **89**, 1611-1615 (1992).

89. T. Cejalvo *et al.*, Ephrin-B-dependent thymic epithelial cell-thymocyte interactions are necessary for correct T cell differentiation and thymus histology organization: relevance for thymic cortex development. *J Immunol* **190**, 2670-2681 (2013).

90. H. L. Holen, K. Nustad, H. C. Aasheim, Activation of EphA receptors on CD4+CD45RO+ memory cells stimulates migration. *J Leukoc Biol* **87**, 1059-1068 (2010).

91. Y. Hu *et al.*, Role of EFNB1 and EFNB2 in Mouse Collagen-Induced Arthritis and Human Rheumatoid Arthritis. *Arthritis & rheumatology (Hoboken, N.J.)* **67**, 1778-1788 (2015).

92. W. Jin, S. Qi, H. Luo, T cell-specific deletion of EFNB2 minimally affects T cell development and function. *Mol Immunol* **52**, 141-147 (2012).

93. H. Kawano *et al.*, A novel feedback mechanism by Ephrin-B1/B2 in T-cell activation involves a concentration-dependent switch from costimulation to inhibition. *Eur J Immunol* **42**, 1562-1572 (2012).

94. T. Kitamura *et al.*, Enhancement of lymphocyte migration and cytokine production by ephrinB1 system in rheumatoid arthritis. *American journal of physiology. Cell physiology* **294**, C189-196 (2008).

95. H. Luo *et al.*, EphrinB1 and EphrinB2 regulate T cell chemotaxis and migration in experimental autoimmune encephalomyelitis and multiple sclerosis. *Neurobiol Dis* **91**, 292-306 (2016).

96. T. M. Nguyen, A. Arthur, J. D. Hayball, S. Gronthos, EphB and Ephrin-B interactions mediate human mesenchymal stem cell suppression of activated T-cells. *Stem cells and development* **22**, 2751-2764 (2013).

97. G. Yu, H. Luo, Y. Wu, J. Wu, EphrinB1 is essential in T-cell-T-cell co-operation during T-cell activation. *J Biol Chem* **279**, 55531-55539 (2004).

98. N. Sharfe *et al.*, EphA and ephrin-A proteins regulate integrin-mediated T lymphocyte interactions. *Molecular immunology* **45**, 1208-1220 (2008).

99. J. G. Wohlfahrt *et al.*, Ephrin-A1 suppresses Th2 cell activation and provides a regulatory link to lung epithelial cells. *J Immunol* **172**, 843-850 (2004).

100. G. Yu, H. Luo, Y. Wu, J. Wu, Mouse ephrinB3 augments T-cell signaling and responses to T-cell receptor ligation. *J Biol Chem* **278**, 47209-47216 (2003).

101. A. Maddigan *et al.*, EphB receptors trigger Akt activation and suppress Fas receptor-induced apoptosis in malignant T lymphocytes. *J Immunol* **187**, 5983-5994 (2011).

102. L. M. Smith *et al.*, EphA3 is induced by CD28 and IGF-1 and regulates cell adhesion. *Experimental cell research* **292**, 295-303 (2004).

103. H. L. Holen, K. Nustad, H.-C. Aasheim, Activation of EphA receptors on CD4+CD45RO+ memory cells stimulates migration. *Journal of Leukocyte Biology* **87**, 1059-1068 (2010).

104. D. Pfaff, U. Fiedler, H. G. Augustin, Emerging roles of the Angiopoietin-Tie and the ephrin-Eph systems as regulators of cell trafficking. *Journal of leukocyte biology* **80**, 719-726 (2006).

105. T. N. Campbell, S. M. Robbins, The Eph receptor/ephrin system: an emerging player in the invasion game. *Curr Issues Mol Biol* **10**, 61-66 (2008).

106. J. Wu, H. Luo, Recent advances on T-cell regulation by receptor tyrosine kinases. *Curr Opin Hematol* **12**, 292-297 (2005).

107. S. Suenobu *et al.*, A role of EphB4 receptor and its ligand, ephrin-B2, in erythropoiesis. *Biochemical and Biophysical Research Communications* **293**, 1124-1131 (2002).

108. H. Kwak *et al.*, Sinusoidal ephrin receptor EPHB4 controls hematopoietic progenitor cell mobilization from bone marrow. *J Clin Invest* **126**, 4554-4568 (2016).

109. Z. Wang *et al.*, Receptor tyrosine kinase, EphB4 (HTK), accelerates differentiation of select human hematopoietic cells. *Blood* **99**, 2740-2747 (2002).

110. A. Merlos-Suárez *et al.*, The Intestinal Stem Cell Signature Identifies Colorectal Cancer Stem Cells and Predicts Disease Relapse. *Cell Stem Cell* **8**, 511-524 (2011).

111. E. Batlle *et al.*, β-Catenin and TCF Mediate Cell Positioning in the Intestinal Epithelium by Controlling the Expression of EphB/EphrinB. *Cell* **111**, 251-263 (2002).

112. T. M. Nguyen *et al.*, EphB4 Expressing Stromal Cells Exhibit an Enhanced Capacity for Hematopoietic Stem Cell Maintenance. *Stem cells (Dayton, Ohio)* **33**, 2838-2849 (2015).

113. P. Lazarova *et al.*, Growth factor receptors in hematopoietic stem cells: EPH family expression in CD34+ and CD133+ cell populations from mobilized peripheral blood. *International journal of immunopathology and pharmacology* **19**, 49-56 (2006).

114. H. C. Aasheim *et al.*, A splice variant of human ephrin-A4 encodes a soluble molecule that is secreted by activated human B lymphocytes. *Blood* **95**, 221-230 (2000).

115. H. Luo, G. Yu, Y. Wu, J. Wu, EphB6 crosslinking results in costimulation of T cells. *The Journal of Clinical Investigation* **110**, 1141-1150 (2002).

116. G. Yu, H. Luo, Y. Wu, J. Wu, Ephrin B2 induces T cell costimulation. *J Immunol* **171**, 106-114 (2003).

117. H. Luo, G. Yu, J. Tremblay, J. Wu, EphB6-null mutation results in compromised T cell function. *J Clin Invest* **114**, 1762-1773 (2004).

118. H. Luo, X. Wan, Y. Wu, J. Wu, Cross-linking of EphB6 resulting in signal transduction and apoptosis in Jurkat cells. *J Immunol* **167**, 1362-1370 (2001).

119. S. Park, Brain-Region Specific Apoptosis Triggered by Eph/ephrin Signaling. *Experimental neurobiology* **22**, 143-148 (2013).

120. A. Freywald, N. Sharfe, C. D. Miller, C. Rashotte, C. M. Roifman, EphA receptors inhibit anti-CD3-induced apoptosis in thymocytes. *J Immunol* **176**, 4066-4074 (2006).

121. A. Freywald, N. Sharfe, C. Rashotte, T. Grunberger, C. M. Roifman, The EphB6 receptor inhibits JNK activation in T lymphocytes and modulates T cell receptor-mediated responses. *J Biol Chem* **278**, 10150-10156 (2003).

122. S. Montero-Herradon, J. Garcia-Ceca, B. Sanchez Del Collado, D. Alfaro, A. G. Zapata, Eph/ephrin-B-mediated cell-to-cell interactions govern MTS20(+) thymic epithelial cell development. *Histochemistry and cell biology* **146**, 167-182 (2016).

123. M. A. Stimamiglio *et al.*, EphB2-mediated interactions are essential for proper migration of T cell progenitors during fetal thymus colonization. *J Leukoc Biol* **88**, 483-494 (2010).

124. T. Cejalvo *et al.*, Conditioned deletion of ephrinB1 and/or ephrinB2 in either thymocytes or thymic epithelial cells alters the organization of thymic medulla and favors the appearance of thymic epithelial cysts. *Histochemistry and cell biology* **143**, 517-529 (2015).

125. J. J. Munoz *et al.*, Expression and function of the Eph A receptors and their ligands ephrins A in the rat thymus. *J Immunol* **169**, 177-184 (2002).

126. D. Alfaro *et al.*, EphrinB1-EphB signaling regulates thymocyte-epithelium interactions involved in functional T cell development. *Eur J Immunol* **37**, 2596-2605 (2007).

127. H. Luo *et al.*, Efnb1 and Efnb2 proteins regulate thymocyte development, peripheral T cell differentiation, and antiviral immune responses and are essential for interleukin-6 (IL-6) signaling. *J Biol Chem* **286**, 41135-41152 (2011).

128. D. Alfaro *et al.*, Alterations in the thymocyte phenotype of EphB-deficient mice largely affect the double negative cell compartment. *Immunology* **125**, 131-143 (2008).

129. J. J. Muñoz *et al.*, Thymic Alterations in EphA4-Deficient Mice. *The Journal of Immunology* **177**, 804-813 (2006).

130. G. D. Victora, SnapShot: the germinal center reaction. *Cell* **159**, 700-700.e701 (2014).

131. H. G. Augustin, Y. Reiss, EphB receptors and ephrinB ligands: regulators of vascular assembly and homeostasis. *Cell Tissue Res* **314**, 25-31 (2003).

132. T. Makinen *et al.*, PDZ interaction site in ephrinB2 is required for the remodeling of lymphatic vasculature. *Genes Dev* **19**, 397-410 (2005).

133. N. Konda, N. Saeki, S. Nishino, K. Ogawa, Truncated EphA2 likely potentiates cell adhesion via integrins as well as infiltration and/or lodgment of a monocyte/macrophage cell line in the red pulp and marginal zone of the mouse spleen, where ephrin-A1 is prominently expressed in the vasculature. *Histochemistry and cell biology* **147**, 317-339 (2017).

134. B. de Saint-Vis *et al.*, Human dendritic cells express neuronal Eph receptor tyrosine kinases: role of EphA2 in regulating adhesion to fibronectin. *Blood* **102**, 4431-4440 (2003).

135. E. Munthe, E. F. Finne, H. C. Aasheim, Expression and functional effects of Eph receptor tyrosine kinase A family members on Langerhans like dendritic cells. *BMC Immunol* **5**, 9 (2004).

136. E. M. Trinidad, A. G. Zapata, L. M. Alonso-Colmenar, Eph-ephrin bidirectional signaling comes into the context of lymphocyte transendothelial migration. *Cell Adhesion & Migration* **4**, 363-367 (2010).

137. N. Sharfe *et al.*, EphA and ephrin-A proteins regulate integrin-mediated T lymphocyte interactions. *Molecular Immunology* **45**, 1208-1220 (2008).

138. H. C. Aasheim, J. Delabie, E. F. Finne, Ephrin-A1 binding to CD4+ T lymphocytes stimulates migration and induces tyrosine phosphorylation of PYK2. *Blood* **105**, 2869-2876 (2005).

139. H. S. Hjorthaug, H. C. Aasheim, Ephrin-A1 stimulates migration of CD8+CCR7+ T lymphocytes. *Eur J Immunol* **37**, 2326-2336 (2007).

140. S. D. Funk, A. C. Finney, A. Yurdagul, Jr., C. B. Pattillo, A. W. Orr, EphA2 stimulates VCAM-1 expression through calcium-dependent NFAT1 activity. *Cell Signal* **49**, 30-38 (2018).

141. N. Sharfe, A. Freywald, A. Toro, H. Dadi, C. Roifman, Ephrin stimulation modulates T cell chemotaxis. *European Journal of Immunology* **32**, 3745-3755 (2002).

142. Y. Chen, A. K. Fu, N. Y. Ip, Eph receptors at synapses: implications in neurodegenerative diseases. *Cell Signal* **24**, 606-611 (2012).

143. M. G. Coulthard *et al.*, Eph/Ephrin signaling in injury and inflammation. *Am J Pathol* **181**, 1493-1503 (2012).

144. S. D. Funk, A. W. Orr, Ephs and ephrins resurface in inflammation, immunity, and atherosclerosis. *Pharmacological research* **67**, 42-52 (2013).

145. E. B. Pasquale, Eph receptors and ephrins in cancer: bidirectional signalling and beyond. *Nature reviews. Cancer* **10**, 165-180 (2010).

146. M. Cisse, F. Checler, Eph receptors: new players in Alzheimer's disease pathogenesis. *Neurobiol Dis* **73**, 137-149 (2015).

147. V. A. Malik, B. Di Benedetto, The Blood-Brain Barrier and the EphR/Ephrin System: Perspectives on a Link Between Neurovascular and Neuropsychiatric Disorders. *Frontiers in molecular neuroscience* **11**, 127 (2018).

148. A. Barquilla, E. B. Pasquale, Eph receptors and ephrins: therapeutic opportunities. *Annu Rev Pharmacol Toxicol* **55**, 465-487 (2015).

149. A. Lodola, C. Giorgio, M. Incerti, I. Zanotti, M. Tognolini, Targeting Eph/ephrin system in cancer therapy. *European journal of medicinal chemistry* **142**, 152-162 (2017).

150. P. A. Aaron, M. Jamklang, J. P. Uhrig, A. Gelli, The blood-brain barrier internalises Cryptococcus neoformans via the EphA2-tyrosine kinase receptor. *Cellular microbiology* **20**, (2018).

151. A. A. TerBush, F. Hafkamp, H. J. Lee, L. Coscoy, A Kaposi's Sarcoma-Associated Herpesvirus Infection Mechanism Is Independent of Integrins alpha3beta1, alphaVbeta3, and alphaVbeta5. *Journal of virology* **92**, (2018).

152. J. Chen *et al.*, Ephrin receptor A2 is a functional entry receptor for Epstein-Barr virus. *Nature microbiology* **3**, 172-180 (2018).

153. H. Zhang *et al.*, Ephrin receptor A2 is an epithelial cell receptor for Epstein-Barr virus entry. *Nature microbiology* **3**, 1-8 (2018).

154. A. Kaushansky *et al.*, Malaria parasites target the hepatocyte receptor EphA2 for successful host infection. *Science* **350**, 1089-1092 (2015).

155. E. B. Pasquale, Eph receptors and ephrins in cancer: bidirectional signalling and beyond. *Nat Rev Cancer* **10**, 165-180 (2010).

156. J. K. McCarron, B. W. Stringer, B. W. Day, A. W. Boyd, Ephrin expression and function in cancer. *Future Oncol* **6**, 165-176 (2010).

157. T. Yamashita *et al.*, Hypoxia-inducible transcription factor-2alpha in endothelial cells regulates tumor neovascularization through activation of ephrin A1. *J Biol Chem* **283**, 18926-18936 (2008).

158. C. Hafner *et al.*, Differential Gene Expression of Eph Receptors and Ephrins in Benign Human Tissues and Cancers. *Clinical Chemistry* **50**, 490-499 (2004).

159. G. Zhuang *et al.*, Elevation of receptor tyrosine kinase EphA2 mediates resistance to trastuzumab therapy. *Cancer Res* **70**, 299-308 (2010).

160. J. Wykosky, W. Debinski, The EphA2 receptor and ephrinA1 ligand in solid tumors: function and therapeutic targeting. *Mol Cancer Res* **6**, 1795-1806 (2008).

161. S. R. Kumar *et al.*, The receptor tyrosine kinase EphB4 is overexpressed in ovarian cancer, provides survival signals and predicts poor outcome. *Br J Cancer* **96**, 1083-1091 (2007).

162. A. A. Merchant *et al.*, EPHB4 is a therapeutic target in AML and promotes leukemia cell survival via AKT. *Blood advances* **1**, 1635-1644 (2017).

163. E. Batlle *et al.*, EphB receptor activity suppresses colorectal cancer progression. *Nature* **435**, 1126-1130 (2005).

164. N. Keane, C. Freeman, R. Swords, F. J. Giles, EPHA3 as a novel therapeutic target in the hematological malignancies. *Expert review of hematology* **5**, 325-340 (2012).

165. R. T. Swords *et al.*, KB004, a first in class monoclonal antibody targeting the receptor tyrosine kinase EphA3, in patients with advanced hematologic malignancies: Results from a phase 1 study. *Leuk Res* **50**, 123-131 (2016).

166. A. Caivano *et al.*, Epha3 acts as proangiogenic factor in multiple myeloma. *Oncotarget* **8**, 34298-34309 (2017).

167. S. Charmsaz *et al.*, EphA2 Is a Therapy Target in EphA2-Positive Leukemias but Is Not Essential for Normal Hematopoiesis or Leukemia. *PLoS One* **10**, e0130692 (2015).

168. E. Oricchio *et al.*, The Eph-receptor A7 is a soluble tumor suppressor for follicular lymphoma. *Cell* **147**, 554-564 (2011).

169. S. Q. Kuang *et al.*, Aberrant DNA methylation and epigenetic inactivation of Eph receptor tyrosine kinases and ephrin ligands in acute lymphoblastic leukemia. *Blood* **115**, 2412-2419 (2010).

170. N. K. Noren, G. Foos, C. A. Hauser, E. B. Pasquale, The EphB4 receptor suppresses breast cancer cell tumorigenicity through an Abl-Crk pathway. *Nat Cell Biol* **8**, 815-825 (2006).

171. N. Li *et al.*, Chimeric Antigen Receptor-Modified T Cells Redirected to EphA2 for the Immunotherapy of Non-Small Cell Lung Cancer. *Translational oncology* **11**, 11-17 (2018).

172. H. Shi *et al.*, EphA2 chimeric antigen receptor-modified T cells for the immunotherapy of esophageal squamous cell carcinoma. *Journal of thoracic disease* **10**, 2779-2788 (2018).

173. Z. Yi, B. L. Prinzing, F. Cao, S. Gottschalk, G. Krenciute, Optimizing EphA2-CAR T Cells for the Adoptive Immunotherapy of Glioma. *Molecular therapy. Methods & clinical development* **9**, 70-80 (2018).

174. S. Taki *et al.*, A Novel Bispecific Antibody against Human CD3 and Ephrin Receptor A10 for Breast Cancer Therapy. *PLoS One* **10**, e0144712 (2015).

175. Y. Huo, K. F. Ley, Role of platelets in the development of atherosclerosis. *Trends in cardiovascular medicine* **14**, 18-22 (2004).

176. N. Prévost *et al.*, Eph kinases and ephrins support thrombus growth and stability by regulating integrin outside-in signaling in platelets. *Proceedings of the National Academy of Sciences of the United States of America* **102**, 9820-9825 (2005).

177. N. Prevost, D. Woulfe, T. Tanaka, L. F. Brass, Interactions between Eph kinases and ephrins provide a mechanism to support platelet aggregation once cell-to-cell contact has occurred. *Proceedings of the National Academy of Sciences of the United States of America* **99**, 9219-9224 (2002).

178. E. Tournoij *et al.*, The platelet P2Y12 receptor contributes to granule secretion through Ephrin A4 receptor. *Platelets* **23**, 617-625 (2012).

179. A. Sakamoto *et al.*, Expression and function of ephrin-B1 and its cognate receptor EphB2 in human atherosclerosis: from an aspect of chemotaxis. *Clinical Science* **114**, 643-650 (2008).

180. A. Sakamoto *et al.*, Expression profiling of the ephrin (EFN) and Eph receptor (EPH) family of genes in atherosclerosis-related human cells. *J Int Med Res* **39**, 522-527 (2011).

181. T. A. Wynn, Cellular and molecular mechanisms of fibrosis. *The Journal of pathology* **214**, 199-210 (2008).

182. D. Lagares *et al.*, ADAM10-mediated ephrin-B2 shedding promotes myofibroblast activation and organ fibrosis. *Nat Med* **23**, 1405-1415 (2017).

183. Y. Goldshmit, J. Bourne, Upregulation of EphA4 on astrocytes potentially mediates astrocytic gliosis after cortical lesion in the marmoset monkey. *J Neurotrauma* **27**, 1321-1332 (2010).

184. T. Frugier *et al.*, Expression and activation of EphA4 in the human brain after traumatic injury. *J Neuropathol Exp Neurol* **71**, 242-250 (2012).

185. J. Fabes *et al.*, Accumulation of the inhibitory receptor EphA4 may prevent regeneration of corticospinal tract axons following lesion. *Eur J Neurosci* **23**, 1721-1730 (2006).

186. K. Berer, G. Krishnamoorthy, Microbial view of central nervous system autoimmunity. *FEBS letters* **588**, 4207-4213 (2014).

187. R. A. Sobel, Ephrin A receptors and ligands in lesions and normal-appearing white matter in multiple sclerosis. *Brain Pathol* **15**, 35-45 (2005).

188. L. Lin, T. G. Lesnick, D. M. Maraganore, O. Isacson, Axon guidance and synaptic maintenance: preclinical markers for neurodegenerative disease and therapeutics. *Trends Neurosci* **32**, 142-149 (2009).

189. A. C. Naj *et al.*, Common variants at MS4A4/MS4A6E, CD2AP, CD33 and EPHA1 are associated with late-onset Alzheimer's disease. *Nat Genet* **43**, 436-441 (2011).

190. M. I. Bonaparte *et al.*, Ephrin-B2 ligand is a functional receptor for Hendra virus and Nipah virus. *Proc Natl Acad Sci U S A* **102**, 10652-10657 (2005).

191. J. J. W. Wong *et al.*, Monomeric ephrinB2 binding induces allosteric changes in Nipah virus G that precede its full activation. *Nature communications* **8**, 781 (2017).

192. A. S. Hahn *et al.*, The ephrin receptor tyrosine kinase A2 is a cellular receptor for Kaposi's sarcoma-associated herpesvirus. *Nat Med* **18**, 961-966 (2012).

193. A. Kaushansky *et al.*, Malaria parasites target the hepatocyte receptor EphA2 for successful host infection. *Science* **350**, 1089-1092 (2015).

194. A. C. Langlois, C. Marinach, G. Manzoni, O. Silvie, Plasmodium sporozoites can invade hepatocytic cells independently of the Ephrin receptor A2. *PLoS One* **13**, e0200032 (2018).

195. M. Khounlotham, S. Subbian, R. Smith, 3rd, S. L. Cirillo, J. D. Cirillo, Mycobacterium tuberculosis interferes with the response to infection by inducing the host EphA2 receptor. *J Infect Dis* **199**, 1797-1806 (2009).

196. S. J. Meding, S. C. Cheng, B. Simon-Haarhaus, J. Langhorne, Role of gamma interferon during infection with Plasmodium chabaudi chabaudi. *Infection and Immunity* **58**, 3671-3678 (1990).

197. A. Chandele, P. Mukerjee, G. Das, R. Ahmed, V. S. Chauhan, Phenotypic and functional profiling of malaria-induced CD8 and CD4 T cells during blood-stage infection with Plasmodium yoelii. *Immunology* **132**, 273-286 (2011).

198. G. Süss, K. Eichmann, E. Kury, A. Linke, J. Langhorne, Roles of CD4- and CD8-bearing T lymphocytes in the immune response to the erythrocytic stages of Plasmodium chabaudi. *Infection and Immunity* **56**, 3081-3088 (1988).

199. S. J. Meding, J. Langhorne, CD4+ T cells and B cells are necessary for the transfer of protective immunity to Plasmodium chabaudi chabaudi. *European Journal of Immunology* **21**, 1433-1438 (1991).

200. D. A. Brake, C. A. Long, W. P. Weidanz, Adoptive protection against Plasmodium chabaudi adami malaria in athymic nude mice by a cloned T cell line. *The Journal of Immunology* **140**, 1989-1993 (1988).

201. A. N. Jayawardena, D. B. Murphy, C. A. Janeway, R. K. Gershon, T cell-mediated immunity in malaria. I. The Ly phenotype of T cells mediating resistance to Plasmodium yoelii. *The Journal of Immunology* **129**, 377-381 (1982).

202. P. Guermonprez *et al.*, Inflammatory Flt3l is essential to mobilize dendritic cells and for T cell responses during Plasmodium infection. *Nature medicine* **19**, 730-738 (2013).

203. T. Imai *et al.*, Involvement of CD8+ T cells in protective immunity against murine blood-stage infection with Plasmodium yoelii 17XL strain. *European Journal of Immunology* **40**, 1053-1061 (2010).

204. C. R. Engwerda, M. F. Good, Interactions between malaria parasites and the host immune system. *Current opinion in immunology* **17**, 381-387 (2005).

205. A. Villegas-Mendez *et al.*, IFN-gamma-producing CD4+ T cells promote experimental cerebral malaria by modulating CD8+ T cell accumulation within the brain. *J Immunol* **189**, 968-979 (2012).

206. W.-L. Chang *et al.*, CD8+-T-Cell Depletion Ameliorates Circulatory Shock in Plasmodium berghei-Infected Mice. *Infection and Immunity* **69**, 7341-7348 (2001).

207. T. N. Shaw *et al.*, Perivascular Arrest of CD8+ T Cells Is a Signature of Experimental Cerebral Malaria. *PLoS Pathog* **11**, e1005210 (2015).

208. S. Pai *et al.*, Real-Time Imaging Reveals the Dynamics of Leukocyte Behaviour during Experimental Cerebral Malaria Pathogenesis. *PLoS Pathog* **10**, e1004236 (2014).

209. A. Haque *et al.*, Granzyme B Expression by CD8+ T Cells Is Required for the Development of Experimental Cerebral Malaria. *The Journal of Immunology* **186**, 6148-6156 (2011).

210. J. A. McQuillan *et al.*, Coincident parasite and CD8 T cell sequestration is required for development of experimental cerebral malaria. *International Journal for Parasitology* **41**, 155-163 (2011).

211. I. Galea *et al.*, An antigen-specific pathway for CD8 T cells across the blood-brain barrier. *The Journal of Experimental Medicine* **204**, 2023-2030 (2007).

212. T. E. Taylor *et al.*, Differentiating the pathologies of cerebral malaria by postmortem parasite counts. *Nat Med* **10**, 143-145 (2004).

213. K. Haldar, S. C. Murphy, D. A. Milner, T. E. Taylor, Malaria: mechanisms of erythrocytic infection and pathological correlates of severe disease. *Annu Rev Pathol* **2**, 217-249 (2007).

214. A. G. Craig *et al.*, The role of animal models for research on severe malaria. *PLoS Pathog* **8**, e1002401 (2012).

215. N. H. Hunt *et al.*, Murine cerebral malaria: the whole story. *Trends Parasitol* **26**, 272-274 (2010).

216. N. J. White, G. D. Turner, I. M. Medana, A. M. Dondorp, N. P. Day, The murine cerebral malaria phenomenon. *Trends Parasitol* **26**, 11-15 (2010).

217. V. Barrera *et al.*, Comparison of CD8(+) T Cell Accumulation in the Brain During Human and Murine Cerebral Malaria. *Frontiers in immunology* **10**, 1747 (2019).

218. V. Amani *et al.*, Involvement of IFN-γ receptor-mediated signaling in pathology and anti-malarial immunity induced by Plasmodium berghei infection. *European Journal of Immunology* **30**, 1646-1655 (2000).

219. L. S. Lau *et al.*, Blood-Stage Plasmodium berghei Infection Generates a Potent, Specific CD8+ T-Cell Response Despite Residence Largely in Cells Lacking MHC I Processing Machinery. *Journal of Infectious Diseases* **204**, 1989-1996 (2011).

220. R. J. Lundie *et al.*, Blood-stage Plasmodium infection induces CD8+ T lymphocytes to parasite-expressed antigens, largely regulated by CD8α+ dendritic cells. *Proceedings of the National Academy of Sciences* **105**, 14509-14514 (2008).

221. E. Belnoue *et al.*, On the Pathogenic Role of Brain-Sequestered αβ CD8+ T Cells in Experimental Cerebral Malaria. *The Journal of Immunology* **169**, 6369-6375 (2002).

222. D. M. Yañez, D. D. Manning, A. J. Cooley, W. P. Weidanz, H. C. van der Heyde, Participation of lymphocyte subpopulations in the pathogenesis of experimental murine cerebral malaria. *The Journal of Immunology* **157**, 1620-1624 (1996).

223. S. W. Howland *et al.*, Brain microvessel cross-presentation is a hallmark of experimental cerebral malaria. *EMBO Molecular Medicine* **5**, 984-999 (2013).

224. S. W. Howland, C. M. Poh, L. Rénia, Activated Brain Endothelial Cells Cross-Present Malaria Antigen. *PLoS Pathog* **11**, e1004963 (2015).

225. J. Nitcheu *et al.*, Perforin-Dependent Brain-Infiltrating Cytotoxic CD8+ T Lymphocytes Mediate Experimental Cerebral Malaria Pathogenesis. *The Journal of Immunology* **170**, 2221-2228 (2003).

226. E. Belnoue *et al.*, Control of pathogenic CD8+ T cell migration to the brain by IFN-γ during experimental cerebral malaria. *Parasite Immunology* **30**, 544-553 (2008).

227. T. N. Ramos *et al.*, Experimental Cerebral Malaria Develops Independently of Endothelial Expression of Intercellular Adhesion Molecule-1 (ICAM-1). *Journal of Biological Chemistry* **288**, 10962-10966 (2013).

228. J. Li *et al.*, Intercellular adhesion molecule 1 is important for the development of severe experimental malaria but is not required for leukocyte adhesion in the brain. *J Investig Med* **51**, 128-140 (2003).

229. A. R. Berendt, D. L. Simmons, J. Tansey, C. I. Newbold, K. Marsh, Intercellular adhesion molecule-1 is an endothelial cell adhesion receptor for Plasmodium falciparum. *Nature* **341**, 57-59 (1989).

230. J. D. Smith *et al.*, Identification of a Plasmodium falciparum intercellular adhesion molecule-1 binding domain: A parasite adhesion trait implicated in cerebral malaria. *Proceedings of the National Academy of Sciences* **97**, 1766-1771 (2000).

231. K. Willimann, H. Matile, N. A. Weiss, B. A. Imhof, In vivo sequestration of Plasmodium falciparum-infected human erythrocytes: a severe combined immunodeficiency mouse model for cerebral malaria. *The Journal of Experimental Medicine* **182**, 643-653 (1995).

232. R. Idro, K. Marsh, C. C. John, C. R. J. Newton, Cerebral Malaria; Mechanisms Of Brain Injury And Strategies For Improved Neuro-Cognitive Outcome. *Pediatric research* **68**, 267-274 (2010).

233. R. Idro, N. E. Jenkins, C. R. J. C. Newton, Pathogenesis, clinical features, and neurological outcome of cerebral malaria. *The Lancet Neurology* **4**, 827-840.

234. S. J. Chakravorty, A. Craig, The role of ICAM-1 in Plasmodium falciparum cytoadherence. *European Journal of Cell Biology* **84**, 15-27 (2005).

235. J. A. Rowe, A. Claessens, R. A. Corrigan, M. Arman, Adhesion of Plasmodium falciparum-infected erythrocytes to human cells: molecular mechanisms and

therapeutic implications. *Expert Reviews in Molecular Medicine* **11**, null-null (2009).

236. I. W. Sherman, S. Eda, E. Winograd, Cytoadherence and sequestration in Plasmodium falciparum: defining the ties that bind. *Microbes and Infection* **5**, 897-909 (2003).

237. L. Turner *et al.*, Severe malaria is associated with parasite binding to endothelial protein C receptor. *Nature* **498**, 502-505 (2013).

238. S. Adams, H. Brown, G. Turner, Breaking down the blood–brain barrier: signaling a path to cerebral malaria? *Trends in Parasitology* **18**, 360-366.

239. I. M. Medana, G. D. H. Turner, Plasmodium falciparum and the Blood-Brain Barrier—Contacts and Consequences. *Journal of Infectious Diseases* **195**, 921-923 (2007).

240. A. Nacer *et al.*, Neuroimmunological Blood Brain Barrier Opening in Experimental Cerebral Malaria. *PLoS Pathog* **8**, e1002982 (2012).

241. S. Potter *et al.*, Perforin mediated apoptosis of cerebral microvascular endothelial cells during experimental cerebral malaria. *International Journal for Parasitology* **36**, 485-496 (2006).

242. W. B. Fang *et al.*, Overexpression of EPHA2 receptor destabilizes adherens junctions via a RhoA-dependent mechanism. *Journal of Cell Science* **121**, 358-368 (2008).

243. N. Zhou *et al.*, Inactivation of EphA2 promotes tight junction formation and impairs angiogenesis in brain endothelial cells. *Microvasc Res* **82**, 113-121 (2011).

244. J. Larson, S. Schomberg, W. Schroeder, T. C. Carpenter, Endothelial EphA receptor stimulation increases lung vascular permeability. *American Journal of Physiology - Lung Cellular and Molecular Physiology* **295**, L431-L439 (2008).

245. M. Tanaka, R. Kamata, R. Sakai, EphA2 Phosphorylates the Cytoplasmic Tail of Claudin-4 and Mediates Paracellular Permeability. *Journal of Biological Chemistry* **280**, 42375-42382 (2005).

246. I. Gramaglia *et al.*, Platelets activate a pathogenic response to blood-stage Plasmodium infection but not a protective immune response. *Blood* **129**, 1669-1679 (2017).

247. I. Gramaglia *et al.*, Cell- rather than antibody-mediated immunity leads to the development of profound thrombocytopenia during experimental Plasmodium berghei malaria. *J Immunol* **175**, 7699-7707 (2005).

248. P. Gerardin *et al.*, Prognostic value of thrombocytopenia in African children with falciparum malaria. *Am J Trop Med Hyg* **66**, 686-691 (2002).

249. U. M. Jadhav, V. S. Patkar, N. N. Kadam, Thrombocytopenia in malaria--correlation with type and severity of malaria. *The Journal of the Association of Physicians of India* **52**, 615-618 (2004).

250. R. D. Horstmann, M. Dietrich, U. Bienzle, H. Rasche, Malaria-induced thrombocytopenia. *Blut* **42**, 157-164 (1981).

251. G. E. Grau *et al.*, Platelet accumulation in brain microvessels in fatal pediatric cerebral malaria. *J Infect Dis* **187**, 461-466 (2003).

252. S. C. Wassmer *et al.*, Platelets reorient Plasmodium falciparum-infected erythrocyte cytoadhesion to activated endothelial cells. *J Infect Dis* **189**, 180-189 (2004).

253. E. Pongponratn, M. Riganti, T. Harinasuta, D. Bunnag, Electron microscopy of the human brain in cerebral malaria. *The Southeast Asian journal of tropical medicine and public health* **16**, 219-227 (1985).

254. S. E. Hochman *et al.*, Fatal Pediatric Cerebral Malaria Is Associated with Intravascular Monocytes and Platelets That Are Increased with HIV Coinfection. *mBio* **6**, e01390-01315 (2015).

255. S. Kho *et al.*, Platelets kill circulating parasites of all major Plasmodium species in human malaria. *Blood* **132**, 1332-1344 (2018).

256. A. Pain *et al.*, Platelet-mediated clumping of Plasmodium falciparum-infected erythrocytes is a common adhesive phenotype and is associated with severe malaria. *Proc Natl Acad Sci U S A* **98**, 1805-1810 (2001).

257. C. M. Hawrylowicz, G. L. Howells, M. Feldmann, Platelet-derived interleukin 1 induces human endothelial adhesion molecule expression and cytokine production. *J Exp Med* **174**, 785-790 (1991).

258. O. P. Barry, D. Pratico, J. A. Lawson, G. A. FitzGerald, Transcellular activation of platelets and endothelial cells by bioactive lipids in platelet microparticles. *J Clin Invest* **99**, 2118-2127 (1997).

259. O. P. Barry, D. Pratico, R. C. Savani, G. A. FitzGerald, Modulation of monocyte-endothelial cell interactions by platelet microparticles. *J Clin Invest* **102**, 136-144 (1998).

260. D. J. Bridges *et al.*, Rapid activation of endothelial cells enables Plasmodium falciparum adhesion to platelet-decorated von Willebrand factor strings. *Blood* **115**, 1472-1474 (2010).

261. P. H. Kuijper *et al.*, Platelet-dependent primary hemostasis promotes selectin- and integrin-mediated neutrophil adhesion to damaged endothelium under flow conditions. *Blood* **87**, 3271-3281 (1996).

262. P. H. Kuijper *et al.*, Platelet associated fibrinogen and ICAM-2 induce firm adhesion of neutrophils under flow conditions. *Thrombosis and haemostasis* **80**, 443-448 (1998).

263. G. E. Grau, J. Lou, TNF in vascular pathology: the importance of platelet-endothelium interactions. *Research in immunology* **144**, 355-363 (1993).

264. H. C. van der Heyde, I. Gramaglia, G. Sun, C. Woods, Platelet depletion by anti-CD41 (alphaIIb) mAb injection early but not late in the course of disease protects against Plasmodium berghei pathogenesis by altering the levels of pathogenic cytokines. *Blood* **105**, 1956-1963 (2005).

265. N. O'Regan *et al.*, A novel role for von Willebrand factor in the pathogenesis of experimental cerebral malaria. *Blood* **127**, 1192-1201 (2016).

266. A. A. Aggrey, K. Srivastava, S. Ture, D. J. Field, C. N. Morrell, Platelet induction of the acute-phase response is protective in murine experimental cerebral malaria. *J Immunol* **190**, 4685-4691 (2013).

267. B. J. McMorran *et al.*, Platelets kill intraerythrocytic malarial parasites and mediate survival to infection. *Science* **323**, 797-800 (2009).

268. F. Peyron, B. Polack, D. Lamotte, L. Kolodie, P. Ambroise-Thomas, Plasmodium falciparum growth inhibition by human platelets in vitro. *Parasitology* **99 Pt 3**, 317-322 (1989).

269. C. N. Morrell, Understanding platelets in malaria infection. *Curr Opin Hematol* **21**, 445-449 (2014).

270. G. L. Birbeck *et al.*, Blantyre Malaria Project Epilepsy Study (BMPES) of neurological outcomes in retinopathy-positive paediatric cerebral malaria survivors: a prospective cohort study. *The Lancet. Neurology* **9**, 1173-1181 (2010).

271. H. Brown *et al.*, Blood-brain barrier function in cerebral malaria in Malawian children. *Am J Trop Med Hyg* **64**, 207-213 (2001).

272. I. M. Medana, G. D. Turner, Human cerebral malaria and the blood-brain barrier. *Int J Parasitol* **36**, 555-568 (2006).

273. D. J. Grab, S. J. Chakravorty, H. van der Heyde, M. F. Stins, How can microbial interactions with the blood-brain barrier modulate astroglial and neuronal function? *Cellular microbiology* **13**, 1470-1478 (2011).

274. A. K. Tripathi, D. J. Sullivan, M. F. Stins, Plasmodium falciparum-infected erythrocytes decrease the integrity of human blood-brain barrier endothelial cell monolayers. *J Infect Dis* **195**, 942-950 (2007).

275. S. J. Chakravorty, A. Craig, The role of ICAM-1 in Plasmodium falciparum cytoadherence. *European journal of cell biology* **84**, 15-27 (2005).

276. C. R. Engwerda *et al.*, Locally up-regulated lymphotoxin alpha, not systemic tumor necrosis factor alpha, is the principle mediator of murine cerebral malaria. *J Exp Med* **195**, 1371-1377 (2002).

277. J. B. de Souza, J. C. Hafalla, E. M. Riley, K. N. Couper, Cerebral malaria: why experimental murine models are required to understand the pathogenesis of disease. *Parasitology* **137**, 755-772 (2010).

278. E. M. Riley *et al.*, Neuropathogenesis of human and murine malaria. *Trends Parasitol* **26**, 277-278 (2010).

279. A. Haque *et al.*, Granzyme B expression by CD8+ T cells is required for the development of experimental cerebral malaria. *Journal of immunology (Baltimore, Md. : 1950)* **186**, 6148-6156 (2011).

280. M. A. Huggins *et al.*, Perforin Expression by CD8 T Cells Is Sufficient To Cause Fatal Brain Edema during Experimental Cerebral Malaria. *Infect Immun* **85**, (2017).

281. M. G. Lampugnani *et al.*, Cell confluence regulates tyrosine phosphorylation of adherens junction components in endothelial cells. *J Cell Sci* **110 (Pt 17)**, 2065-2077 (1997).

282. H. de Lavallade *et al.*, Tyrosine kinase inhibitors impair B-cell immune responses in CML through off-target inhibition of kinases important for cell signaling. *Blood* **122**, 227-238 (2013).

283. Y. Yamaguchi, E. B. Pasquale, Eph receptors in the adult brain. *Current opinion in neurobiology* **14**, 288-296 (2004).

284. W. B. Fang *et al.*, Overexpression of EPHA2 receptor destabilizes adherens junctions via a RhoA-dependent mechanism. *Journal of cell science* **121**, 358-368 (2008).

285. D. Togbe *et al.*, Both functional LTbeta receptor and TNF receptor 2 are required for the development of experimental cerebral malaria. *PLoS One* **3**, e2608 (2008).

286. S. W. Howland *et al.*, Brain microvessel cross-presentation is a hallmark of experimental cerebral malaria. *EMBO Mol Med* **5**, 984-999 (2013).

287. C. M. Poh, S. W. Howland, G. M. Grotenbreg, L. Renia, Damage to the blood-brain barrier during experimental cerebral malaria results from synergistic effects of CD8+ T cells with different specificities. *Infect Immun* **82**, 4854-4864 (2014).

288. P. A. Swanson, 2nd *et al.*, CD8+ T Cells Induce Fatal Brainstem Pathology during Cerebral Malaria via Luminal Antigen-Specific Engagement of Brain Vasculature. *PLoS Pathog* **12**, e1006022 (2016).

289. S. D. Funk *et al.*, EphA2 activation promotes the endothelial cell inflammatory response: a potential role in atherosclerosis. *Arterioscler Thromb Vasc Biol* **32**, 686-695 (2012).

290. K. Ieguchi *et al.*, ADAM12-cleaved ephrin-A1 contributes to lung metastasis. *Oncogene* **33**, 2179-2190 (2014).

291. P. W. Janes *et al.*, Cytoplasmic relaxation of active Eph controls ephrin shedding by ADAM10. *PLoS biology* **7**, e1000215 (2009).

292. G. Solanas, C. Cortina, M. Sevillano, E. Batlle, Cleavage of E-cadherin by ADAM10 mediates epithelial cell sorting downstream of EphB signalling. *Nat Cell Biol* **13**, 1100-1107 (2011).

293. K. Salaita *et al.*, Restriction of receptor movement alters cellular response: physical force sensing by EphA2. *Science* **327**, 1380-1385 (2010).

294. M. G. Coulthard *et al.*, Eph/Ephrin Signaling in Injury and Inflammation. *The American Journal of Pathology* **181**, 1493-1503 (2012).

295. P. E. Van den Steen *et al.*, Matrix metalloproteinases, tissue inhibitors of MMPs and TACE in experimental cerebral malaria. *Lab Invest* **86**, 873-888 (2006).

296. S. Davis *et al.*, Ligands for EPH-related receptor tyrosine kinases that require membrane attachment or clustering for activity. *Science* **266**, 816-819 (1994).

297. J. P. Himanen *et al.*, Crystal structure of an Eph receptor-ephrin complex. *Nature* **414**, 933-938 (2001).

298. J. Wykosky *et al.*, Soluble monomeric EphrinA1 is released from tumor cells and is a functional ligand for the EphA2 receptor. *Oncogene* **27**, 7260-7273 (2008).

299. J. P. Himanen *et al.*, Ligand recognition by A-class Eph receptors: crystal structures of the EphA2 ligand-binding domain and the EphA2/ephrin-A1 complex. *EMBO reports* **10**, 722-728 (2009).

300. S. Ferluga *et al.*, Biological and structural characterization of glycosylation on ephrin-A1, a preferred ligand for EphA2 receptor tyrosine kinase. *J Biol Chem* **288**, 18448-18457 (2013).

301. L. B. Holzman, R. M. Marks, V. M. Dixit, A novel immediate-early response gene of endothelium is induced by cytokines and encodes a secreted protein. *Molecular and cellular biology* **10**, 5830-5838 (1990).

302. N. Cheng, J. Chen, Tumor necrosis factor-alpha induction of endothelial ephrin A1 expression is mediated by a p38 MAPK- and SAPK/JNK-dependent but

nuclear factor-kappa B-independent mechanism. *J Biol Chem* **276**, 13771-13777 (2001).

303. A. Pandey, H. Shao, R. M. Marks, P. J. Polverini, V. M. Dixit, Role of B61, the ligand for the Eck receptor tyrosine kinase, in TNF-alpha-induced angiogenesis. *Science* **268**, 567-569 (1995).

304. L. Vandermosten *et al.*, Experimental malaria-associated acute respiratory distress syndrome is dependent on the parasite-host combination and coincides with normocyte invasion. *Malaria journal* **17**, 102 (2018).

305. P. E. Van den Steen *et al.*, Matrix metalloproteinases, tissue inhibitors of MMPs and TACE in experimental cerebral malaria. *Laboratory investigation; a journal of technical methods and pathology* **86**, 873-888 (2006).

306. A. K. Tripathi, W. Sha, V. Shulaev, M. F. Stins, D. J. Sullivan, Plasmodium falciparum–infected erythrocytes induce NF-κB regulated inflammatory pathways in human cerebral endothelium. *Blood* **114**, 4243-4252 (2009).

307. D. P. Harris, S. Bandyopadhyay, T. J. Maxwell, B. Willard, P. E. DiCorleto, Tumor necrosis factor (TNF)-alpha induction of CXCL10 in endothelial cells requires protein arginine methyltransferase 5 (PRMT5)-mediated nuclear factor (NF)-kappaB p65 methylation. *J Biol Chem* **289**, 15328-15339 (2014).

308. E. W. Sorensen *et al.*, CXCL10 stabilizes T cell-brain endothelial cell adhesion leading to the induction of cerebral malaria. *JCI insight* **3**, (2018).

309. R. Chui, K. Dorovini-Zis, Regulation of CCL2 and CCL3 expression in human brain endothelial cells by cytokines and lipopolysaccharide. *Journal of neuroinflammation* **7**, 1 (2010).

310. E. A. Subileau *et al.*, Expression of chemokines and their receptors by human brain endothelium: implications for multiple sclerosis. *J Neuropathol Exp Neurol* **68**, 227-240 (2009).

311. B. Chan, V. P. Sukhatme, Receptor tyrosine kinase EphA2 mediates thrombin-induced upregulation of ICAM-1 in endothelial cells in vitro. *Thrombosis research* **123**, 745-752 (2009).

312. A. R. Hess *et al.*, VE-cadherin regulates EphA2 in aggressive melanoma cells through a novel signaling pathway: implications for vasculogenic mimicry. *Cancer Biol Ther* **5**, 228-233 (2006).

313. J. Thundyil *et al.*, Evidence that the EphA2 receptor exacerbates ischemic brain injury. *PLoS One* **8**, e53528 (2013).

314. E. Hadzijusufovic *et al.*, Nilotinib-induced vasculopathy: identification of vascular endothelial cells as a primary target site. *Leukemia* **31**, 2388-2397 (2017).

315. S. S. Karuppagounder *et al.*, The c-Abl inhibitor, nilotinib, protects dopaminergic neurons in a preclinical animal model of Parkinson's disease. *Scientific reports* **4**, 4874 (2014).

316. M. L. Hebron, I. Lonskaya, C. E. Moussa, Nilotinib reverses loss of dopamine neurons and improves motor behavior via autophagic degradation of alpha-synuclein in Parkinson's disease models. *Human molecular genetics* **22**, 3315-3328 (2013).

317. R. Noberini *et al.*, Small molecules can selectively inhibit ephrin binding to the EphA4 and EphA2 receptors. *J Biol Chem* **283**, 29461-29472 (2008).

318. K. R. Amato *et al.*, Genetic and pharmacologic inhibition of EPHA2 promotes apoptosis in NSCLC. *J Clin Invest* **124**, 2037-2049 (2014).

319. P. Strangward *et al.*, A quantitative brain map of experimental cerebral malaria pathology. *PLoS Pathog* **13**, e1006267 (2017).

320. N. D. Zantek *et al.*, E-cadherin regulates the function of the EphA2 receptor tyrosine kinase. *Cell growth & differentiation : the molecular biology journal of the American Association for Cancer Research* **10**, 629-638 (1999).

321. M. Tanaka, R. Kamata, R. Sakai, EphA2 phosphorylates the cytoplasmic tail of Claudin-4 and mediates paracellular permeability. *The Journal of biological chemistry* **280**, 42375-42382 (2005).

322. B. E. Perez White *et al.*, EphA2 proteomics in human keratinocytes reveals a novel association with afadin and epidermal tight junctions. *J Cell Sci* **130**, 111-118 (2017).

323. M. Teichert *et al.*, Pericyte-expressed Tie2 controls angiogenesis and vessel maturation. *Nature communications* **8**, 16106 (2017).

324. S. Kale *et al.*, Microarray analysis of in vitro pericyte differentiation reveals an angiogenic program of gene expression. *FASEB journal : official publication of the Federation of American Societies for Experimental Biology* **19**, 270-271 (2005).

325. T. B. Puschmann, A. M. Turnley, Eph receptor tyrosine kinases regulate astrocyte cytoskeletal rearrangement and focal adhesion formation. *Journal of neurochemistry* **113**, 881-894 (2010).

326. X. Li *et al.*, Expression of EphA2 in human astrocytic tumors: correlation with pathologic grade, proliferation and apoptosis. *Tumour biology : the journal of the International Society for Oncodevelopmental Biology and Medicine* **28**, 165-172 (2007).

327. I. M. Medana, N. H. Hunt, G. Chaudhri, Tumor necrosis factor-alpha expression in the brain during fatal murine cerebral malaria: evidence for production by microglia and astrocytes. *Am J Pathol* **150**, 1473-1486 (1997).

328. I. M. Medana, T. Chan-Ling, N. H. Hunt, Redistribution and degeneration of retinal astrocytes in experimental murine cerebral malaria: relationship to disruption of the blood-retinal barrier. *Glia* **16**, 51-64 (1996).

329. F. G. Baptista *et al.*, Accumulation of Plasmodium berghei-infected red blood cells in the brain is crucial for the development of cerebral malaria in mice. *Infect Immun* **78**, 4033-4039 (2010).

330. E. B. Gordon *et al.*, Inhibiting the Mammalian target of rapamycin blocks the development of experimental cerebral malaria. *mBio* **6**, e00725 (2015).

331. K. Dorovini-Zis *et al.*, The neuropathology of fatal cerebral malaria in malawian children. *Am J Pathol* **178**, 2146-2158 (2011).

332. J. K. Patnaik *et al.*, Vascular clogging, mononuclear cell margination, and enhanced vascular permeability in the pathogenesis of human cerebral malaria. *Am J Trop Med Hyg* **51**, 642-647 (1994).

333. R. Noberini, I. Lamberto, E. B. Pasquale, Targeting Eph receptors with peptides and small molecules: progress and challenges. *Semin Cell Dev Biol* **23**, 51-57 (2012).

334. A. S. Hahn *et al.*, The ephrin receptor tyrosine kinase A2 is a cellular receptor for Kaposi's sarcoma–associated herpesvirus. *Nat Med* **18**, 961-966 (2012).

335. J. Fonager *et al.*, Reduced CD36-dependent tissue sequestration of Plasmodium-infected erythrocytes is detrimental to malaria parasite growth in vivo. *J Exp Med* **209**, 93-107 (2012).

336. T. Au - Ruck, S. Au - Bittner, L. Au - Epping, A. M. Au - Herrmann, S. G. Au - Meuth, Isolation of Primary Murine Brain Microvascular Endothelial Cells. *JoVE*, e52204 (2014).

337. M. W. Pfaffl, A new mathematical model for relative quantification in real-time RT-PCR. *Nucleic acids research* **29**, e45 (2001).

338. G. E. Grau *et al.*, TNF-induced microvascular pathology: active role for platelets and importance of the LFA-1/ICAM-1 interaction. *European cytokine network* **4**, 415-419 (1993).

339. P. F. Piguet *et al.*, Delayed mortality and attenuated thrombocytopenia associated with severe malaria in urokinase- and urokinase receptor-deficient mice. *Infect Immun* **68**, 3822-3829 (2000).

340. G. Sun *et al.*, Inhibition of platelet adherence to brain microvasculature protects against severe Plasmodium berghei malaria. *Infect Immun* **71**, 6553-6561 (2003).

341. C. Engwerda, E. Belnoue, A. C. Gruner, L. Renia, Experimental models of cerebral malaria. *Current topics in microbiology and immunology* **297**, 103-143 (2005).

342. H. A. Lagasse *et al.*, Recruited monocytes modulate malaria-induced lung injury through CD36-mediated clearance of sequestered infected erythrocytes. *J Leukoc Biol* **99**, 659-671 (2016).

343. F. E. Lovegrove *et al.*, Parasite burden and CD36-mediated sequestration are determinants of acute lung injury in an experimental malaria model. *PLoS Pathog* **4**, e1000068 (2008).

344. W. H. Kahr *et al.*, Abnormal megakaryocyte development and platelet function in Nbeal2(-/-) mice. *Blood* **122**, 3349-3358 (2013).

345. C. Deppermann *et al.*, Gray platelet syndrome and defective thrombo-inflammation in Nbeal2-deficient mice. *J Clin Invest*, (2013).

346. M. Nishibori *et al.*, The protein CD63 is in platelet dense granules, is deficient in a patient with Hermansky-Pudlak syndrome, and appears identical to granulophysin. *J Clin Invest* **91**, 1775-1782 (1993).

347. W. Bergmeier *et al.*, Flow cytometric detection of activated mouse integrin alphaIIbbeta3 with a novel monoclonal antibody. *Cytometry* **48**, 80-86 (2002).

348. C. R. Engwerda, L. Beattie, F. H. Amante, The importance of the spleen in malaria. *Trends Parasitol* **21**, 75-80 (2005).

349. J. Hearn, N. Rayment, D. N. Landon, D. R. Katz, J. B. de Souza, Immunopathology of cerebral malaria: morphological evidence of parasite sequestration in murine brain microvasculature. *Infect Immun* **68**, 5364-5376 (2000).

350. H. C. van der Heyde *et al.*, Assessing vascular permeability during experimental cerebral malaria by a radiolabeled monoclonal antibody technique. *Infect Immun* **69**, 3460-3465 (2001).

351. B. Franke-Fayard *et al.*, Murine malaria parasite sequestration: CD36 is the major receptor, but cerebral pathology is unlinked to sequestration. *Proc Natl Acad Sci U S A* **102**, 11468-11473 (2005).

352. J. M. Sowerby *et al.*, NBEAL2 is required for neutrophil and NK cell function and pathogen defense. *J Clin Invest* **127**, 3521-3526 (2017).

353. T. A. M. Claushuis *et al.*, Nbeal2 Deficiency Increases Organ Damage but Does Not Affect Host Defense During Gram-Negative Pneumonia-Derived Sepsis. *Arterioscler Thromb Vasc Biol* **38**, 1772-1784 (2018).

354. M. K. Sercundes *et al.*, Targeting Neutrophils to Prevent Malaria-Associated Acute Lung Injury/Acute Respiratory Distress Syndrome in Mice. *PLoS Pathog* **12**, e1006054 (2016).

355. G. Senaldi, C. Vesin, R. Chang, G. E. Grau, P. F. Piguet, Role of polymorphonuclear neutrophil leukocytes and their integrin CD11a (LFA-1) in the pathogenesis of severe murine malaria. *Infect Immun* **62**, 1144-1149 (1994).

356. L. M. Wuescher, A. Takashima, R. G. Worth, A novel conditional platelet depletion mouse model reveals the importance of platelets in protection against Staphylococcus aureus bacteremia. *Journal of thrombosis and haemostasis : JTH* **13**, 303-313 (2015).

357. S. Lindemann *et al.*, Activated platelets mediate inflammatory signaling by regulated interleukin 1beta synthesis. *The Journal of cell biology* **154**, 485-490 (2001).

358. K. Srivastava *et al.*, Platelet factor 4 mediates inflammation in experimental cerebral malaria. *Cell host & microbe* **4**, 179-187 (2008).

359. M. S. Love *et al.*, Platelet factor 4 activity against P. falciparum and its translation to nonpeptidic mimics as antimalarials. *Cell host & microbe* **12**, 815-823 (2012).

360. A. Armulik *et al.*, Pericytes regulate the blood-brain barrier. *Nature* **468**, 557-561 (2010).

361. R. C. Janzer, M. C. Raff, Astrocytes induce blood-brain barrier properties in endothelial cells. *Nature* **325**, 253-257 (1987).

362. H. Ikeshima-Kataoka, M. Yasui, Correlation between astrocyte activity and recovery from blood-brain barrier breakdown caused by brain injury. *Neuroreport* **27**, 894-900 (2016).

363. A. Palmer *et al.*, EphrinB phosphorylation and reverse signaling: regulation by Src kinases and PTP-BL phosphatase. *Molecular cell* **9**, 725-737 (2002).

364. S. A. Green *et al.*, Activated platelet-T-cell conjugates in peripheral blood of patients with HIV infection: coupling coagulation/inflammation and T cells. *AIDS (London, England)* **29**, 1297-1308 (2015).

365. C. Zamora *et al.*, Association of Platelet Binding to Lymphocytes with B Cell Abnormalities and Clinical Manifestations in Systemic Lupus Erythematosus. *Mediators of inflammation* **2019**, 2473164 (2019).

366. S. P. Kurup, N. S. Butler, J. T. Harty, T cell-mediated immunity to malaria. *Nature reviews. Immunology* **19**, 457-471 (2019).

367. D. H. Busch, E. G. Pamer, T cell affinity maturation by selective expansion during infection. *J Exp Med* **189**, 701-710 (1999).

368. L. Malherbe, C. Hausl, L. Teyton, M. G. McHeyzer-Williams, Clonal selection of helper T cells is determined by an affinity threshold with no further skewing of TCR binding properties. *Immunity* **21**, 669-679 (2004).

369. P. A. Savage, J. J. Boniface, M. M. Davis, A kinetic basis for T cell receptor repertoire selection during an immune response. *Immunity* **10**, 485-492 (1999).

370. J. J. Sabatino, J. Huang, C. Zhu, B. D. Evavold, High prevalence of low affinity peptide–MHC II tetramer–negative effectors during polyclonal CD4+ T cell responses. *The Journal of Experimental Medicine* **208**, 81-90 (2011).

371. R. J. Martinez, R. Andargachew, H. A. Martinez, B. D. Evavold, Low-affinity CD4+ T cells are major responders in the primary immune response. *Nature communications* **7**, 13848 (2016).

372. J. Huang *et al.*, The kinetics of two-dimensional TCR and pMHC interactions determine T-cell responsiveness. *Nature* **464**, 932-936 (2010).

373. J. Huang, L. J. Edwards, B. D. Evavold, C. Zhu, Kinetics of MHC-CD8 Interaction at the T Cell Membrane. *The Journal of Immunology* **179**, 7653-7662 (2007).

374. Y. Choi *et al.*, Discovery and structural analysis of Eph receptor tyrosine kinase inhibitors. *Bioorg Med Chem Lett* **19**, 4467-4470 (2009).

375. M. Bantscheff *et al.*, Quantitative chemical proteomics reveals mechanisms of action of clinical ABL kinase inhibitors. *Nat Biotech* **25**, 1035-1044 (2007).

376. Y. Gokmen-Polar *et al.*, Dual targeting of EphA2 and ER restores tamoxifen sensitivity in ER/EphA2-positive breast cancer. *Breast Cancer Res Treat* **127**, 375-384 (2011).

377. C. N. Landen *et al.*, Intraperitoneal delivery of liposomal siRNA for therapy of advanced ovarian cancer. *Cancer Biol Ther* **5**, 1708-1713 (2006).

378. S. Mitra *et al.*, Structure-activity relationship analysis of peptides targeting the EphA2 receptor. *Biochemistry* **49**, 6687-6695 (2010).

379. S. Wang *et al.*, Targeted delivery of paclitaxel to EphA2-expressing cancer cells. *Clin Cancer Res* **19**, 128-137 (2013).

380. H. Okada *et al.*, Induction of CD8+ T-cell responses against novel glioma-associated antigen peptides and clinical activity by vaccinations with {alpha}-type 1 polarized dendritic cells and polyinosinic-polycytidylic acid stabilized by lysine and carboxymethylcellulose in patients with recurrent malignant glioma. *J Clin Oncol* **29**, 330-336 (2011).

381. K. Carles-Kinch, K. E. Kilpatrick, J. C. Stewart, M. S. Kinch, Antibody targeting of the EphA2 tyrosine kinase inhibits malignant cell behavior. *Cancer Res* **62**, 2840-2847 (2002).

382. S. A. Hammond *et al.*, Selective targeting and potent control of tumor growth using an EphA2/CD3-Bispecific single-chain antibody construct. *Cancer Res* **67**, 3927-3935 (2007).

383. R. Shretta *et al.*, Tracking development assistance and government health expenditures for 35 malaria-eliminating countries: 1990-2017. *Malaria journal* **16**, 251 (2017).

384. N. A. Beare, T. E. Taylor, S. P. Harding, S. Lewallen, M. E. Molyneux, Malarial retinopathy: a newly established diagnostic sign in severe malaria. *Am J Trop Med Hyg* **75**, 790-797 (2006).

385. G. Fabiani, J. Orfila, C. M. Prades, [Blood platelet variations during experimental malaria in white rat]. *Comptes rendus des seances de la Societe de biologie et de ses filiales* **152**, 588-589 (1958).

386. S. H. Yun, E. H. Sim, R. Y. Goh, J. I. Park, J. Y. Han, Platelet Activation: The Mechanisms and Potential Biomarkers. *BioMed research international* **2016**, 9060143 (2016).

387. J. D. Eicher *et al.*, Characterization of the platelet transcriptome by RNA sequencing in patients with acute myocardial infarction. *Platelets* **27**, 230-239 (2016).

388. P. F. Bray *et al.*, The complex transcriptional landscape of the anucleate human platelet. *BMC genomics* **14**, 1 (2013).

389. E. A. Middleton *et al.*, Sepsis alters the transcriptional and translational landscape of human and murine platelets. *Blood* **134**, 911-923 (2019).

390. Z. A. Jeremiah, E. K. Uko, Depression of platelet counts in apparently healthy children with asymptomatic malaria infection in a Nigerian metropolitan city. *Platelets* **18**, 469-471 (2007).

391. W. Leowattana *et al.*, Changes in platelet count in uncomplicated and severe falciparum malaria. *The Southeast Asian journal of tropical medicine and public health* **41**, 1035-1041 (2010).

392. S. T. Agnandji *et al.*, A phase 3 trial of RTS,S/AS01 malaria vaccine in African infants. *The New England journal of medicine* **367**, 2284-2295 (2012).

393. S. T. Agnandji *et al.*, First results of phase 3 trial of RTS,S/AS01 malaria vaccine in African children. *The New England journal of medicine* **365**, 1863-1875 (2011).

394. A. Moreno, C. Joyner, Malaria vaccine clinical trials: what's on the horizon. *Curr Opin Immunol* **35**, 98-106 (2015).

395. S. J. Draper *et al.*, Malaria Vaccines: Recent Advances and New Horizons. *Cell host & microbe* **24**, 43-56 (2018).

APPENDIX

Fig. A1

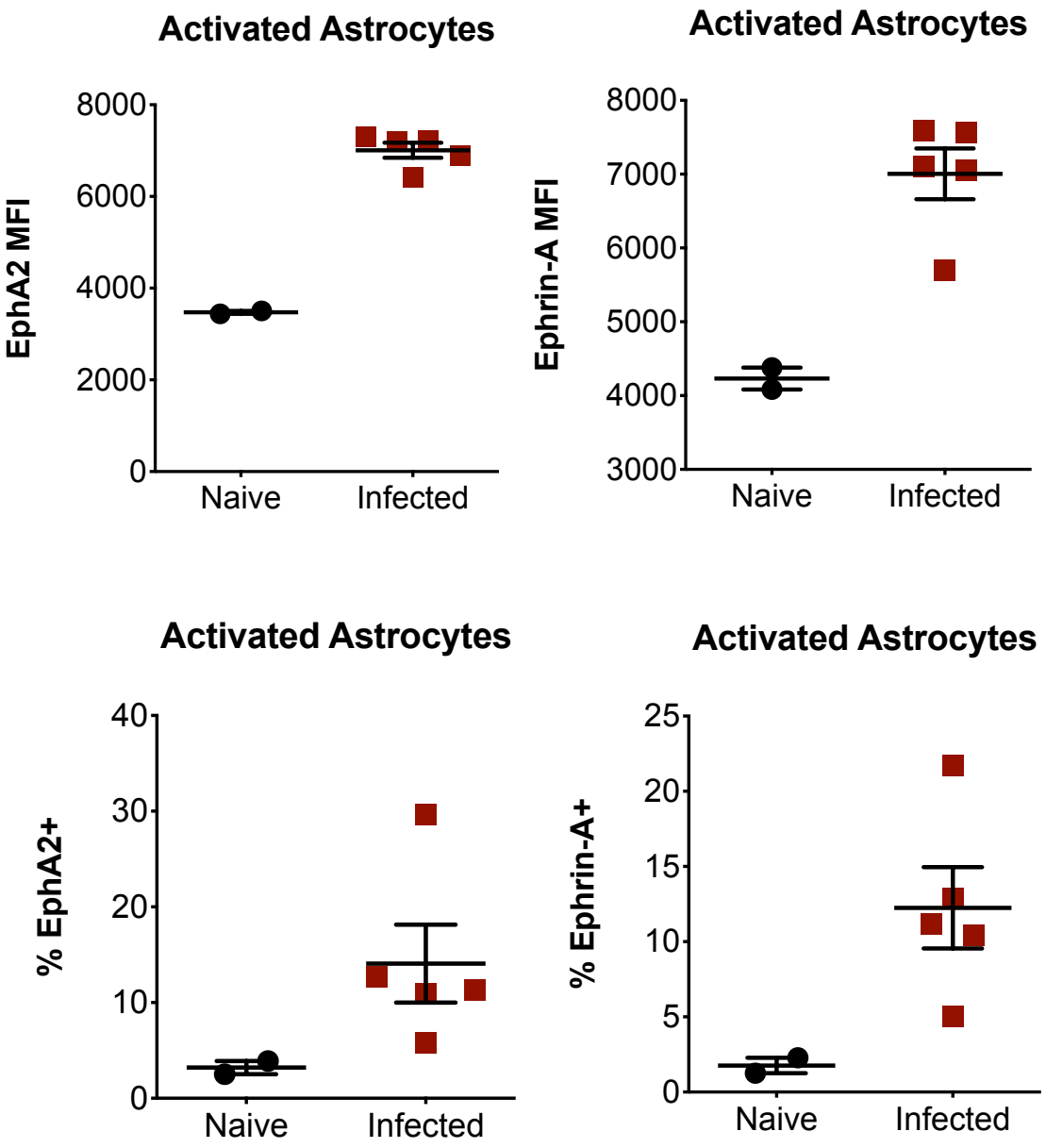
Activated Astrocytes
EphA2 MFI
8000
6000
4000
2000
0
Naive
Infected
Activated Astrocytes
Ephrin-A MFI
8000
7000
6000
5000
4000
3000
Naive
Infected
Activated Astrocytes
% EphA2+
40
30
20
10
0
Naive
Infected
Activated Astrocytes
% Ephrin-A+
25
20
15
10
5
0
Naive
Infected

Appendix Figure 1. Activated astrocytes upregulate EphA2 and ephrin-A ligands in response to *Plasmodium* infection. Median fluorescent intensity (top row) and frequency (bottom row) of EphA2 (left column) and ephrin-A (right column) positive activated astrocytes isolated from brains of C57BL/6J mice six days post-infection with *Pb*A (n=5 mice) in comparison to naïve mice (n=2 mice). Activated astrocytes were identified by GFAP expression. Bars represent the mean ± SEM.

Fig. A2

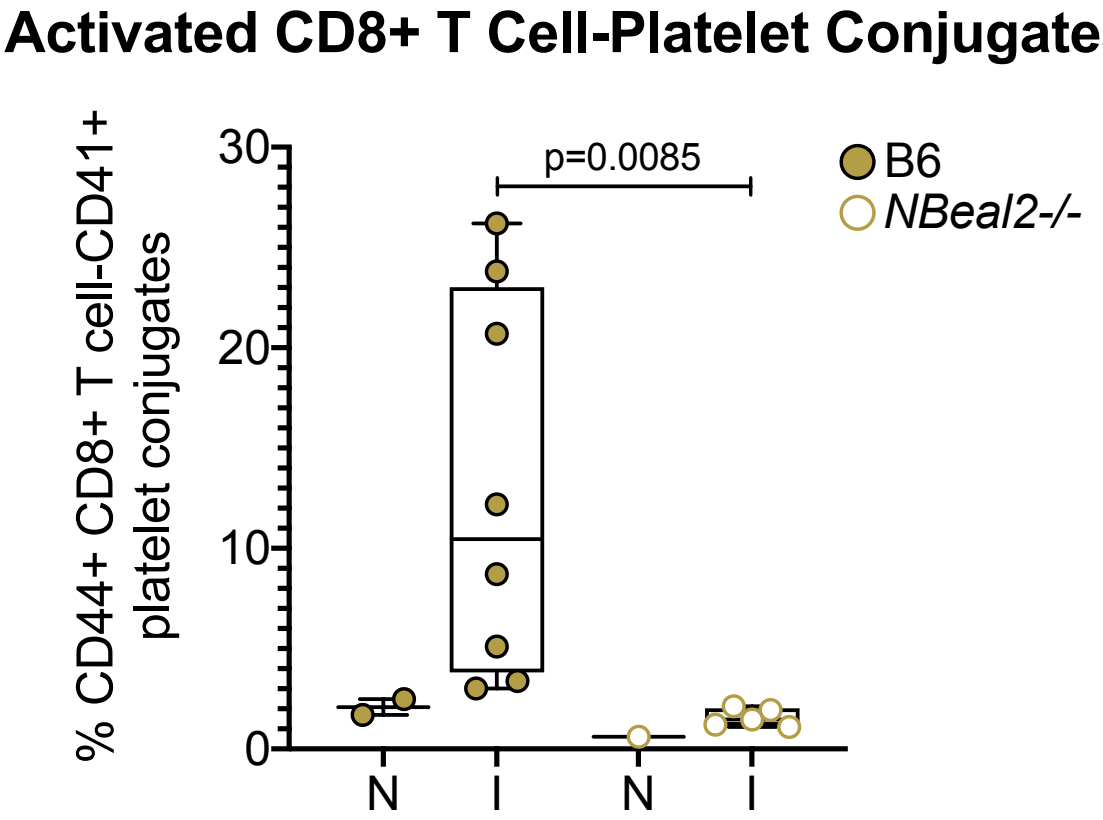
Activated CD8+ T Cell-Platelet Conjugates
% CD44+ CD8+ T cell-CD41+ platelet conjugates
30
20
10
0
p=0.0085
B6
NBeal2-/-
N
I
N
I

Appendix Figure 2. Platelets form conjugates with activated CD8+ T cells during *Plasmodium* infection in an α-granule dependent manner. Frequency of CD44+CD8+CD41+ T cell-platelet conjugates in whole blood of C57BL/6J and *Nbeal2*-/- mice five days after *Pb*A infection (n=5-8 mice/group) in comparison to naïve mice (n=1-2 mice/group). Prior gates include size and granularity, live cells, and CD3+. Boxes represent the median ± the 25th and 75th percentiles with minimum/maximum whiskers. Statistical analyses: Kruskal-Wallis test with Dunn's multiple comparisons. Only statistically significant ($p<0.05$) values are shown.

Fig. A3

Plasmodium-reactive CD8+ T Cells

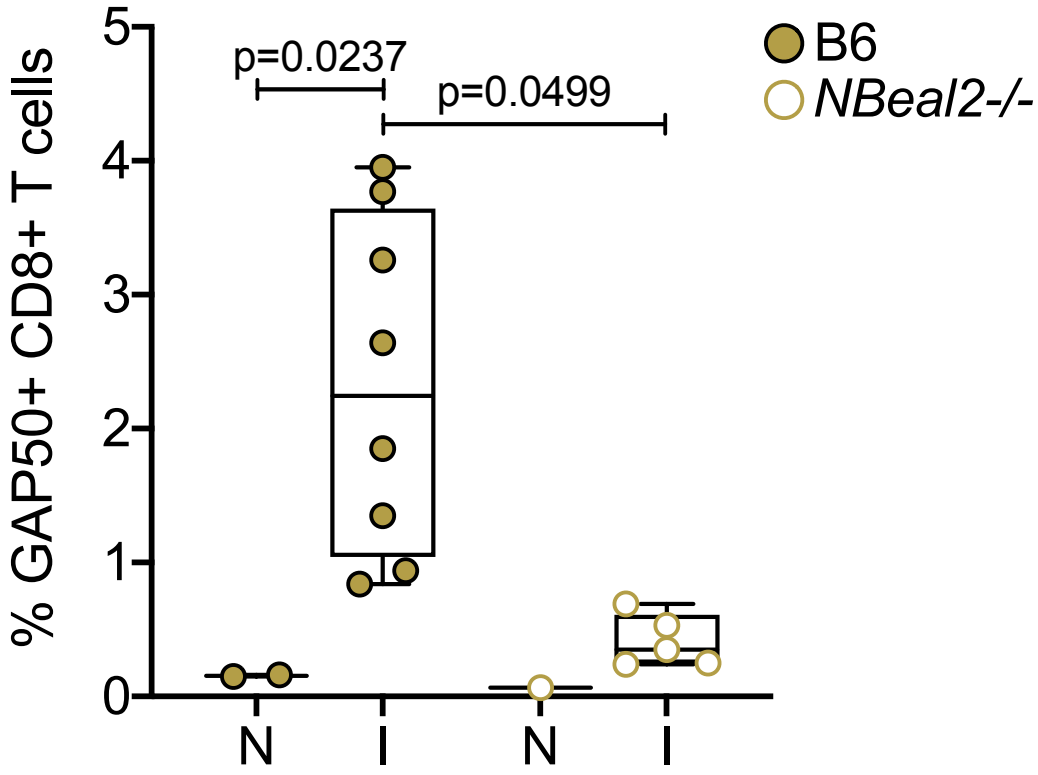

Appendix Figure 3. Mice with dysfunctional platelets have a blunted *Plasmodium*-reactive CD8+ T cell response. Frequency of *Plasmodium*-reactive GAP50+ CD8+ T cells in whole blood of C57BL/6J and *Nbeal2*-/- mice five days after *Pb*A infection (n=5-8 mice/group) in comparison to naïve mice (n=1-2 mice/group). Prior gates include size and granularity, single, live, CD3+, and CD4-CD8+ cells. Boxes represent the median ± the 25th and 75th percentiles with minimum/maximum whiskers. Statistical analyses: Kruskal-Wallis test with Dunn's multiple comparisons. Only statistically significant ($p<0.05$) values are shown.

Fig. A4

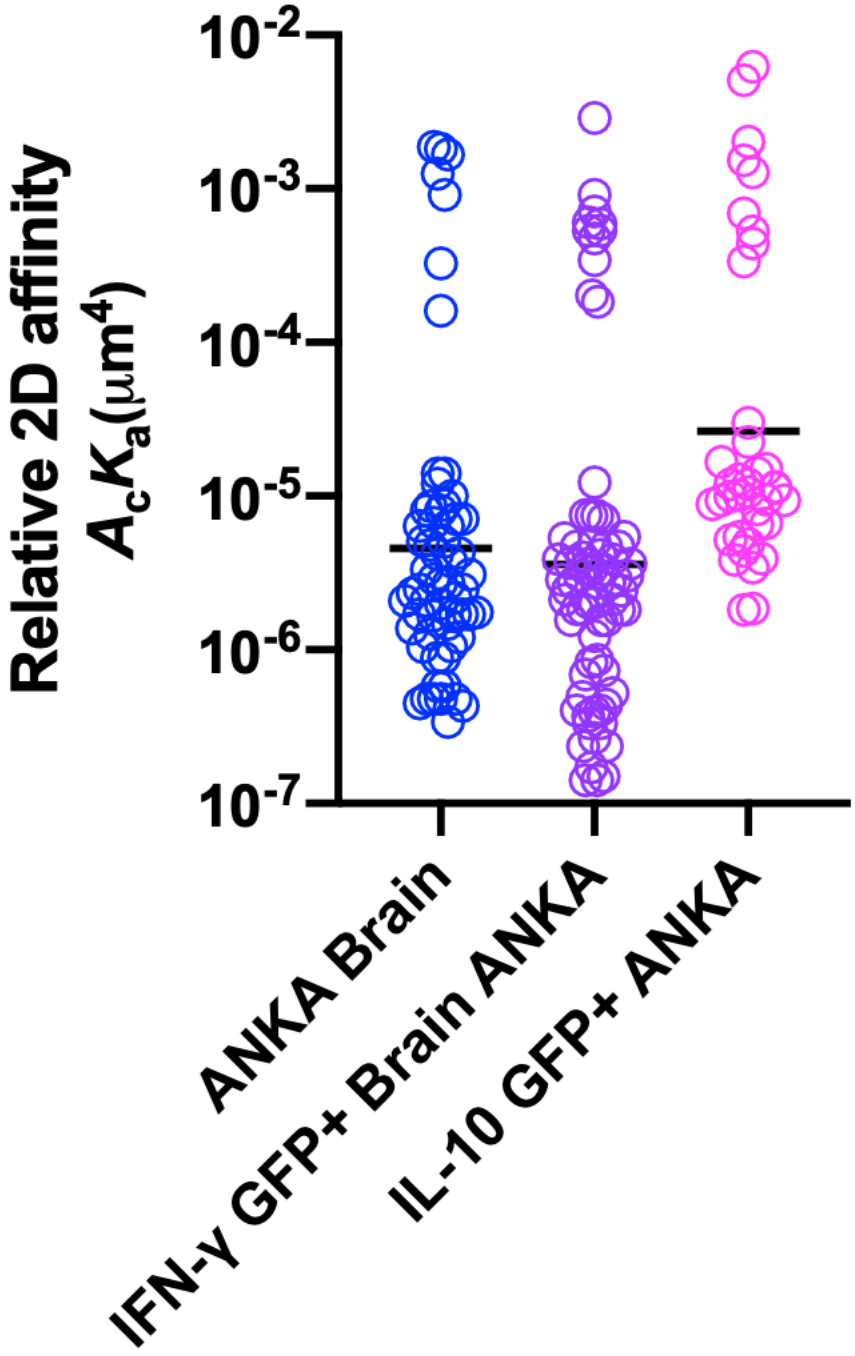
Relative 2D affinity
$A_cK_a(\mu m^4)$
10^{-2}
10^{-3}
10^{-4}
10^{-5}
10^{-6}
10^{-7}
ANKA Brain
IFN-γ GFP+ Brain ANKA
IL-10 GFP+ ANKA

Appendix Figure 4. Functional CD8+ T cells present in the brains of mice with ECM are predominantly low-affinity. Affinities of *Plasmodium* GAP50-reactive CD8+ T cells isolated from the brains of C57BL/6J (left), IFN-γ-GFP reporter mice (center), and IL-10-GFP reporter mice (right) at day 6 post-infection with *Pb*A. Affinities of bulk CD8+ T cells isolated from brains of C57BL/6J mice are shown while affinities specifically from GFP+ CD8+ T cells isolated from brains of IFN-γ-GFP and IL-10-GFP reporter mice are shown. Each point represents an individual CD8+ T cell. Graph includes combined data from 2 (right) or more (left and center) independent experiments.

Interferon-γ: The Jekyll and Hyde of Malaria

The following is a print of a published review:

King T and Lamb T (2015) Interferon-γ: The Jekyll and Hyde of Malaria. *PLoS Pathogens*. 11(10): e1005118. https://doi.org/10.1371/journal.ppat.1005118

PLOS | PATHOGENS

PEARLS

Interferon-γ: The Jekyll and Hyde of Malaria

Thayer King, Tracey Lamb*

Department of Pediatrics, Emory University School of Medicine, Atlanta, Georgia, United States of America

* tracey.j.lamb@emory.edu

Citation: King T, Lamb T (2015) Interferon-γ: The Jekyll and Hyde of Malaria. PLoS Pathog 11(10): e1005118. doi:10.1371/journal.ppat.1005118

Editor: Laura J Knoll, University of Wisconsin Medical School, UNITED STATES

Published: October 1, 2015

Funding: This work was supported by a grant from the National Institute for Neurological Disorders and Stroke (1R21N5085382-01A1), the Emory University Immunology and Molecular Pathogenesis training grant (5T32AI007610-15), the Royal Society, and the Emory Egleston Children's Research Center. The funders had no role in study design, data collection and analysis, decision to publish, or preparation of the manuscript.

Competing Interests: The authors have declared that no competing interests exist.

Introduction

Interferon gamma (IFN-γ) is a key mediator of inflammatory immune responses induced primarily by interleukin-12 (IL-12). IFN-γ secretion by both innate and adaptive immune cells is essential for control of intracellular pathogens and tumors, yet aberrant production of IFN-γ contributes to autoimmunity and inflammation in certain disease settings. These divergent roles are well illustrated in the context of malaria, a disease caused by infection with protozoan parasites of the genus *Plasmodium*. IFN-γ is a central cytokine in controlling *Plasmodium* infection in both the liver and blood stages of the parasite life cycle, but it can also exacerbate the severity of malarial disease depending on the temporal and spatial production of IFN-γ. Here, we review the types of immune cells that produce IFN-γ during malaria and discuss the IFN-γ-induced effector mechanisms that can aid in killing *Plasmodium* parasites but also contribute to the pathogenesis of malaria.

Which Immune Cells Produce IFN-γ during Malaria?

Plasmodium infection induces IFN-γ production from a variety of innate and adaptive immune cell subsets at different stages of the life cycle. Studies in mice have demonstrated that natural killer (NK) cells are one of the earliest sources of IFN-γ during the liver stage [1], as well as blood stage [2], of malaria. For example, C57BL/6J mice depleted of NK cells and infected with a nonlethal *Plasmodium yoelli* strain showed a 58% abrogation of IFN-γ production at 24 hours postinfection [2]. Human NK cells have also been shown to rapidly produce IFN-γ upon incubation with *Plasmodium falciparum*-infected red blood cells (iRBCs) in vitro [3]. Bridging innate and adaptive immunity, both natural killer T (NKT) cells and γδ T cells can contribute to IFN-γ production during *Plasmodium* infection. Studies suggest a significant proportion (50%) of γδ T cells from humans infected with *P. falciparum* secrete IFN-γ [4], while NKT cells in mice secrete IFN-γ in response to sporozoites and liver stage parasites [5]. While there is likely significant redundancy in IFN-γ production from leukocytes in response to both liver stage and blood stage *Plasmodium* parasites, studies using IFN-γ eYFP reporter mice infected with *P. berghei* ANKA suggest that NK cells contribute greater to IFN-γ production than both NKT and γδ T cells at early time points postinfection, and the production of IFN-γ from NKT and γδ T cells remains fairly stable over time [6].

Once an adaptive immune response is initiated, both $CD4^+$ and $CD8^+$ T cells become a major source of IFN-γ in response to both liver stage [7] and blood stage malaria. The finding that both $CD4^+$ [8] and $CD8^+$ [9] T cells isolated from *Plasmodium*-infected humans produce IFN-γ is also observed in many mouse models of malaria. Secretion of IFN-γ by both $CD4^+$ and $CD8^+$ T cells increases around day seven postinfection with blood stage *P. berghei* ANKA in both the spleen and brain [6]. While IFN-γ is the canonical cytokine that has been used to define $CD4^+$ T cells as Th1 cells, it has been widely observed that Th1 cells can simultaneously produce other inflammatory cytokines including IL-2, TNF-α, and IL-17 during an adaptive

immune response. A subset of IFN-γ/IL-10 double-producing $CD4^+$ T cells have been observed in humans infected with *Plasmodium* [8,10], and mouse models of malaria suggest that IFN-γ/IL-10 double-producing cells are an important source of IL-10 that limit immunopathogenesis of malaria [11] at the cost of inhibiting control of the infection [12].

What Evidence Suggests That IFN-γ Is Protective during Malaria?

There have been several correlations between IFN-γ levels in the periphery and protection against severe malaria in humans. The protective capacity of IFN-γ in malaria appears to be, in part, related to the timing of IFN-γ production with the early appearance of IFN-γ after infection in humans correlated with protection against the development of clinical symptoms of malaria in some studies [13]. However, study conclusions are often complicated by factors that include differing patterns of *Plasmodium* transmission between study sites or varying levels of pathogen coinfection giving rise to conflicting data. Experiments in mice also suggest that early IFN-γ production is protective against experimental cerebral malaria (ECM), and peripheral levels of IFN-γ can drop just before the onset of ECM [14] with a similar phenomenon potentially occurring in humans [15]. This introduces a time-dependent sampling variable that can pose problems when attempting to establish a correlation between disease severity and peripheral IFN-γ levels. Nevertheless, in a study where human volunteers were infected over time with several low doses of *Plasmodium* iRBCs and treated to clear the infection, protection from a challenge infection was positively correlated with numbers of circulating IFN-γ-producing $CD4^+$ T cells [16]. The natural resistance of the Fulani tribe in Mali to *Plasmodium* infection has also been correlated with elevated levels of IFN-γ [17], suggesting a protective role for IFN-γ against malaria.

Similar to human malaria, IFN-γ also appears to play a protective role against blood stage *Plasmodium* infection in mice. Mice lacking IFN-γ experience higher and more prolonged blood stage parasitemia compared to IFN-γ-sufficient mice when infected with the rodent parasites *P. yoelii yoelii* or *P. chabaudi adami* [18]. Additionally, a separate study found that IFN-γ levels were markedly higher 24 hours post blood stage infection in mice infected with nonlethal strains of *P. chabaudi* or *P. yoelli* when compared to mice infected with lethal strains of *P. yoelli* or *P. berghei* [2] emphasizing the potential benefits of IFN-γ to disease control in mice.

The prevalence of IFN-γ-producing $CD4^+$ and $CD8^+$ T cells has been associated with a greater likelihood of uncomplicated malaria [8], as well as reduced severe malarial anemia [9] in humans. However, experiments in mice have demonstrated that IFN-γ production by NK cells, NKT cells, and γδ T cells can also play a major role in the control of *Plasmodium* infection. NKT cells have been shown to inhibit parasite growth within hepatocytes in a partially IFN-γ-dependent manner [5]. Also, despite the prominent role of $CD4^+$ and $CD8^+$ T cells in contributing to serum IFN-γ levels during malaria, γδ T cells in mice are able to control liver stage *Plasmodium* infection in the absence of αβ T cells [19], demonstrating that γδ T cells are an important source of IFN-γ with respect to parasite control.

What Immune Effector Mechanisms Responsible for Controlling *Plasmodium* Infection Are Activated by IFN-γ?

IFN-γ secreted by $CD4^+$ Th1 cells is critical for optimal activation of $CD8^+$ T cells, B cells, and macrophages, all of which perform vital roles in the control of *Plasmodium* infection (Fig 1). The primary immune effector mechanisms by which IFN-γ can influence destruction of *Plasmodium*-infected cells include increasing the cytotoxic potential of $CD8^+$ T cells, inducing production of cytophilic antibodies by B cells and enhancing phagocytic abilities of immune cells

PLOS | PATHOGENS

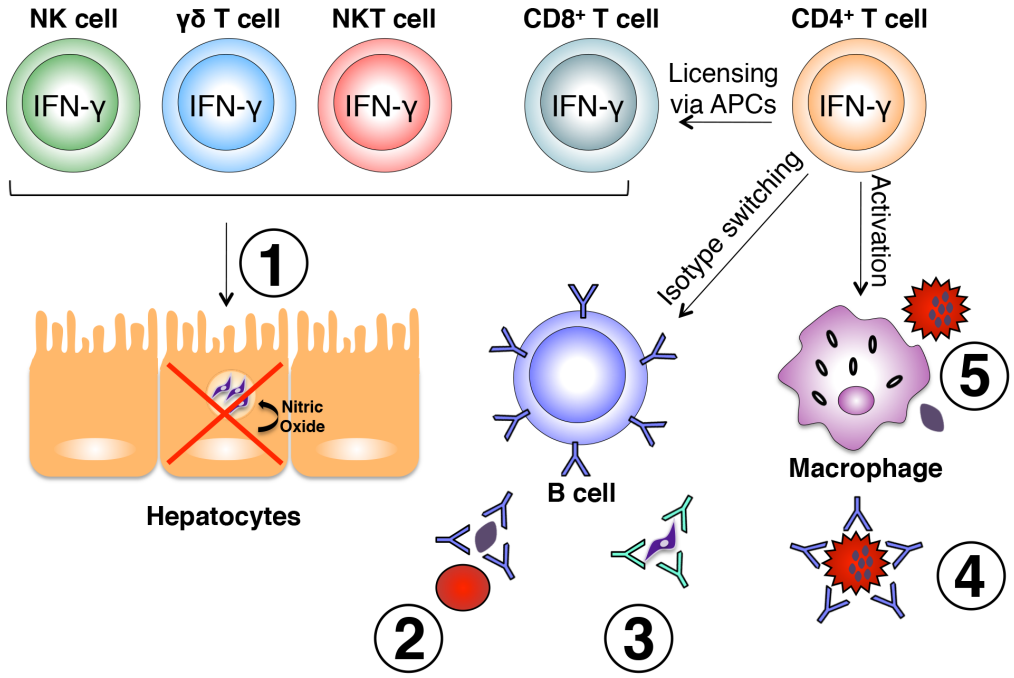

Fig 1. Effector mechanisms induced by IFN-γ during malaria. Various immune cell subsets produce IFN-γ in response to *Plasmodium* infection. NK, γδ, and NKT cells are largely responsible for early production of IFN-γ in response to liver and blood stages of the parasite and play a role in early control of parasite growth. IFN-γ-producing $CD8^+$ T cells have also been shown to limit intrahepatic parasite growth through an IFN-γ-inducible, nitric oxide-dependent mechanism (**1**). Once an adaptive immune response is initiated, IFN-γ produced by $CD4^+$ T cells optimally activates $CD8^+$ T cells, B cells, and macrophages. IFN-γ influences isotype switching in B cells leading to production of cytophilic antibodies capable of binding free parasites and blocking red blood cell invasion (**2**), mediating parasite clearance through opsonization (**3**), and binding the surface of infected red blood cells promoting antibody-dependent phagocytosis (**4**). Production of IFN-γ from $CD4^+$ T cells also optimally activates macrophages to phagocytose infected red blood cells and free parasites (**5**). All of these mechanisms are important for optimal control of parasite growth during *Plasmodium* infection.

doi:10.1371/journal.ppat.1005118.g001

such as macrophages. It should be noted that the latter two functions are not mutually exclusive.

IFN-γ exerts its effects on immune cells that express the IFNGR1/2 cell surface receptor, and signaling through this receptor results in activation of transcription factors such as IRF1, STAT1, JAK2, IRF9, CIITA [20], and T-bet [21]. This leads to expression of a number of proteins such as nitric oxide synthase and FcγRI (CD64, a high-affinity Fc receptor) [20], as well as induction of B cell class-switching to the IgG2a antibody isotype [21]. As a result, the aforementioned events can lead to enhanced phagocytosis and destruction of intracellular pathogens.

Regarding liver stage parasite development in mice, $CD8^+$ T cells induced by a DNA vaccination encoding the gene for a *P. yoelli* liver stage antigen were shown to be absolutely essential for protection of mice from a *P. yoelli* sporozoite challenge infection [22]. This protection was entirely dependent on IFN-γ production from *Plasmodium*-specific $CD8^+$ T cells as well as IFN-γ-inducible nitric oxide synthase production from *Plasmodium*-infected hepatocytes [22] leading to direct intracellular parasite killing.

Although $CD8^+$ T cell responses have also been implicated in control of blood stage *Plasmodium* infection in an IFN-γ-dependent manner [23], the mechanism by which this could occur

jk

remains unclear since infected red blood cells do not express the major histocompatibility complex class I (MHC-I) which is required for $CD8^+$ T cell recognition. On the contrary, antibodies are known to be key effector molecules in *Plasmodium* infection and perform many well-characterized functions important for parasite control and clearance such as blocking parasite reinvasion, parasite opsonization, and targeting of parasites for phagocytosis. IFN-γ impacts the antibody response and isotypes of malaria-specific antibodies produced, which is evident in IFN-$\gamma^{-/-}$ mice that produce significantly less parasite-specific IgM, IgG3, and cytophilic IgG2a than wild-type mice [24]. Thus, the role of IFN-γ in the isotype switching of B cells to a cytophilic antibody isotype such as IgG2a increases the opsonic potential of antibodies.

IFN-γ is a potent activator of macrophages and can increase canonical macrophage activities such as phagocytosis and the production of both proinflammatory cytokines and reactive oxygen intermediates. In mice, IFN-γ has been shown to enhance phagocytosis of *P. chabaudi* AS iRBCs and free merozoites by peritoneal macrophages with mice lacking IFN-γ exhibiting lower levels of parasite phagocytosis than wild-type mice [25]. The phagocytosis-enhancing role of IFN-γ has been further demonstrated in vitro as macrophages isolated from C57BL/6J mice treated with IFN-γ exhibit enhanced phagocytosis of iRBCs, an effect inhibited by IL-10 treatment [25]. Since phagocytosis of iRBCs can occur in an antibody-dependent or antibody-independent manner, the role of IFN-γ on B cells and phagocytes is likely synergistic leading to increased phagocytosis of opsonized parasites and parasite products.

How Does IFN-γ Cause Pathology during Malaria?

The pathology associated with malaria is caused by the blood stages of *Plasmodium* infection and, in particular, immune responses targeting iRBCs sequestered in various organs. In susceptible C57BL/6J mice infected with *P. berghei* ANKA, which develop experimental cerebral malaria (ECM), the IFN-γ-induced immune response against iRBCs sequestered in the brain and lung is required for pathogenesis of infection [6]. Furthermore, IFN-$\gamma^{-/-}$ mice that are resistant to ECM show decreased parasite and leukocyte accumulation in the brain [26]. This finding has been attributed to robust IFN-γ-induced expression of canonical adhesion molecules such as ICAM-1 [26], as well as $CD4^+$ T cell IFN-γ-induced expression of the chemokines CXCL9 and CXCL10 that recruit IFN-γ-producing $CD8^+$ T cells to the brain during ECM [6]. These pathogenic T cells induce cerebral pathology [6] most likely through perforin- and granzyme-dependent disruption of the blood-brain barrier upon recognition of malaria-derived peptides presented in the context of MHC-I on brain endothelial cells [27]. Thus, while IFN-γ is necessary for the recruitment of $CD8^+$ T cells to the brain during ECM [28], other effector molecules produced by activated $CD8^+$ T cells such as perforin and granzyme B are the critical mediators of pathology [29].

Perspectives

Studies in both humans and mice suggest a fine line between IFN-γ-associated protection versus immunopathology in the immune response to malaria in which a threshold level is needed for optimal control of parasitemia, yet aberrant expression can lead to pathology and the complications of severe malaria. It is tempting to explore boosting the IFN-γ response during malaria therapeutically, given the associations between IFN-γ and improved disease outcome. For example, phase IIa clinical trials for the RTS,S pre-erythrocytic malaria vaccine candidate showed a correlation between prolonged $CD4^+$ and $CD8^+$ T cell IFN-γ responses against a malaria-specific protein and protection upon challenge infection in human volunteers [30]. In mice, the loss of protective immunity against *P. chabaudi* is associated with a decrease in memory $CD4^+$ Th1 cells after parasite clearance along with a concomitant decrease in IFN-γ

production from splenocytes [31]. Splenic IFN-γ has been shown to be required for optimal priming of effector and effector memory T cells by splenic innate cells [32], demonstrating the importance of this cytokine in maintenance of optimal immunity. However, it is clear that the dynamic roles of IFN-γ during malaria are complex, and more work is needed to understand the delicate balance of IFN-γ necessary for achieving optimal protection while minimizing pathology.

References

1. Miller JL, Sack BK, Baldwin M, Vaughan AM, Kappe SH. Interferon-mediated innate immune responses against malaria parasite liver stages. Cell Rep. 2014 Apr 4; 7(2):436–47. doi: 10.1016/j.celrep.2014.03.018 PMID: 24703850
2. De Souza JB, Williamson KH, Otani T, Playfair JH. Early gamma interferon responses in lethal and non-lethal murine blood-stage malaria. Infect Immun. 1997 May 4; 65(5):1593–8. PMID: 9125535
3. Artavanis-Tsakonas K, Riley EM. Innate immune response to malaria: rapid induction of IFN-gamma from human NK cells by live Plasmodium falciparum-infected erythrocytes. J Immunol. 2002 Sep; 169 (6):2956–63. PMID: 12218109
4. Hviid L, Kurtzhals JA, Adabayeri V, Loizon S, Kemp K, Goka BQ, et al. Perturbation and proinflammatory type activation of V delta 1(+) gamma delta T cells in African children with Plasmodium falciparum malaria. Infect Immun. 2001 May 2; 69(5):3190–6. PMID: 11292740
5. Pied S, Roland J, Louise A, Voegtle D, Soulard V, Mazier D, et al. Liver CD4-CD8- NK1.1+ TCR alpha beta intermediate cells increase during experimental malaria infection and are able to exhibit inhibitory activity against the parasite liver stage in vitro. J Immunol. 2000 Feb 2; 164(3):1463–9. PMID: 10640763
6. Villegas-Mendez A, Greig R, Shaw TN, de Souza JB, Gwyer Findlay E, Stumhofer JS, et al. IFN-γ-producing CD4+ T cells promote experimental cerebral malaria by modulating CD8+ T cell accumulation within the brain. J Immunol. 2012 Jul; 189(2):968–79. doi: 10.4049/jimmunol.1200688 PMID: 22723523
7. Connelly M, King CL, Bucci K, Walters S, Genton B, Alpers MP, et al. T-cell immunity to peptide epitopes of liver-stage antigen 1 in an area of Papua New Guinea in which malaria is holoendemic. Infect Immun. 1997 Dec 1; 65(12):5082–7. PMID: 9393799
8. Walther M, Jeffries D, Finney OC, Njie M, Ebonyi A, Deininger S, et al. Distinct roles for FOXP3 and FOXP3 CD4 T cells in regulating cellular immunity to uncomplicated and severe Plasmodium falciparum malaria. PLoS Pathog. 2009 Apr 3; 5(4):e1000364. doi: 10.1371/journal.ppat.1000364 PMID: 19343213
9. Ong'echa JM, Lal AA, Terlouw DJ, Ter Kuile FO, Kariuki SK, Udhayakumar V, et al. Association of interferon-gamma responses to pre-erythrocytic stage vaccine candidate antigens of Plasmodium falciparum in young Kenyan children with improved hemoglobin levels: XV. Asembo Bay Cohort Project. Am J Trop Med Hyg. 2003 May 4; 68(5):590–7. PMID: 12812352
10. Jagannathan P, Eccles-James I, Bowen K, Nankya F, Auma A, Wamala S, et al. IFNγ/IL-10 co-producing cells dominate the CD4 response to malaria in highly exposed children. PLoS Pathog. 2014 Jan 3; 10(1):e1003864. doi: 10.1371/journal.ppat.1003864 PMID: 24415936
11. Freitas do Rosário AP, Lamb T, Spence P, Stephens R, Lang A, Roers A, et al. IL-27 promotes IL-10 production by effector Th1 CD4+ T cells: a critical mechanism for protection from severe immunopathology during malaria infection. J Immunol. 2012 Feb 3; 188(3):1178–90. doi: 10.4049/jimmunol.1102755 PMID: 22205023
12. Couper KN, Blount DG, Wilson MS, Hafalla JC, Belkaid Y, Kamanaka M, et al. IL-10 from CD4CD25Foxp3CD127 adaptive regulatory T cells modulates parasite clearance and pathology during malaria infection. PLoS Pathog. 2008 Feb 5; 4(2):e1000004. doi: 10.1371/journal.ppat.1000004 PMID: 18401464
13. D'Ombrain MC, Robinson LJ, Stanisic DI, Taraika J, Bernard N, Michon P, et al. Association of early interferon-gamma production with immunity to clinical malaria: a longitudinal study among Papua New Guinean children. Clin Infect Dis. 2008 Dec 1; 47(11):1380–7. doi: 10.1086/592971 PMID: 18947328
14. Mitchell AJ, Hansen AM, Hee L, Ball HJ, Potter SM, Walker JC, et al. Early cytokine production is associated with protection from murine cerebral malaria. Infect Immun. 2005 Sep 4; 73(9):5645–53. PMID: 16113282
15. Prakash D, Fesel C, Jain R, Cazenave P-AA, Mishra GC, Pied S. Clusters of cytokines determine malaria severity in Plasmodium falciparum-infected patients from endemic areas of Central India. J Infect Dis. 2006 Jul 6; 194(2):198–207. PMID: 16779726

16. Pombo DJ, Lawrence G, Hirunpetcharat C, Rzepczyk C, Bryden M, Cloonan N, et al. Immunity to malaria after administration of ultra-low doses of red cells infected with Plasmodium falciparum. Lancet. 2002 Aug 6; 360(9333):610–7. PMID: 12241933

17. McCall MBB, Hopman J, Daou M, Maiga B, Dara V, Ploemen I, et al. Early interferon-gamma response against Plasmodium falciparum correlates with interethnic differences in susceptibility to parasitemia between sympatric Fulani and Dogon in Mali. J Infect Dis. 2010 Jan 5; 201(1):142–52. doi: 10.1086/648596 PMID: 19929378

18. Van der Heyde HC, Pepper B, Batchelder J, Cigel F, Weidanz WP. The time course of selected malarial infections in cytokine-deficient mice. Exp Parasitol. 1997 Feb 6; 85(2):206–13. PMID: 9030670

19. Tsuji M, Mombaerts P, Lefrancois L, Nussenzweig RS, Zavala F, Tonegawa S. Gamma delta T cells contribute to immunity against the liver stages of malaria in alpha beta T-cell-deficient mice. Proc Natl Acad Sci USA. 1994 Jan 2; 91(1):345–9. PMID: 8278391

20. Waddell SJ, Popper SJ, Rubins KH, Griffiths MJ, Brown PO, Levin M, et al. Dissecting interferon-induced transcriptional programs in human peripheral blood cells. PLoS ONE. 2010 Jan 5; 5(3):e9753. doi: 10.1371/journal.pone.0009753 PMID: 20339534

21. Xu W, Zhang JJ. Stat1-dependent synergistic activation of T-bet for IgG2a production during early stage of B cell activation. J Immunol. 2005 Dec 4; 175(11):7419–24. PMID: 16301649

22. Doolan DL, Sedegah M, Hedstrom RC, Hobart P, Charoenvit Y, Hoffman SL. Circumventing genetic restriction of protection against malaria with multigene DNA immunization: CD8+ cell-, interferon gamma-, and nitric oxide-dependent immunity. J Exp Med. 1996 Apr 1; 183(4):1739–46. PMID: 8666931

23. Imai T, Shen J, Chou B, Duan X, Tu L, Tetsutani K, et al. Involvement of CD8+ T cells in protective immunity against murine blood-stage infection with Plasmodium yoelii 17XL strain. Eur J Immunol. 2010 Apr 4; 40(4):1053–61. doi: 10.1002/eji.200939525 PMID: 20101613

24. Su Z, Stevenson MM. Central role of endogenous gamma interferon in protective immunity against blood-stage Plasmodium chabaudi AS infection. Infect Immun. 2000 Aug 2; 68(8):4399–406. PMID: 10899836

25. Su Z, Fortin A, Gros P, Stevenson MM. Opsonin-independent phagocytosis: an effector mechanism against acute blood-stage Plasmodium chabaudi AS infection. J Infect Dis. 2002 Nov 5; 186(9):1321–9. PMID: 12402202

26. Amani V, Vigário AM, Belnoue E, Marussig M, Fonseca L, Mazier D, et al. Involvement of IFN-gamma receptor-medicated signaling in pathology and anti-malarial immunity induced by Plasmodium berghei infection. Eur J Immunol. 2000 Jun 4; 30(6):1646–55. PMID: 10898501

27. Howland SW, Poh CM, Gun SY, Claser C, Malleret B, Shastri N, et al. Brain microvessel cross-presentation is a hallmark of experimental cerebral malaria. EMBO Mol Med. 2013 Jul 1; 5(7):916–31. doi: 10.1002/emmm.201202273 PMID: 23681698

28. Belnoue E, Potter SM, Rosa DS, Mauduit M, Grüner AC, Kayibanda M, et al. Control of pathogenic CD8+ T cell migration to the brain by IFN-gamma during experimental cerebral malaria. Parasite Immunol. 2008 Oct 3; 30(10):544–53. doi: 10.1111/j.1365-3024.2008.01053.x PMID: 18665903

29. Haque A, Best SE, Unosson K, Amante FH, de Labastida F, Anstey NM, et al. Granzyme B expression by CD8+ T cells is required for the development of experimental cerebral malaria. J Immunol [Internet]. 2011 Jun 3; 186(11):6148–56. http://www.jimmunol.org/cgi/pmidlookup?view=long&pmid=21525386

30. McCall MBB, Sauerwein RW. Interferon-γ—central mediator of protective immune responses against the pre-erythrocytic and blood stage of malaria. J Leukoc Biol. 2010 Dec 3; 88(6):1131–43. doi: 10.1189/jlb.0310137 PMID: 20610802

31. Freitas do Rosário AP, Muxel SM, Rodríguez-Málaga SMM, Sardinha LR, Zago CAA, Castillo-Méndez SI, et al. Gradual decline in malaria-specific memory T cell responses leads to failure to maintain long-term protective immunity to Plasmodium chabaudi AS despite persistence of B cell memory and circulating antibody. J Immunol. 2008 Dec 1; 181(12):8344–55. PMID: 19050251

32. Da Silva HB, de Salles EM, Panatieri RH, Boscardin SB, Rodríguez-Málaga SMM, Alvarez JMM, et al. IFN-γ-induced priming maintains long-term strain-transcending immunity against blood-stage Plasmodium chabaudi malaria. J Immunol. 2013 Nov 5; 191(10):5160–9. doi: 10.4049/jimmunol.1300462 PMID: 24133169